AN ABSTRACT OF THE THESIS OF

David Esteban Rodriguez Matiz for the degree of Master of Science in Civil Engineering presented on November 20, 2015.

Title: Evaluation of the Effect of Chloride Ingress and Freeze-Thaw Cycles on Electrical Resistivity of Reinforced Concrete

Abstract approved:

_____

Jason H. Ideker O. Burkan Isgor

Performing bridge inspections can be a very daunting task for every department of transportation (DOT) in the country. Because the leading cause of deterioration in reinforced concrete bridge decks is corrosion of the steel reinforcement, the ability to detect the concentration of corrosion-causing chlorides in the concrete, using a non-destructive method, would save DOTs time and resources by allowing reparative action to take place early in the deterioration process. These are the contexts in which the current investigation was carried out, with the primary objective of investigating the potential for surface resistivity to be used as a non-destructive tool to assess the deterioration of concrete due to chloride ingress and freeze-thaw action. In this study, electrical resistivity measurements were taken on concrete cylinders and at various locations on reinforced concrete slabs that were saturated with chlorides from commercially available magnesium chloride de-icing solution, which contained a corrosion inhibitor. The study also provides a deeper understanding of the effect of freeze-thaw cycles on chloride ingress and surface resistivity measurements taken on

concrete slabs previously exposed to a de-icing solution. Additionally, chloride profiles were taken congruently with the electrical resistivity measurements to monitor the ingress of chlorides. Surface resistivity values for all concrete increased during the early part of the study, partly due to the hydration of the concrete. However, surface resistivity decreased at the latter half for the chloride-exposed concrete, while water-saturated concrete did not vary. This suggests that SR measurements could identify chloride ingress. As chlorides ingressed in the concrete over time, the amount of bound chlorides increase; however, this increase was dominated by the amount of free chlorides that were retained at a specific depth in the concrete. The increase in free chloride concentrations, which are known to initiate corrosion, may be a cause of the decrease in surface resistivity measurements. This observation was also confirmed by thermodynamic modeling; however, this will need to be studied further. Though the cause of behavior observed on the surface resistivity measurements that underwent freeze-thaw action is not clear, it is evident that freeze-thaw action has a significant negative impact on the rate of chloride ingress on the slabs. The chloride profiles strongly indicated that the penetrability of the OPC mixtures increased compared to the same slab that did not go through freeze-thaw action. An increase in transport of chlorides was not apparent for the HPC mixture and was not seen in the chloride profiles. It is suggested that additional freeze-thaw cycles continue in this study, especially until the concrete starts to fail, in order to evaluate the impact and permanency of deterioration on surface resistivity.

Evaluation of the Effect of Chloride Ingress and Freeze-Thaw Cycles on Electrical Resistivity of Reinforced Concrete

by
David Esteban Rodriguez Matiz

A THESIS

submitted to

Oregon State University

in partial fulfillment of
the requirements for the
degree of

Master of Science

Presented November 20, 2015
Commencement June 2016

Master of Science thesis of David Esteban Rodriguez Matiz presented on November 20, 2015

APPROVED:

Co-major Professor, representing Civil Engineering

Co-major Professor, representing Civil Engineering

Head of the School of Civil and Construction Engineering

Dean of the Graduate School

I understand that my thesis will become part of the permanent collection of Oregon State University libraries. My signature below authorizes release of my thesis to any reader upon request.

David Esteban Rodriguez Matiz, Author

ACKNOWLEDGEMENTS

I would like to extend my deepest thanks to my co-advisors, Dr. Jason H. Ideker and Dr. O. Burkan Isgor. You have each shown me a great amount of guidance, patience, and encouragement, and for that I am incredibly appreciative. Thank you for believing in me.

To my committee members, Dr. Jason H. Ideker, O. Burkan Isgor, and Dr. David Trejo, Dr. Lech Muszynski, thank you for all your guidance and support throughout this project.

To the post doctorate, Vahid Azad, thank you for your patience and all the hours of modeling work you put in this project. To my fellow Materials graduate research assistants, Tyler Deboodt, Chang Li, Tengfei Fu, Monica Morales, and Matt Adams, I am so grateful for the wealth of knowledge and experience you have shared with me over the years. Thank you for all your support and camaraderie. I will miss working with you all.

A huge thank you to the undergraduate students who have put in countless hours of hard work, rain or shine, to help me get here. Christine Baker, Walter Webster, Kristin Jones, Aaron Strand, and Raven Merritt-Shorb, thank you for your eagerness to learn and for your support as we worked through the ups and downs of this project.

To my parents, Gladys Matiz and Hugo Rodriguez, thank you for teaching me the value of hard work and for instilling in me the value of education. I would not have accomplished what I have without the encouragement and support you have given me throughout my whole life.

To my partner Ashby Conwell, thank you for the unbelievable support and encouragement you have given me all these years. I am a better person because of you.

CONTRIBUTION OF AUTHORS

Drs. Jason H. Ideker O. Burkan Isgor, and David Trejo advised on data collection, analysis, interpretation, and writing of Chapters 1, 2, 3, and 4. Dr. Vahid Jafari Azad assisted in the writing, data interpretation, and modeling work in Chapter 2 and Chapter 3.

TABLE OF CONTENTS

Page

TABLE OF CONTENTS (Continued)

Page

TABLE OF CONTENTS (Continued)

Page

LIST OF FIGURES

LIST OF FIGURES (Continued)

Figure Page

LIST OF TABLES

LIST OF EQUATIONS

Equation Page

1 General Introduction and Literature Review

1.1. Scope and Layout of this Thesis

This Master's thesis follows the manuscript option guidelines provided by the Oregon State University Graduate School Thesis Guide 2015-2016. This thesis states the results and discussion of experimental procedures performed through the use of electrical resistivity to develop a better understanding of the chloride ingress due to de-icer solution exposure on reinforced concrete. The experimental investigations evaluated selected reinforced concrete properties, such as concrete cover depth, the use of SCMs, varying air content and a range of water-to-cement ratios. Deterioration means, such as chloride ingress and freeze-thaw attack, were evaluated in concurrence with electrical resistivity measurements to establish a correlation. The thesis is structured as follows:

Chapter 1: *General Introduction* – This chapter provides an overview of the importance of developing accurate techniques that can detect deterioration of bridge decks at early age. A literature review that includes the deterioration mechanisms due to chloride ingress and freeze-thaw action, as well as the emphasis of the use of electrical resistivity as a durability-related quantitative performance indicator and its limitations.

Chapter 2: *Manuscript 1* – The first manuscript titled "Evaluation on the Effect of Chloride Ingress in Reinforced Concrete on Surface Resistivity Measurements" investigates the potential for surface resistivity, using the four-point Wenner probe technique, to be used as a non-destructive evaluation tool to assess the deterioration of

concrete due to chloride ingress. The manuscript evaluates the parameters that can affect the surface resistivity measurements, such as moisture, internal relative humidity and temperature, reinforcement, concrete mixture properties, porosity, chloride ingress and free vs. bound chlorides. The manuscript, considering the parameters stated, provides the correlations found between the surface resistivity measurements and chloride ingress.

Chapter 3: *Manuscript 2* – The second manuscript titled "The Effect of Freeze-Thaw Action on Electrical Resistivity Measurements Taken on Concrete Saturated with Magnesium Chloride De-Icing Solution" investigates the effect that freeze-thaw cycles have on surface resistivity and bulk resistivity measurements taken on concrete cylinders as well as concrete slabs that were exposed to a commercially available magnesium chloride de-icing solution that contained a corrosion inhibitor. The testing method practices are discussed and suggested when using electrical resistivity to analyze freeze thaw action and chloride ingress. The effect that freeze-thaw action has on specimens with and with-out air entrainment is examined as well as the ability for chloride to ingress concrete after freeze-thaw exposure. Additional experimental work is proposed to have a better understanding of the concrete performance.

Chapter 4: *General Conclusions* – Chapter 4 summarizes the overview of the main experimental work performed as well as the overall conclusions with recommendations for future work.

Appendix – The appendix contains the composition of the cement and SCMs used, as well as images of various types of deterioration from specimens observed throughout the experimental study.

1.2. Background and Introduction

Performing bridge inspections can be a very daunting task for every department of transportation (DOT) in the country. Due to the number of bridges and the limited resources available to the DOT for bridge repairs, it is imperative that each test or evaluation done during inspections is rapid and accurate. The most significant type of deterioration in reinforced structures is corrosion of the reinforcing steel with an estimated $276 billion dollars in cost to the US economy which is one of the largest single expenses in the country (Koch et al. 2002). The main contributors to corrosion of reinforced concrete bridge decks are de-icing chemicals and marine salts. Detection of corroding steel in bridge decks is time consuming and sometimes destructive. An obvious sign of corrosion of the reinforcing steel is visible damage; however, once corrosion is visible, the time required and the resources needed to mitigate it may be unfeasible. The solution to mitigating corrosion of the reinforcing steel is to prevent corrosion initiation. Each year, DOTs use coatings, overlays and sealants on the surface of bridge decks to prevent chlorides from infiltrating the concrete. Still, determining which bridge deck to seal or coat can be challenging due to the time consuming and destructive testing needed to detect the amount of chlorides in the concrete matrix.

In an effort to increase the service life of bridge decks by preventing steel corrosion in reinforced concrete, the Oregon Department of Transportation (ODOT), according to their Bridge Inspection Program Manual, currently performs biennial visual inspections. The manual provides guidelines for inspectors to follow during each evaluation, however, the manual states that "Such an evaluation is frequently based on the personal judgment, intuition, and perhaps experience of each inspector. As a result, different inspectors may assess a given bridge differently" (2013). It is noted that visual inspections may not provide accurate information on the condition of the bridge decks, and due to the amount of bridges in Oregon, a detailed inspection that provides mapping, sampling and testing is simply not practical; there is no established protocol in place for evaluating the remaining service-life of bridge decks based on a system that combines computable measurements with time-to-damage predictions. An established system that can predict the deterioration rate of these decks would be beneficial to the DOT, as it would allow ODOT to take action during the early stages of deterioration of the concrete, thereby saving the DOT resources. Whatever measures are used, data obtained during inspection needs to be turned into predictions about time to corrosion damage in order to provide a proactive approach to repair that would optimize financial and material resources required to repair bridge decks before significant damage occurs.

1.2.1. Destructive and Non-destructive Testing

The current destructive testing methods used to determine the durability or service life of a structure can be expensive and time consuming. Destructive testing methods often entail taking a sufficient number of cores from the structure to validate results obtained

from various tests, which can be detrimental to the structural integrity of a building or bridge. These tests include Rapid Chloride Penetration (ASTM C1202), which takes 24 hours to run, acid-soluble chloride content (ASTM C1152), which involves extracting powders at various depths into the structure and quantifying the amount of acid-soluble chlorides in the concrete, and petrographic examination of hardened concrete (ASTM C856), which is a common but expensive test as a licensed petrographer has to analyze the samples.

According to the Transportation Board of the National Academies (Gucunski 2013), there is not a single technology that can provide information on deterioration accurately. Combining technologies provide the most precise information on deterioration of bridge decks. Some of the more common, non-destructive testing methods, which can help evaluate the performance of the structure, include Schmidt rebound hammer test (ASTM C805), which determines the compressive strength of the concrete, chain drag (ASTM D4580) provides the location of delaminated areas, ultrasonic pulse velocity test (ASTM C597), which provides insight on the quality of the concrete although the reinforcing steel of the concrete structure can affect the results, ground penetrating radar (ASTM D6432) which supplies information of the subsurface, and impact echo test (ASTM C1383), which uses impact waves to help identify internal cracks or flaws. Half-cell potential mapping (ASTM C876) can be very useful in identifying potential corrosion in the reinforcing steel, and electrical surface resistivity (SR) measurements can be used as an indicator of concrete deterioration.

A study done by the University of Genova (Brencich et al. 2013) concluded that the Schmidt hammer test results were greatly affected by the properties of the materials and the limited area in which the test is performed which suggests that this test may only provide a rough estimation of the strength of concrete. A separate study by the University of Malaya (Shariati et al. 2011), also determined that the use alone of rebound hammer test was not enough to determine compressive strengths. The study reiterated that combining the rebound hammer test with ultrasonic pulse velocity would provide a much higher degree of accuracy. A study focused on detecting bridge deck deterioration by Maser et al. (2012) analyzed the accuracy of hammer sounding, ultrasonic impact echo, half-cell potential and ground penetrating radar, and concluded that the combination of ground penetrating radar with half-cell potential was the most useful technique for detecting deterioration of bridge decks early on in its service life. The findings in these studies showing that combining test methods, for either, destructive or non-destructive methods provide more accurate results is well established and is supported by various researchers (Jianhong et al. 2008, Khalim et al. 2011, Gucunski 2013, Sadowski 2013).

In addition to various testing methods for detection of deterioration of bridge decks, there seems to be a lack of documented information about the bridge decks that can be vital when assessing one. A study in the State of Oregon (Huang 2014) concluded that issues with data availability and quality were identified and it is recommended that deicer type and application rate, traffic volume, weather condition information, and bridge mix design data should be documented. This additional information will provide inspectors

and researchers a better understanding of problems that may arise throughout the service life of the structures.

1.3. Electrical Surface Resistivity (SR) of Concrete

1.3.1. Introduction

In recent years, electrical resistivity of concrete has emerged as a durability-related quantitative performance indicator (Andrade et al. 2013). Several investigations have shown the existence of relationships between electrical resistivity and other durability-related parameters, such as corrosion rate of steel reinforcement and transport properties of concrete. Lopez and Gonzalez (1993), and Gowers and Millard (1999) reported that concrete resistivity and corrosion rate are inversely proportional over a wide range of concrete resistivity values. The literature also shows that concrete resistivity is strongly affected by the concrete characteristics, the degree of concrete pore saturation, and the chloride concentration (Hussain et al. 1995, Morris et al. 2004, Song et al. 2007). Low resistivity values are associated with high water-to-cement ratios, high moisture contents, and presence of chlorides (Neville 1996, Morris et al. 2004). All these developments have led to increased efforts to standardize SR measurement procedures (AASHTO TP 095-11UL 2011; CAN/CSA A23.2 2009; ASTM WK37880 2014). A number of jurisdictions even started requiring resistivity measurements as part of ongoing construction and maintenance procedures (FM 5-578 2004; MTO LS-444 2013). Resistivity of concrete can be measured in a number of ways; however, the four-point Wenner probe technique is the most commonly used approach for field application because of its speed, simplicity, and practicality. It can be used to measure resistivity of concrete cores

extracted from concrete structures, but it can also be used directly on concrete surfaces without the need of coring or without the need for access to the steel reinforcement (as in the case of half-cell potential measurements). In all cases measurements are made in seconds. An image and function schematic of the four-point Wenner probe is provided in Figure 1.1(a and b).

(a)

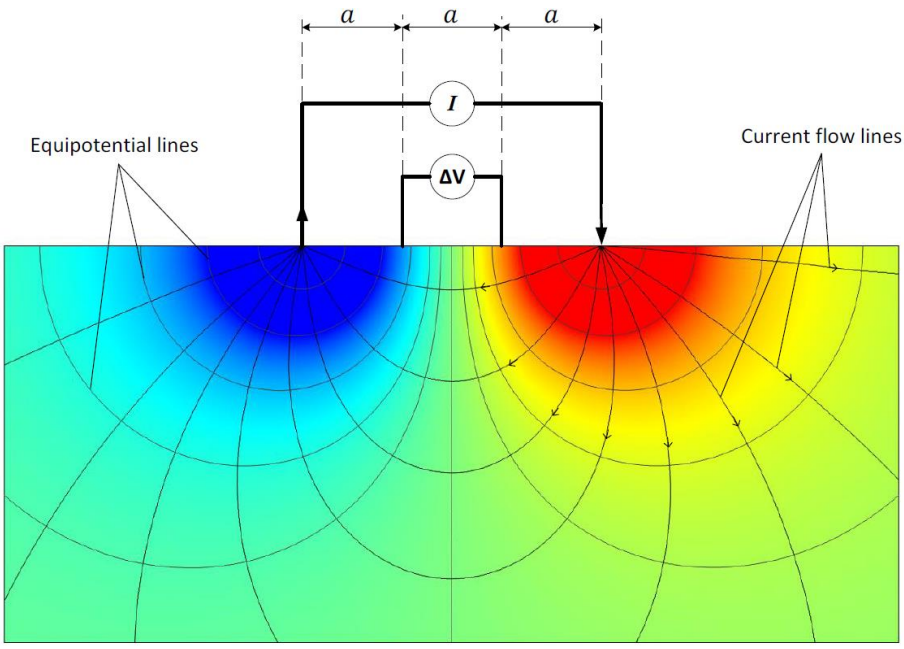

(b)

Figure 1.1 – (a) A commercial Wenner probe. (b) Function schematic of four point Wenner probe.

When the probe makes contact with the concrete, a voltage differential is created and measured between the two inner electrodes due to a current that's applied through the two outer electrodes. Knowing the voltage difference, V, the spacing between the electrodes, a, and the current, I, resistivity, ρ, can be calculated via:

$$\rho = \frac{2\pi aV}{I} \tag{1.1}$$

1.3.2. SR vs. RCPT

An established method for determining the durability of a concrete sample is to test its resistance to ionic ingress. The more vulnerable the concrete to ionic ingress, the more likely it is to deteriorate at a faster rate. The most common standard for estimating the resistance of concrete to chloride ingress is ASTM C1202 Standard Test Method for Electrical Indication of Concrete's Ability to Resist Chloride Ion Penetration, also known as RCPT. This test can provide insight on the concrete's resistance to chloride ion penetration and it does so by applying a constant voltage through a two-inch by four-inch diameter sample that on one side is submerged with sodium chloride and the other side with sodium hydroxide. The test takes 18 hours to prepare and six hours to run. The total amount of charge that passes through the concrete sample during the six hours is then compared to a table on the standard that indicates the penetrability of the sample. Table 1.1 shows the chloride ion penetrability potential from ASTM C1202.

Table 1.1 - Chloride Ion Penetrability - ASTM C1202

Charge Passed (coulombs)	Chloride Ion Penetrability
>4,000	High
2,000–4,000	Moderate
1,000–2,000	Low
100–1,000	Very Low
<100	Negligible

The RCPT determines the electrical conductance of the concrete sample, which inversely provides its resistance to chloride ion penetration. RCPT however, has its limitations. Since the test takes six hours, the conductivity and temperature of the sample may change due to the movement of chloride ions and the porosity of the sample. Nevertheless, the use of electrical resistivity as it has been used in RCPT and surface resistivity methods, seem to prove to be a good indicator for determining chloride penetrability. Surface resistivity devices have emerged in the last few years and have proven to be more practical and reliable methods for measuring the electrical resistivity of concrete because, while both tests provide a measure of resistance of concrete to ionic movement under an applied electrical potential difference, they differ in terms of precision and time required to complete the test. In most cases, RCPT and SR measurements have nearly perfect correlation (Rupnow 2011, Jackson 2013), but while RCPT takes 24 hours to complete and is prone to testing errors, SR measurements can be taken accurately in seconds.

1.3.3. Limitations of SR Measurement Devices

There are, however, a number of gaps in the literature and practical challenges to address before SR data can provide quantitative insight into the corrosion risk of bridge decks. Most studies that demonstrated strong correlations between SR measurements and

durability-related performance indicators (e.g. water permeability, RCPT data, and bulk chloride diffusivity) have been conducted on cores extracted from concrete structures or laboratory-produced concrete cylinders. Establishing such correlations on concrete surfaces of bridge decks will establish a faster, more accurate and non-destructive method for bridge inspections. Some limitations that need to be considered when using surface resistivity meters to assess the condition of concrete structures are the moisture in the concrete, temperature, reinforcing steel size, spacing, depth and orientation.

1.3.3.1. Moisture and temperature

The moisture content of concrete affects electrical resistivity measurements; therefore, for the same concrete with the same amount of chloride ingress, different resistivities will be measured depending on the degree of saturation of concrete (Neville 1996, Hussain 2011, Ryu et al. 2011, Wang et al. 2014). Since electrical conductivity is greater through a liquid phase compared to a solid phase, the higher the moisture content in the concrete matrix, the lower the SR. To obtain consistent and comparable SR measurements, the moisture content of concrete needs to be relatively similar between distinct specimens. This can be achieved fairly easily in extracted cores by consistently measuring SR after saturating the specimens; however, saturating the bridge decks before collecting SR measurements will seldom be practical. Therefore, a new method for correcting for the effect of moisture content of concrete will need to be developed to ascertain that the SR values measured at different times are comparable, even though moisture contents of the deck might differ in each measurement. Since surface resistivity measurements are

influenced greatly by temperature, all measurements can be normalized to a reference temperature using the Hinrichsen-Rasch law (Hope 1987) which is given by:

$$\rho_2 = \rho_1 * exp\left[2900\left(\frac{1}{T_1} - \frac{1}{T_2}\right)\right] \quad (1.2)$$

where ρ1 is the measured resistivity, ρ2 is the normalized resistivity, T1 (K) is the temperature of the concrete during the measurement, and T2, is the normalized temperature.

1.3.3.2. Reinforcing steel

A number of researchers (Gowers et al. 1999, Weydert et al. 1999, Presuel-Moreno et al. 2009, Sengul 2009, Salehi 2013, Garzon et al. 2014) have shown that electrical resistivity measurements can be affected by the depth, bar size, type, and orientation of steel reinforcement with respect to the probe in the deck. Aforementioned studies showed that the distance from the rebar to the measured location is what most influences the measurements. The size of the rebar caused minimal disturbance in the readings, but the spacing between the rebar was inversely correlated to the margin of error. A separate study performed by Morales (2015) focused on the orientation of the surface resistivity probe when taking measurements and found that the most accurate measurements were made when the probe was oriented perpendicular to the topmost rebar and parallel to the bottommost rebar.

1.4. Chlorides Ingress

1.4.1. Chloride Transport Properties in Concrete

When chloride solutions reach the surface of the concrete, either from exposure to marine environments or de-icing chemicals, the chlorides penetrate through the concrete matrix. Porosity of the concrete plays a significant role in the ingress rate of chlorides because of the connecting pores that provide a path through which chlorides and moisture can move through. Factors that change the porosity of concrete include age, supplementary cementitious materials (SCM), and water content. It is well established that the porosity of concrete decreases as water-to-cement ratio decreases which is beneficial because less permeable concrete is more resistant to the penetration of chloride ions (Mutale 2014).

Transport of chloride solutions occurs mostly through advection, diffusion and electrical migration. In addition, adsorption occurs at the surface of the concrete, however, it takes a very small role in the amount of chloride mass being moved into the concrete, hence it is typically ignored when assessing deterioration of concrete (Lingen 1998). Advection is the movement of the chlorides in concrete with moving water as in the case of wetting-drying action or capillary suction. Diffusion, is the process by which ions pass through the concrete matrix due to a concentration gradient. Electrical migration is the movement of ions under an electrical potential or due to ionic interactions among each other. ASTM C1556 provides a standard for determining the apparent chloride diffusion coefficient of concrete, D_a, which combines all possible chloride ingress mechanisms under a diffusion-type process by fitting chloride profile data to the solution of the Fick's Second Law as given by Equation 1.3 using nonlinear regression analysis:

$$C(x,t) = C_s - (C_s - C_i) \cdot erf\left(\frac{x}{\sqrt{4 \cdot D_a \cdot t}}\right) \quad (1.3)$$

where the chloride concentration, C(x,t), is measured at a depth, x, and exposure time, t, by mass percent. C_s is the surface concertation on concrete, C_i is the initial chloride concentration of the cementitious mixture prior to submersion in the exposure solution, x s the depth below the exposed surface measured in millimeters, D_a is the apparent chloride diffusion coefficient, t is the exposure time in seconds, and erf is the error function. Surface concertation, C_s, and apparent diffusion coefficient, D_a, are obtained through the nonlinear regression analysis (ASTM C1556).

1.4.2. Bound and Free chlorides

When chloride ions travel through the concrete matrix, some ions may become bound physically and chemically to the hydration products of the binder in the concrete. If enough chlorides are present, the free chlorides can eventually reach the surface of the reinforcing steel, and once they reach a certain concentration on the surface, corrosion can initiate. The ability to measure free and bound chloride concentrations, therefore, is crucial in understanding the corrosion risks of a certain structure. Research has been done on quantifying the chloride binding process in ordinary portland cement (OPC) mixtures because this would enhance the ability to predict the duration or service-life of concrete structures exposed to marine environments or de-icing chemicals, as well as find ways to decrease the amount of chlorides reaching the steel surface. According to Neville (1996), from “Properties of Concrete”, the main form of chemical binding of chloride ions is through the reaction of the cement compound tricalcium aluminate, C_3A,

and the formation of Friedel salt. A similar reaction with the cement compound tetracalcium aluminoferrite, C_4AF, results in calcium chloroferrite. From the stoichiometry of these reactions, it can be calculated that one gram of C_3A will consume 0.263 grams of chloride, while one gram of C_4AF will consume 0.146 grams of chlorides. The testing procedures for determining free chlorides are very time consuming and intricate. ASTM C1218 is the most commonly used testing procedure for finding concentrations of water-soluble chlorides which can represent the amount of free chlorides. ASTM C1152 standard provides the acid soluble chloride concentration which is also known to provide the "acid soluble chloride" concentration, which is an indicator of total chlorides. The values are typically shown in chloride percentage by weight of cement. In a study done by Sirivivatnanon et al. (2012), chlorides were tested using both, acid soluble and water soluble methods following ASTM C 1202 and ASTM C1218 respectively. This study concluded that the extractive techniques and level of aggressiveness determine the type and amount of chlorides. It was found that the aggressive solvents and surface area of the materials tested controlled the amount and type of chlorides extracted. The use of boiling water on materials passing an 850 micron sieve offered the most accurate amount of free chloride content. This is important to establish since quantifying chloride content, for either total or free chlorides, is a very delicate procedure. Once the accurate chloride content is determined, the appropriate corrosion mitigation techniques can be made.

1.4.3. De-icing solutions

In environments where freeze-and-thaw (F-T) action is common, DOTs can remove ice off the surface of the concrete by plowing, using de-icers and anti-icers (2004). The DOTs either use anti-icing agents, which lower the freezing point so that when precipitation falls, it does not freeze, or use de-icing chemicals on the roads to decrease the freezing point, melting any ice formed on them, allowing vehicles to drive safely. This practice of applying salts to roads during freezing weather was first implemented in the 1930s (Lord 1988), and since then, numerous types of de-icing chemicals have been developed to provide safe travel conditions. Some of the more common de-icing chemicals used today, based on the FHWA manual of practice for an effective anti-icing program include sodium chloride (NaCl), calcium chloride ($CaCl_2$), and magnesium chloride ($MgCl_2$).

While the use of de-icing chemicals has proven to be effective, these chemicals are harmful to the environment and to the reinforcing steel in concrete structures. Environmental concerns regarding the use of de-icing chemicals, according to Lord, (1988), include drinking water contamination and degradation of habitats surrounding areas where salt accumulates from runoff. These chemicals also have a detrimental effect on structures. The corrosion of structures, specifically bridge decks, has been of high concern for the last few decades. Corrosion occurs when chlorides from de-icing chemicals infiltrate the concrete and reach the steel reinforcement. A study by Conciatori (2008), determined that chloride ingress was controlled mainly by the concentration of the de-icing chemicals the composition of the concrete, due to the density and

permeability of the materials used (Jaegermann 1990, Hong 1999), and by the weather conditions. Weather conditions are vital when analyzing the chloride ingress since cyclic wetting and drying environments promote a faster rate of chloride ingress (Hong 1999, Ji 2009). Hot weather also influences the rate of ingress. A study performed by Yuan (2008), evaluated the temperature effect on migration of chlorides. The results showed that the greater the temperature of the concrete, the greater the diffusion coefficients. They also concluded that the chloride penetration, while influenced by temperature, did not change the chloride profile trends. Once the chlorides build to a critical level corrosion of the reinforcing steel can initiate. Various studies have concluded that concrete, that is saturated with de-icer solutions, undergoing freeze-thaw cycles shows considerable deterioration including mass change, expansion, decrease in dynamic modulus of elasticity, and increase in permeability (Sutter et al. 2008; Cody et al.1994; Cody et al. 1996; Mussato 2004; Kozikowski et al. 2007). These studies concluded that the magnesium chloride ($MgCl_2$) de-icer solution physically and chemically reacted with hardened cement paste at a fast rate and performed poorly in various durability tests when compared to the other de-icing solutions. Interestingly, samples which were saturated with $MgCl_2$ solution did not show significant salt scaling, which was contrary to expectation. These samples showed similar scaling to the specimens saturated with other de-icing solutions.

1.4.4. De-icing Solutions, Chloride Ingress and Electrical Resistivity

It is well known that chlorides, once they reach a critical level, in a concrete matrix break down the passive layer of the reinforcing steel, which can lead to corrosion initiation.

Developing a non-destructive technique that can accurately predict the amount of chlorides available in a concrete structure could provide better insight regarding the deterioration of a structure and a quicker mode of corrosion initiation mitigation. The use of surface resistivity measurements in the last few years has increased in popularity due to its accurate and immediate results. Surface resistivity measurements can provide information about the performance of the concrete over time. Very few researchers have performed studies trying to correlate surface resistivity and chloride ingress. A study done by Morris et al. (2004), investigated a method to determine chloride threshold. The chloride threshold defines the point at which steel reinforcement becomes susceptible to corrosion. Because this limit varies greatly between situations, Morris proposed a relationship between the chloride threshold and concrete resistivity based on the similarities in factors affecting each, such as concrete quality and exposure conditions. To prove this correlation between the chloride threshold and resistivity, corrosion potential and current density were considered along with resistivity and chloride concentration. Four concrete mixtures were considered and samples of these were both immersed in a saline solution and subjected to seashore exposure. Morris observed that the specimens exposed to seashore environment provided resistivity values three times higher than the values observed for the immersed specimens. Resistivity values were also three times greater for the sample with the lowest w/cm ratio (0.40) and greater cement content (400 kg^{-3}) than the standard samples (w/cm ratio of 0.60 and cement content of 300 kg m^{-3}). When considering chloride content and concrete resistivity, they determined that as resistivity increased, the chloride threshold increased as well. It was suggested that lower resistivity values could be explained by a high concentration of free chlorides.

1.5 Freeze-Thaw (F-T) Action

Concrete exposed to F-T action can deteriorate at a rapid rate due to water expansion in the concrete pores. According to the Portland Cement Association (PCA) (Kosmatka et al. 2011), water expands around 9% when frozen. When the water in the concrete matrix freezes, the expansion provides internal tensile forces which cause cracks. These cracks continue to escalate with continuous freezing and thawing action. F-T cycles also cause scaling and spalling on the surface of the concrete. The bond between the aggregate and the paste weakens and causes the aggregates to separate causing "pop-outs". The most effective way to protect concrete from freeze-thaw deterioration is to develop a proper air entrainment system. Air-entraining admixtures provide evenly distributed air voids throughout the concrete matrix to alleviate internal or localized tensile forces that create cracks in the concrete during freeze-thaw cycling. In order to determine if a concrete sample has adequate protection from freeze-thaw action, the standard test method ASTM C666 can be used to test the resistance of concrete to rapid freezing and thawing. This test method can be utilized when the concrete samples undergo rapid freezing and thawing in water, or freezing in air and thawing in water. Regardless of the type of environment in which the samples are placed, they undergo 300 F-T cycles or the number of cycles until the original relative dynamic modulus is reduced below 60%. This test method states that the specimens' mass needs to be recorded and tested for fundamental transverse frequency every 36 cycles. There is a gap in literature for relating SR to freeze-thaw action. One group was able to use electrical resistivity to assess frost damage (Wang et al. 2014, 2015). Wang showed that as temperature decreased, electrical resistivity increased, and as F-T cycles continued, the resistivity continued to increase.

This increase was attributed to frost damage that was progressively resulting in more micro fracturing of the concrete and thus a loss of connectivity within the specimen. Frost damage was also confirmed by the loss of strength and visible cracks on their specimens. No literature specifically regarding SR values with chloride ingress and F-T action was found, which is of great concern since de-icing chemicals are used only in environments in which F-T occurs.

1.6 References

ASTM C597-09 Standard test method for pulse velocity through concrete. (2010). ASTM International, West Conshohocken, PA.

ASTM C666/C666M-15 Standard test method for resistance of concrete to rapid freezing and thawing. (2015). ASTM International, West Conshohocken, PA.

ASTM C1152 Standard test method for acid-soluble chloride in mortar and concrete. (2012). ASTM International, West Conshohocken, PA.

Andrade, C., M. Prieto, P. Tanner, F. Tavares, R. d'Andrea. (2013). "Testing and modelling chloride penetration into concrete." Construction and Building Materials 39: 9-18.

Blackburn, R., D. Amsler, K. Bauer (2004). Snow removal and ice control technology. Sixth International Symposium on Snow Removal and Ice Control Technology, Transportation Research Board of the National Academies, Spokane, WA.

Brencich, A., G. Cassini, D. Pera, G. Riotto (2013). "Calibration and Reliability of the Rebound (Schmidt) Hammer Test." Civil Engineering and Architecture 1(3): 66-78.

Conciatori, D, H. Sadouki, E. Brühwiler. (2008). "Capillary suction and diffusion model for chloride ingress into concrete." Cement and Concrete Research 38(12): 1401-1408.

Garzon, A. J., J. Sanchez, C. Andrade, N. Rebolledo, E. Menéndez, J. Fullea. (2014). "Modification of four point method to measure the concrete electrical resistivity in presence of reinforcing bars." Cement and Concrete Composites 53: 249-257.

Koch, G.H., M. Brongers, N. Thompson, Y. Virmani, J. Payer. (2002). "Corrosion Costs and Preventive Strategies in the United States." FHWA-RD-01-156 (Final Report): 773 pp.

Gowers, K. R., S. G. Millard. (1999). "Measurement of concrete resistivity for assessment of corrosion severity of steel using Wenner technique." ACI Materials Journal 96(5): 536-541.

Gucunski, N., I. Arezoo; F. Romero, S. Zanarian, D. Yuan, H. Wiggenhauser, P. Shokouhi, A. Taffe, D. Kutrubes. (2013). Nondestructive testing to identify concrete bridge deck deterioration. Transportation Research Board. Washington, D.C.

Hong, K. (1999). Cyclic wetting and drying and its effects on chloride ingress in concrete. National Library of Canada, Ottawa, ON.

Hope, B, A. Ip. (1987). "Chloride Corrosion Threshold in Concrete." Materials Journal 84(4): 306-314.

Huang, J., W. Shaowei, J. Chaudhari, S. Soltesz, X. Shi. (2014). Deicer Effect on Concrete Bridge Decks: Practitioners Perspective and a Method of Developing Exposure Maps. Transportation Research Board Annual Meeting: 1-13. Washington, DC.

Hussain, R. R. (2011). "Effect of moisture variation on oxygen consumption rate of corroding steel in chloride contaminated concrete." Cement and Concrete Composites 33(1): 154-161.

Hussain, S., E.,Rasheeduzzafar, A. Almusallam, A. S. Algahtani. (1995). "Factors affecting threshold chloride for reinforcement corrosion in concrete." Cement and Concrete Research 25(7): 1543-1555.

Jackson, L. (2013). "Surface resistivity test evaluation as an Indicator of the Chloride Permeability of Concrete." Tech brief. Publication no. FHWA-HRT-13-024, McLean, VA.

Jaegermann, C. (1990). "Effect of water-cement ratio and curing on chloride penetration into concrete exposed to Mediterranean Sea climate." Materials Journal 87(4): 333-339.

Ji, Y., T. Zan, Y. Yuan. (2009). "Chloride Ion Ingress in Concrete Exposed to a Cyclic Wetting and Drying Environment." American Society of Agricultural and Biological Engineers 52(1): 239-245.

Jianhong, C., B. Dylan, J. Frank, H. Dryver. (2008). Concrete bridge deck condition assessment with automated multisensor techniques. Bridge Maintenance, Safety Management, Health Monitoring and Informatics. Burlington, VT, Taylor & Francis.

Khalim, A. R., D. Sagar, M. D. Kumruzzaman, A. S. M. Z. Hasan. (2011). "Combination of nondestructive evaluations for reliable assessment of bridge deck." Facta universitatis - series: Architecture and Civil Engineering 9(1): 11-22.

Kosmatka, S. H., M. L. Wilson. (2011). "Design and Control of Concrete Mixtures." 15th Edition: 444, Portland Cement Association, Washington, D.C.

Lingen, R. T. (1998). "Concrete in coastal structures." 301. London, U.K., Thomas Telford Limited.

López, W., J. A. González. (1993). "Influence of the degree of pore saturation on the resistivity of concrete and the corrosion rate of steel reinforcement." Cement and Concrete Research 23(2): 368-376.

Lord, B. N. (1988). "Program to reduce deicing chemical usage." Federal Highway Administration: 13 pp., McLean, VA.

Shariati, M., H. Sulong, M. Arabnejad, P. Shafigh, H. Sinaei. (2011). "Assessing the strength of reinforced concrete structures through ultrasonic pulse velocity and Schmidt Rebound Hammer tests." Scientific Research and Essays 6 (1): 213-220.

Morales, M. T. (2015). Experimental investigation of the effects of embedded rebar, cracks, chloride ingress and corrosion on electrical resistivity measurements of reinforced concrete: 174 pp.

Morris, W., A. Vico, M. Vázquez. (2004). "Chloride induced corrosion of reinforcing steel evaluated by concrete resistivity measurements." Electrochimica Acta 49(25): 4447-4453.

Mussato, B. T.,O. K. Gepraegs and G. Farnden (2004). "Relative effects of sodium chloride and magnesium chloride 0n reinforced concrete: state of the art." Transportation research record.(1866): 59-66.

Mutale, L. (2014). An investigation into the relationship between surface concrete resistivity and chloride conductivity tests: 105 pp.

Neville, A. M. (1996). Properties of Concrete: Fourth Edition. 844. Hoboken, NJ, Wiley.

Presuel-Moreno, F., Y. Liu, M. Paredes (2009). Understanding The Effect Of Rebar Presence And/Or Multilayered Concrete Resistivity On The Apparent Surface Resistivity Measured Via The Four-Point Wenner Method. Corrosion Conference 2009. Atlanta, GA, NACE International.

Qiang, Y., A. Katrien, S. Caijun, S. Geert De. (2008). Effect of temperature on transport of chloride ions in concrete. Concrete Repair, Rehabilitation and Retrofitting II, CRC Press: 159-160.

Rupnow, T., I. Patrick. (2011). Evaluation of surface resistivity measurements as an alternative to the rapid chloride permeability test for quality assurance and acceptance. Louisiana Transportation Research Center: 68 pp.

Ryu, D,W. Ko, T. Noguchi. (2011). "Effects of simulated environmental conditions on the internal relative humidity and relative moisture content distribution of exposed concrete." Cement and Concrete Composites 33(1): 142-153.

Sadowski, L. (2013). "Methodology for assessing the probabilty of corrosion in concrete structures on the basis of half-cell potential and concrete resistivity measurements." Scientific World Journal. 2013: 8. Article ID 714501.

Salehi, M. (2013). Numerical investigation of the effects of cracking and embedded reinforcement on surface concrete resistivity measurements using Wenner probe. Civil and Environmental Engineering. Ottawa, ON, Carleton University. Master of Applied Science in Civil Engineering: 155 pp.

Sengul, O. G., E. Odd. (2009). "Effect of Embedded Steel on Electrical Resistivity Measurements on Concrete Structures." 106 (1): 11-18.

Sirivivatnanon, V., W. A. Thomas, K. Waye. (2012). Determination of free chlorides in aggregates and concrete. Australian Journal of Structural Engineering. 151-158.

Song, H. W., V. Saraswathy. (2007). "Corrosion monitoring of reinforced concrete structures - A review." International Journal of Electrochemical Scienc. 2(1): 1-28.

Swanstrom, J., T. Rogers, G. Bowling, S. Tuttle (2013). ODOT bridge inspection program manual 2013. Oregon Department of Transportation: 1-381, OR.

Wang, Z., Q. Zeng, L. Wang, Y. Yao, K. Li. (2014). "Effect of moisture content on freeze–thaw behavior of cement paste by electrical resistance measurements." Journal of Materials Science. 49(12): 4305-4314.

Weydert, R., C. Gehlen. (1999). "Electrolytic resistivity of cover concrete: Relevance, measurement and interpretation." Proceedings of the 8th International Conference on Durability of Building Materials and Components. 409-419. NRC Research Press, Vancouver, Canada.

Wang, Q. Z., L. Wang, Y. Yao, K. Li. (2015). "Electrical resistivity of cement pastes undergoing cyclic freeze-thaw action." Journal of Materials in Civil Engineering. 27(1).

2 First Manuscript

Evaluation of the Effect of Chloride Ingress in Reinforced Concrete on Surface Resistivity Measurements

David Esteban Rodriguez Matiz, Vahid J. Azad, David Trejo,

Jason H. Ideker, O. Burkan Isgor

Abstract: It would be beneficial to measure the chloride ingress in concrete bridge decks resulting from application of de-icing chemicals or exposure to marine environments directly from the surface without the need to extract cores. It is in this context that the current investigation was carried out with the primary objective of investigating the potential for surface resistivity (SR) to be used as a non-destructive evaluation tool to assess the deterioration of concrete due to chloride ingress. In this study, surface resistivity measurements were taken using a four-point Wenner probe at various locations on reinforced slabs that were saturated with magnesium chloride based de-icing solution which contained a corrosion inhibitor. Chloride profiles were taken to monitor the ingress of chlorides. SR values decreased for the chloride-saturated concrete after concrete matured, while SR measurements for water-saturated concrete did not change significantly. This indicates that SR measurements may be used to identify chloride ingress. An increase in free chloride concentrations, which are known to initiate corrosion, are likely a cause of the decrease in surface resistivity measurements. This observation was also confirmed by thermodynamic modeling; however, it is recommended that this be further studied in future investigations.

2.1. Introduction

Corrosion of the steel in reinforced concrete (RC) bridge decks is an important issue for structures that are exposed to chloride-containing de-icing chemicals or marine salts. Once the amount of chloride at the steel reinforcement reaches a critical level, corrosion is likely to initiate. Pre-emptive actions that can prevent corrosion initiation are generally more cost effective than repair or replacement of bridge decks that have already experienced corrosion. An obvious indicator of a corrosion problem is visible damage; unfortunately, if corrosion damage is visible, the window for preventive action is likely closed.

Most departments of transportation (DOT) in the United States use chloride depth profiling on occasion to provide quantitative insight into the corrosion risk of bridge elements, but the method is time consuming and relatively expensive. Chloride profiling is also not practical for routine monitoring of bridge decks with current limited DOT resources. Other measurement technologies are at various stages of maturity and may be useful either by themselves or when used in combination with other technologies. Whatever measures are used, values need to be turned into predictions about time to corrosion damage and when to apply these pre-emptive actions. Much valuable research is already available on detection technologies and models to predict corrosion are available.

In recent years, electrical resistivity of concrete has emerged as a durability-related quantitative performance indicator (Alonso et al. 1988). Several investigations have

shown the existence of relationships between electrical resistivity and other durability-related parameters such as corrosion rate of steel reinforcement and transport properties of concrete. López et al. (1993) and Gowers et al. (1999) reported that concrete resistivity and corrosion rate are inversely proportional over a wide range of concrete resistivity values. The literature also shows that concrete resistivity is strongly affected by the concrete characteristics, the degree of concrete pore saturation, and the chloride concentration (Hussain et al. 1995, Morris et al. 2004, Song et al. 2007). Low resistivity values are associated with high water-to-cement ratio and/or high moisture contents (Neville 1981, Morris et al. 2004).

Lately, surface resistivity (SR) measurements of concrete cores have been replacing the widely-used Rapid Chloride Permeability Test (RCPT) because both tests provide a measure of resistance of concrete to ionic movement under an applied electrical potential difference. In most cases, RCPT and SR measurements have good correlation (Rupnow 2011, Hooton et al. 2012, Jackson 2013); While RCPT takes many hours to complete, SR measurements can be taken in seconds. Several researchers have also shown in studies on cores extracted from RC structures and laboratory-produced cylinders that SR measurements are also well correlated with water permeability (Kessler et al. 2005) and the bulk chloride diffusion coefficient of concrete (Hamilton et al. 2007, Sengul et al. 2008).

All these developments have led to increased efforts to standardize SR measurement procedures (AASHTO TP 095-11-UL; CAN/CSA A23.2 2009; ASTM WK37880). A number of jurisdictions even started requiring resistivity measurements as part of ongoing

construction and maintenance procedures (FM 5-578 2004; MTO LS-444 2013). Consequently, a number of companies producing SR measurement devices have been increasing, while the cost of units for SR measurements has been declining.

The electrical resistivity of concrete can be measured in a number of ways; however, the four-point Wenner probe technique (ASTM 2014) is the most commonly used approach for field applications because of its speed, simplicity, and practicality. It can be used to measure resistivity of concrete cores extracted from concrete structures, but it can also be used directly on concrete surfaces without the need of coring or without the need for access to the steel reinforcement (as in the case of half-cell potential measurements). In all cases, measurements are made in seconds. It has been shown by a number of researchers (Gowers et al. 1999, Weydert et al. 1999, Presuel-Moreno et al. 2009, Sengul et al. 2009, Salehi 2013) that SR measurements can be affected by the density, depth, diameter, type, and orientation of steel reinforcement (with respect to the probe) in the deck. The use of SR data as a quantitative decision-making aid for selecting treatment options and timing for bridge decks require correction of the measurements to minimize the reinforcement effect. A recent study by Morales (2015) provided a detailed literature review on these factors and outlined instructions to minimize the errors associated with them. This will assist in allowing SR data to be used for realistic condition assessment of reinforced concrete bridge decks.

The ability to measure the chloride ingress on concrete bridge from the surface without the need to extract cores could be extremely beneficial. If this can be accomplished, large surfaces could be mapped over relatively short durations with resistivity measurements. If

a routine, quantitative methodology based on SR measurements can be coupled with time-to-damage predictions, DOTs will reduce the subjectivity and costs that are associated with the selection and timing of the treatments of bridge decks to protect them from de-icing chemicals. Although SR measurements do not provide the actual chloride depth profile of the deck, the resistivity measurements coupled with time-to-damage predictions could indicate if chloride profiling is necessary, and if so, at which locations on the deck it should be conducted. DOTs will not have to spend valuable resources and time on excessive and unnecessary chloride profiling and will minimize the risk of not conducting chloride profiling at critical areas of the bridge decks. Overall subjectivity of the current practices can be replaced with quantitative and repeatable protocols.

Although SR measurements have been correlated with transport properties of concrete (Kessler et al. 2005, Hamilton et al. 2007, Sengul et al. 2008), they do not provide a measurement of the amount of chlorides present nor do they provide a chloride profile through the depth of the concrete. However, transport properties that are revealed by SR measurements may be used in chloride ingress models that can then be used to predict chloride profiles in concrete. The accuracy of the predictions will improve with additional quantitative data such as environmental history (temperature, relative humidity, and precipitation) and amount of salt exposure. Some of this additional quantitative data are readily available, but further data is needed to fully develop predictive models for chloride ingress. These predictions, coupled with SR data, may also indicate if additional chloride profiling is necessary and, if so, at which locations the testing should be conducted. It is in these contexts that the current investigation was

carried out with the primary objective of investigating the potential for surface resistivity to be used as a non-destructive evaluation tool to assess the deterioration of reinforced concrete due to chloride ingress.

2.2. Experimental Procedure

2.2.1. General

The experimental study involved continuous monitoring of surface resistivity measurements, temperature, relative humidity and chloride ingress of reinforced concrete slabs that were cast at the Oregon State University Outdoor Exposure Site. The slabs were designed to represent bridge decks commonly used by Oregon Department of Transportation (ODOT) in Oregon from 1960s to present. Based on concrete mixture properties from three different periods, twenty slabs were cast and investigated. Slab Type 1 (ST1), composed of twelve air-entrained slabs designed per 1960s specifications, Slab Type 2 (ST2) consisted of three non-air-entrained slabs designed per 1960s specifications, Slab Type 3 (ST3) were two air-entrained slabs designed per 1990s specifications and slab Type 4 (ST4) consisted of three air-entrained slabs designed per current specifications.

2.2.2. Materials

2.2.2.1. Concrete

The concrete mixtures were ordered from a local ready-mix concrete plant. The six concrete mixtures were used to construct six different slab types that are representative of Oregon bridge decks that have been built within the past six decades. The mixture

proportions for each concrete type are included in Table 2.1. Slab Type 1 (ST1) contained a Type I/II ordinary portland cement (OPC) concrete mixture with no supplementary cementitious materials (SCMs) as per 1960s specifications. It should be noted that 1960s specifications did not specify w/cm but define the mixture using specified workability requirements. A range of w/cm values (ST1-A, ST1-B, ST1-C) were investigated for concrete of this era and are depicted in Table 2.1. Slab Type 2 (ST2) was also cast with the same OPC as the ST1 specimens but without air entrainment; these slabs represent non-air-entrained bridge decks from the 1960s. Slab Type 3 (ST3) represents bridges from the 1990s; this concrete mixture is an air-entrained concrete with 20% Class F fly ash replacement. Slab Type 4 (ST4) represent modern air-entrained high performance mixture which contained 30% Class F fly ash and 4% silica fume. The chemical compositions of OPC, fly ash and silica fume used in this study are provided in the Appendix. The coarse aggregate used was rounded river rock with a gradation that ranged from 3/4-inch (1.91 cm) to 0.187 inches (.475 cm). The fine aggregate used was natural sand with a fineness modulus of 3.02 and a gradation that ranged from 0.187 inches (.475 cm) to 0.0059 inches (0.0149 cm). Detailed information on the gradation of the coarse and fine aggregates are found in the Appendix.

Fifteen 4-inch by 8-inch (10.16 cm by 20.32 cm) cylinders were cast from each one of the different mixture types. These cylinders were used for additional mechanical property and performance testing. The slabs and the cylinders were each cured under wet burlap for 28 days after casting. Compressive strength testing according to ASTM C39 was performed at 28 and 90 days.

Table 2.1 - Fresh properties and six concrete mixture designs used in this study.

	ST1-A	ST1-B	ST1-C	ST2	ST3	ST4
w/cm ratio	0.60	0.40	0.47	0.53	0.35	0.43
Measured slump, in. (cm)	9.5 (24.1)	1.25 (3.2)	6.25 (15.9)	5.5 (14.0)	3.25 (8.3)	3.5 (8.9)
Measured air (%)	9	3.25	5	1	3	2.5
Measured unit Weight, lb/ft^3 (kg/m^3).	132.1 (2116.0)	145.9 (2337.1)	142.16 (2277.2)	148 (2370.7)	147.52 (2363.0)	145.88 (2336.8)
Cement, lbs. (kg)	525 (238.1)	528 (239.5)	512 (232.2)	515 (233.6)	510 (231.3)	461 (209.1)
Flyash, lbs. (kg)	0	0	0	0	129 (58.5)	204 (92.5)
Silica Fume, lbs. (kg)	0	0	0	0	0	25 (11.3)
Water, lbs. (kg)	317 (143.8)	209 (94.8)	240 (108.9)	275 (124.7)	222 (100.7)	300 (136.1)
3/4" - No.4, lbs. (19.1mm – 4.76mm (kg)	1693 (767.9)	1688 (765.7)	1690 (766.6)	1693 (767.9)	1753 (795.1)	1714 (777.5)
Sand, lbs. (kg)	1133 (513.9)	1456 (660.4)	1196 (542.5)	1401 (635.5)	1306 (592.4)	617 (279.9)
Total, lbs. (kg)	3668 (1663.8)	3881 (1760.4)	3638 (1750.2)	3884 (1761.8)	3920 (1778.1)	3321 (1506.4)

2.2.2.2. Reinforcement

All slabs were reinforced with #5 (5/8 in, 16 mm) ASTM A615 carbon steel rebar. Historical data on bridge decks show that most decks in Oregon are reinforced with #5 (5/8 in., 16 mm) rebar. Although #4 rebar is also common, previous studies showed that resistivity measurements are not affected by the difference between these two bar sizes (Salehi 2013); therefore, for consistency #5 (5/8 in., 16mm) bars were used. In this

research, as shown in Figure 2~~Figure 2~~.1, an unreinforced zone was left in each slab for the extraction of cores to be used in bulk resistivity measurements, mechanical testing, and moisture content determination. Most slabs were reinforced with orthogonal rebar with 8-inch (20.3 cm) center-to-center spacing. Two slabs with 4-inch (10.16 cm) rebar center-to-center spacing were used to verify the results of a parallel investigation. The slabs in this study had either 1-inch (2.54 cm) or 2.5-inch (6.35 cm) concrete cover thickness. Historical data shows that a large number of bridge decks in Oregon have 1-inch (2.54 cm) to 2.5-inch (6.35 cm) concrete covers, and some of these bridge decks are exposed to de-icing chemicals. Therefore, slabs with both a 1-inch (2.54 cm) and 2.5-inch (6.35 cm) cover thickness were investigated. Figure 2~~Figure 2~~.1a and 2b show typical slab dimensions and positioning of the reinforcement.

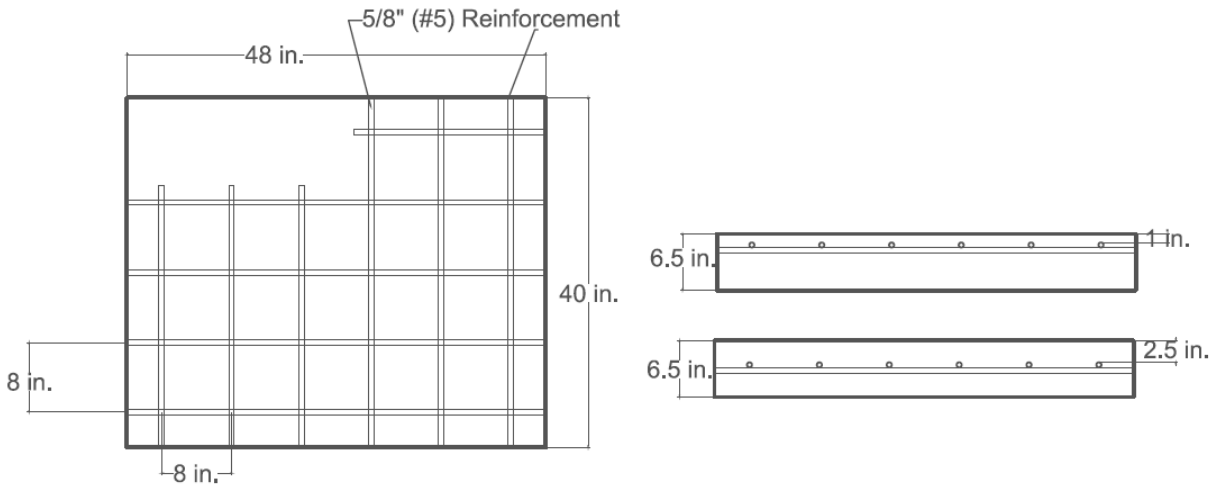

(a)

(b) (c)

Figure 2.1 – (a) Geometrical details of the concrete slabs; (b) a sample slab with placed reinforcement before casting of concrete; (c) a sample concrete slab during ponding with the deicing solution. The section that is unreinforced was used to take measurements and to extract cores for additional testing.

2.2.3. Exposure Regime

2.2.3.1. Ponding cycles

After 28 days of wet curing, the slabs were exposed to commercially available 30% magnesium chloride ($MgCl_2$) deicing solution that contained a corrosion inhibitor in alternating wet/dry cycles to increase chloride ingress rates (see Figure 2.1c). This is the same deicing solution used by ODOT. The composition and type of the corrosion inhibitor are not disclosed by the supplier; therefore the inhibitor type is not reported here. In each cycle, the slabs were ponded with the deicing solution for 96 hours. After 96 hours, the deicing solution was removed by vacuum, then the slabs were exposed to ambient conditions for a 10-day period. The duration of each cycle was decided based on the needs of the project in addition to previous studies that showed this cycling approach increased chloride ion ingress but still remained reasonable compared to field exposure (Hong 1999). After 7 cycles it was determined that chloride ingress was occurring at a

higher rate than expected. Control slabs, one for each type of concrete, also had the same ponding regime. However these slabs were ponded with tap water instead of the de-icing solution. The cycles were postponed for ten weeks after the 7 cycles. During this time the slabs were exposed to the ambient conditions without ponding. After this period, the slabs were exposed to the deicing solution once again continuing the ponding regime.

2.2.3.2. Internal and atmospheric conditions

In-situ Wagner Rapid RH® probes were installed at various depths inside the slabs. These probes measure temperature and relative humidity inside the concrete and data were provided at the time that SR measurements were taken. All control slabs and one slab for each type of concrete had probes thus resulting in 12 slabs having probes. The probes were installed at 1 inch (2.54 cm) and 2.5-inches (6.35 cm) from the surface of the slabs. The depths of the probes were chosen based on practicality. At 1 inch (2.54 cm), it decreased the chance of cracks near the surface and at 2.5-inches (6.35 cm) it provided information regarding the change in temperature and relative humidity with depth compared to the one inch probe. Surface temperature was measured with an infrared temperature gun. In addition to these measurements, a weather station continuously collected weather data onsite. This included relative humidity, wind speed, wind direction, precipitation, barometric pressure, etc. This data was used to calibrate measurements and provide additional information for the companion modeling study.

2.2.4. Testing Methods

The concrete slabs, cylinders, and cores that were extracted from the unreinforced zone of the slabs went through various tests throughout the duration of the project. The tests that were performed on concrete slabs, cylinders, and cores are described in the following sections.

2.2.4.1. Mechanical Testing

Compressive strength of cylindrical concrete specimens was measured after 28 days and 90 days following ASTM C39.

2.2.4.2. Moisture Content

Moisture content of concrete cores were determined from select slabs at select times by taking cores with a handheld core drill and oven drying the cores to determine the free water content inside the concrete matrix. In addition, a side study was performed on wet coring to determine if dry coring to affects the water content when using a coring drill. Six cores 3-inches (7.62 cm) in diameter were taken from a concrete slab; three cores were dry cored and three were wet cored. The samples were then cut in sections of two inches (5.08cm) each to establish a moisture content in relation with depth. The wet samples were surface dried and the mass was recorded for all the samples taken. The samples were then placed in an oven at 230° Fahrenheit (110 °C) for 24 hours and the mass was recorded once again. The evaporable moisture content of the concrete samples was then determined. Once the study was completed, cores were taken from each type of concrete in two different occasions to determine the evaporable moisture content of the

concrete slabs. Cylinders that were cast with the slabs were also tested for moisture content. Three cylinders from each type of concrete were placed in a fog room the mass did not increase. Once the cylinders were fully saturated, they were placed in an oven at 230° Fahrenheit (110 °C) for 24 hours and the mass was recorded once again. The evaporable moisture content of the concrete samples was then determined.

2.2.4.3. Chloride Profiling

Chloride profiling was performed on each slab at various ages using a field profile grinder. There were nine possible chloride profiling sites on each slab due to the location of rebar and the unreinforced zone. Collected powders were analyzed for acid soluble and water soluble chloride content following ASTM C1152 and ASTM C1218 respectively and profiles were generated for determination of chloride transport properties per ASTM C1556. After each chloride profile was taken, the area where the grinding occurred was sealed with a commercial self-consolidating, shrinkage-compensating concrete repair material that is also used by ODOT.

2.2.4.4. Surface Resistivity Measurements

SR measurements were taken using a four-point Wenner probe at two locations on the slab surface. Five readings were taken on the unreinforced section of the slabs and five readings were taken on the reinforced section. The median value was taken for each set of measurements as suggested by the RILEM TC-154 (Andrade et al. 2004). When taking SR measurements in sections where rebar was present, the probe was oriented

perpendicular to the topmost rebar and parallel to the bottommost rebar. The orientation of the probe and procedure was decided following the study performed on probe orientation (Morales 2015). Because these measurements were rapid, they were performed weekly or bi-weekly, depending on the ponding cycles, they were taken when chloride profiles were performed and they were taken half way through the dry period of the ponding cycle for consistency.

2.3. Experimental Results and Discussion

2.3.1. Compressive Strength

Compressive strength of cylindrical concrete specimens was measured after 28 days and 90 days following ASTM C39. Table 2.2 shows the compressive strengths of the six types of concrete used in this study.

Table 2.2 - Compressive strengths of the six types of concrete at 28 days and 90 days.

	ST1-A	ST1-B	ST1-C	ST2	ST3	ST4
28 Day, MPa (psi)	12.3 (1784.0)	24.4 (3539.0)	20.9 (3031.3)	28.3 (4104.6)	27.8 (4032.0)	24.6 (3567.9)
90 Day, MPa (psi)	17.1 (2480.1)	27.5 (3988.5)	28.3 (4104.6)	37.3 (5409.9)	34.0 (4931.3)	33.1 (4800.7)

Overall, the compressive strengths of all the mixtures were lower than the design strengths. A reason for this can be attributed to the temperature at the time of casting which was 45°F (7.2°C) and the temperature fluctuated at around 45°F (7.2°C) by $\pm$ 10°F (5.5°C) over their wet curing time since the slabs were cast outside. ST2 mixture had the highest compressive strength, even though its w/cm was 0.53 for ST2 and it did not contain any SCMs, which can be attributed to the fact that it contained no air-

entrainment. The slabs with SCMs (ST3 and ST4) had greater compressive strengths than the ST1 mixtures that only contained OPC. Although ST4 was expected to have a higher strength than ST3 due to the addition of silica fume and fly ash, ST3 had a lower w/cm than ST4 (0.35 vs. 0.43), which controlled the strength.

2.3.2. Moisture Content

The evaporable moisture content of the concrete was determined first by using a wet core and a dry core to determine the effect that an outside water source has on the internal moisture of the samples. Table 2.3 shows the moisture content of samples cored with a wet and dry coring drill.

Table 2.3 - Comparison of moisture content using a wet coring drill and a dry coring drill.

	Moisture Content (%)	
	Dry Cores	**Wet Cores**
1A 0-2" (0-5.1 cm)	5.6	5.5
1B 2-4” (5.1 – 10.2 cm)	5.6	5.6
1C 4-6" (10.2 – 15.2 cm)	5.0	5.9
Average	5.4	5.7
2A 0-2" (0-5.1 cm)	5.2	5.6
2B 2-4” (5.1 – 10.2 cm)	5.3	5.5
2C 4-6" (10.2 – 15.2 cm)	5.3	5.8
Average	5.3	5.6
3A 0-2" (0-5.1 cm)	5.4	5.9
3B 2-4” (5.1 – 10.2 cm)	5.2	5.7
3C 4-6" (10.2 – 15.2 cm)	-	5.8
Average	5.3	5.8

It can be observed from Table 2.3 that the core extraction techniques did not significantly affect the moisture content of concrete significantly. The moisture content of the samples

remained 5 to 6% regardless of the depth or the extraction method used. The difference between the two methods was negligible and it was determined that wet coring, being the most practical method, was an accurate and acceptable technique to use on the concrete slabs. Therefore, subsequent cores were taken from each type of concrete after five ponding cycles and after 14 ponding cycles using the wet coring method. The moisture contents of these cores are reported in Table 2.4.

Table 2.4 - Moisture content taken from extracted cores corresponding to each type of concrete that underwent 5 and 14 de-icing solution ponding cycles.

	Moisture content (%)	
	After 5 Cycles	**After 14 Cycles**
ST1-A	8.2	6.5
ST1-B	7.1	5.4
ST1-C	7.3	5.0
ST2	7.5	5.4
ST3	6.0	4.3
ST4	6.8	4.9

The water-to-cement ratio plays an important role in the porosity and transport properties of the concrete and this can be seen in Table 2.4, which shows the moisture content from six different types of concrete. The moisture of the concrete after five ponding cycles decreased in order of w/cm for all cases except for ST4, the modern high performance concrete, which had the second lowest moisture content. ST1-A having a w/cm of 0.6, had the highest moisture at 8.2% and ST3, having a w/cm of 0.35, had the lowest at 6.0%. While the moisture content did decrease with decreasing w/cm, the difference between all the moistures of ST1 and ST2, which only contained OPC, is negligible. However, there is a clear difference when comparing the OPC mixtures with the mixtures

containing SCMs, which show that the use of SCMs provide a less porous concrete matrix. The moisture of the concrete decreased in all cases as the concrete slabs continued to undergo cycling ponding, After 14 ponding cycles, the ST1-A specimen still contained the highest amount of moisture, and ST3 had the least amount of moisture, 6.5% and 4.9% respectively. The decrease of moisture is attributed partly to the continuing microstructure formation, high increasing ambient temperatures (owing to seasonal change) and the presence of Magnesium Chloride which absorbs water into its structure.

Chloride Profiles

Chloride profiles were taken periodically throughout the 14 ponding cycles. Figure 2.2 shows the total chloride ingress for all six types of concrete at the end of the 14 ponding cycle regime. From Figure 2.2, it is clear how important of a role the w/cm and porosity have on chloride ingress. From the experiments, it is evident that the higher the w/cm, the greater the chloride ingress. This can be supported by various studies which prove that a decrease in w/cm increases resistance to chloride penetration. A study done by Jaegermann (1990) concluded that the porosity inside the concrete is mainly governed by the w/cm, hence the effect of the w/cm on the amount of chlorides.

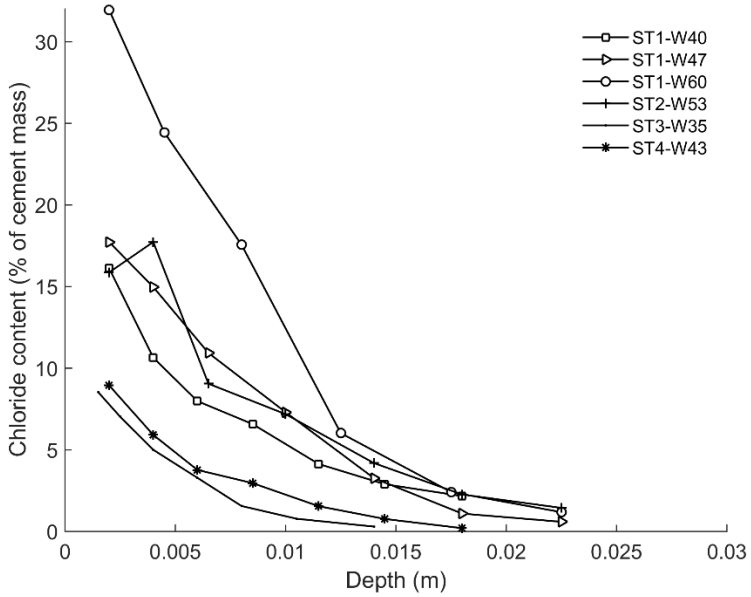

Figure 2.2 – Total chloride profiles are shown on the six types of concrete after 14 ponding cycles. ST1-W40 had a w/c ratio of 0.40, ST1-W47 had a w/c ratio of 0.47, ST1-W60 had a w/c ratio of 0.60, ST2-W53 had a w/c ratio of 0.53, ST3 had a w/c ratio of 0.35 and ST4 had a w/c ratio of 0.43

Two types of concrete mixtures in this study contained SCMs. ST3 contained 20% replacement of cement with fly ash and ST4 contained 4% and 30% of silica fume and fly ash, respectively. From Figure 2.2, it is clear that both ST3 and ST4 have a lower chloride contents than all mixtures which contained only ordinary portland cement (ST1). The use of SCMs helped densify the concrete matrix by filling the voids in between the cement particles, increasing the resistance against penetrating chlorides. In this study, all the concrete slabs were air entrained except for ST2. From Figure 2.2, it can be noted that ST2 had a similar chloride profile as ST1-W47. ST2 had the highest unit weight out of all the concrete mixture because it contained no air entrainment, which could provide a greater resistance to chloride ingress. However, the high w/cm ration may increase porosity which provides space for chlorides to travel through. Chloride profiles were

taken periodically throughout the 14 ponding cycles to have a better understanding of the migration of chlorides through the concrete matrix and can be seen in Figure 2.3 (a-f).

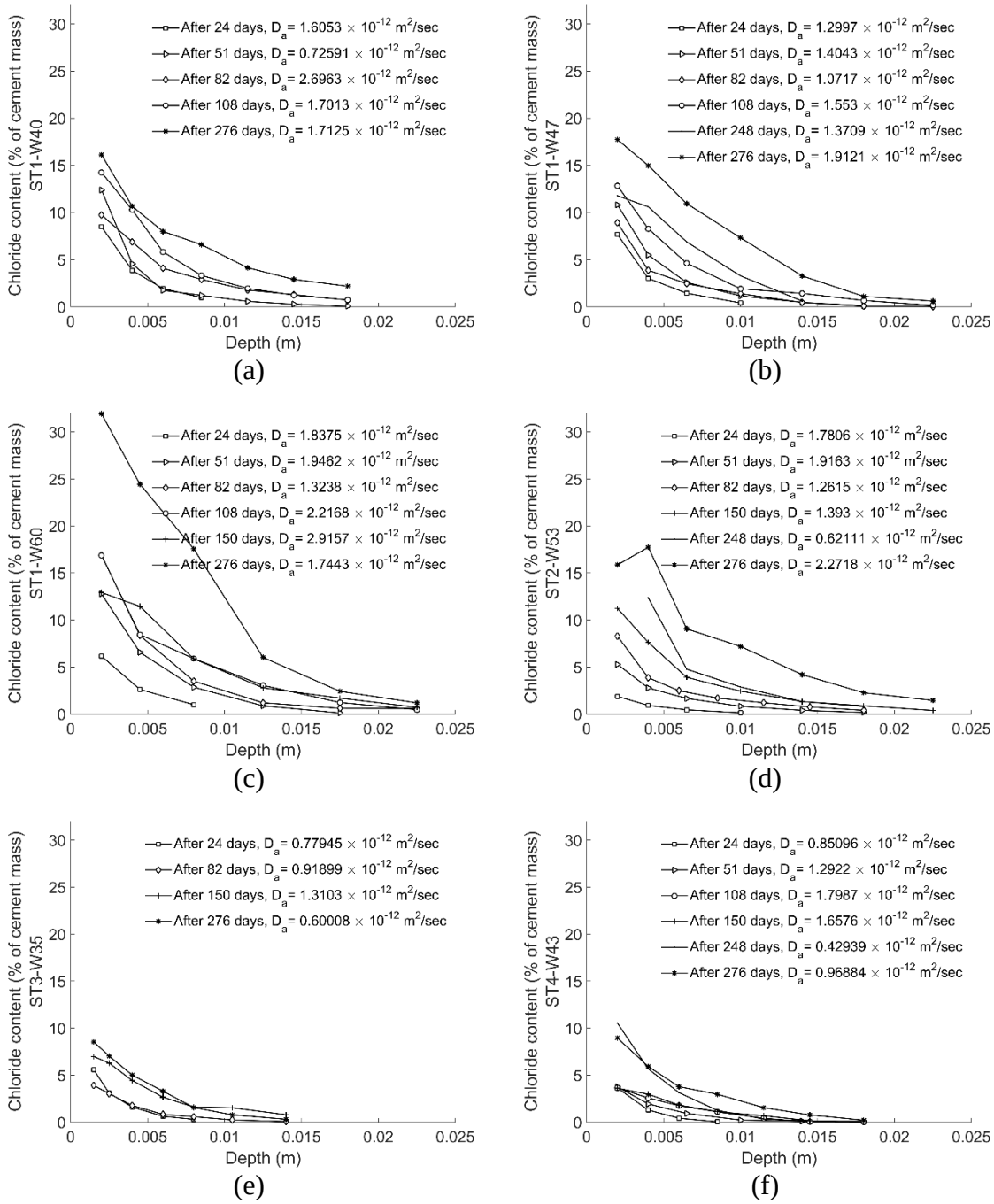

Figure 2.3 - Chloride concentrations by weight of cement throughout 276 days of cyclic ponding with their respective apparent diffusion coefficients. (a) is ST1 with w/c ratio of 0.40, (b) is ST1 with w/c ratio of 0.47, (c) is ST1 with w/c ratio of 0.60, (d) is ST2 with w/c ratio of 0.53, (e) is ST3 with w/c ratio of 0.35 and (f) is ST4 with w/c ratio of 0.43.

It is evident that all the ST1 (a,b and c) mixtures had a lower resistance to chloride penetration and ST3 and ST4, as expected, due to the addition of SCM's, are more resistant to chloride penetration. After 24 days from ponding initiation, or 2 ponding cycles, the chlorides of all ST1 had already reached at least a concentration of total chlorides greater than 6% by weight of cement at 2 mm, and went on to reach a maximum of 32% by the end of the 14th cycle indicating high transport of chlorides of the concrete mixtures containing no SCMs. Figure 2.3c shows the type of concrete with the greatest amount of acid soluble chlorides in the system, which happens to be the concrete with the highest w/cm and the highest air content at 9%. When performing routine ponding of the slabs, surface cracking began showing on this type of concrete. The cracks presented themselves during the summer months. The combination or high temperatures, low relative humidity, high porosity and chlorides present attributed to these cracks which created a direct path for chlorides to enter. The high ingress of chlorides for these slabs is evident in the figure. A fluctuation can be seen in some of the profiles in Figure 2.3 (b and d). The specimens show a lower concentration of chlorides closer to the surface. Martin-Perez (Martin-Perez 1999) explains this fluctuation as a result of when the concrete surface is wet, capillary suction occurs and pulls chlorides into the pore structure, and when the slabs are going through the dry period of the cycle, the water evaporates leaving the chloride ions in the concrete matrix leaving the maximum concentration of chlorides a few millimeters from the surface of the concrete. Figure 2.3e and 4f show a relatively higher resistance to chloride ingress. Neither of the two concrete mixtures, which contained SCMs, got near the surface of the reinforcement which was embedded at 1 (2.54cm) and 2.5-inches (6.35cm). If the concentration of chlorides that

reach the surface of the reinforcement is high enough to disturb the passive layer, corrosion will initiate. This total chloride threshold can range from 0.2 to 0.6% by mass of cement. Figure 2.3a, c and d show that after 14 ponding cycles, the total chloride profiles may have exceeded this threshold, suggesting corrosion initiation. However, it is widely reported that only free chlorides can cause corrosion initiation and it is recognized by the ACI 222 committee. Due to the low amount of powders collected from profile grinding, there is limited data available on free chlorides, however, Figure 2.4 shows the free and bound chloride concentration at 0.394 in. (10 mm) over time.

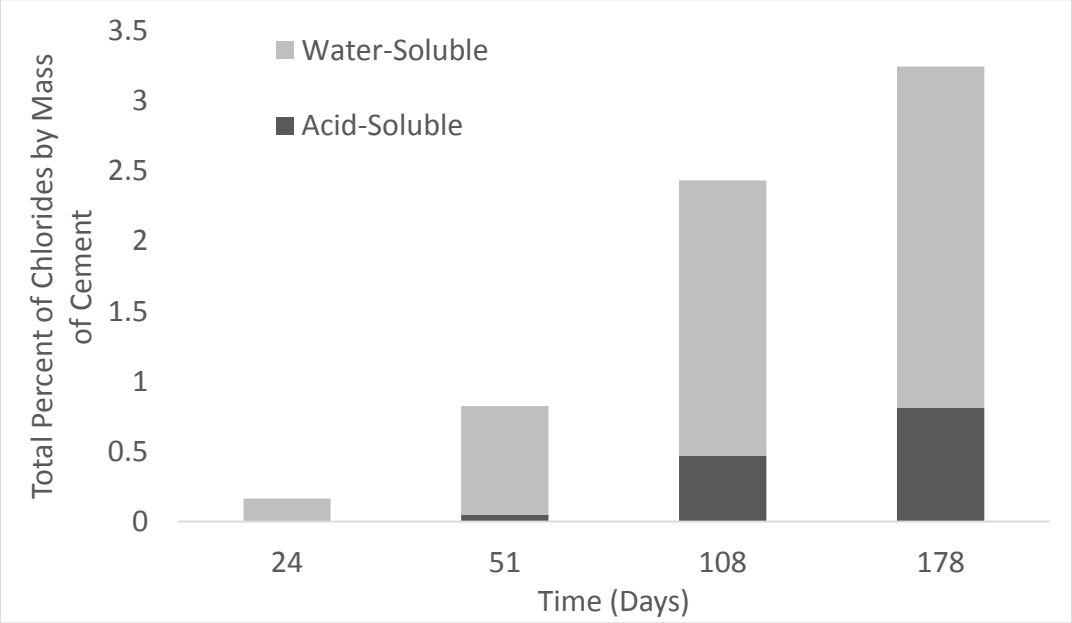

Figure 2.4 - Free and bound chloride concentration of ST2 at 10 mm in depth over time.

The concentration of total chlorides shown in Figure 2.4 increases over time at 0.394 inch (10 mm) depth. In the first 24 days of cyclic ponding, all the chlorides at this depth were free chlorides. Over time, the amount of bound chlorides increased, however, this increase was minimal compared to the amount of free chlorides that were retained at this

depth. Nevertheless, by 178 days, 25% of the total chlorides were bound chlorides. It is expected that the amount of bound chlorides will continue to increase over time, while the amount of free chlorides also continues to increase, however, once the concrete matrix cannot bind more chlorides, the amount of bound chlorides will plateau or decrease.

2.3.3. Internal and Atmospheric Conditions

Because the concrete slabs were placed at an outdoor exposure site, they endured various temperature and relative humidity ranges over the duration of the study, which played a key role in the development of concrete setting and chloride ingress so temperature and relative humidity were monitored both at the exposure site and within the concrete slabs. Figure 2.5 and 2.6 show the temperature and relative humidity changes that the de-icer-ponded concrete slabs went through, respectively. The internal, surface and air temperature can be seen in Figure 2.5 for all types of slabs. The increase and decrease in temperatures are due to the change in seasons. The internal and surface temperatures seem to follow a trend of being greater than the air temperature even at the hottest days of the year. This is due to the microstructure of concrete. It is important to identify this increase in temperature, especially internally since it affects the chloride diffusion coefficients. A study performed by Qiang et al. (2008) looked into the effect of temperature transport of chlorides in concrete and the study concluded that an increase in temperature results in a higher diffusion coefficient. According to this study, the temperatures do not affect the chloride profile trends, but the surface chloride concentration and diffusion coefficients are affected by the temperature change.

Additional information can be drawn from the relative humidity in Figure 2.6. Since the concrete slabs were relatively new when the ponding of de-icing solution began, the slabs had an internal relative humidity near 100%. The figures show a decrease of relative humidity over time, and correlates with the decrease in moisture content measured from core samples. The decrease in internal moisture and relative humidity is due to the hydration process of the concrete and the decrease of relative humidity in the air. The concrete type that contained no air entrainment had the smallest change in relative humidity. Since the concrete has no air-entrainment, the passage way for water vapor to move is very limited so the rate in which the relative humidity decreases is expected to be less than the rest of the concrete slabs.

Figure 2.7shows the relative humidity of the concrete slabs that underwent cyclic water ponding. It is interesting to note that all six slabs, regardless of the type of concrete, continued to have a relative humidity that was close to 100% during the entire study. During the time that ponding stopped for 10 weeks, the relative humidity began to decrease and once the ponding continued, the relative humidity increased once again.

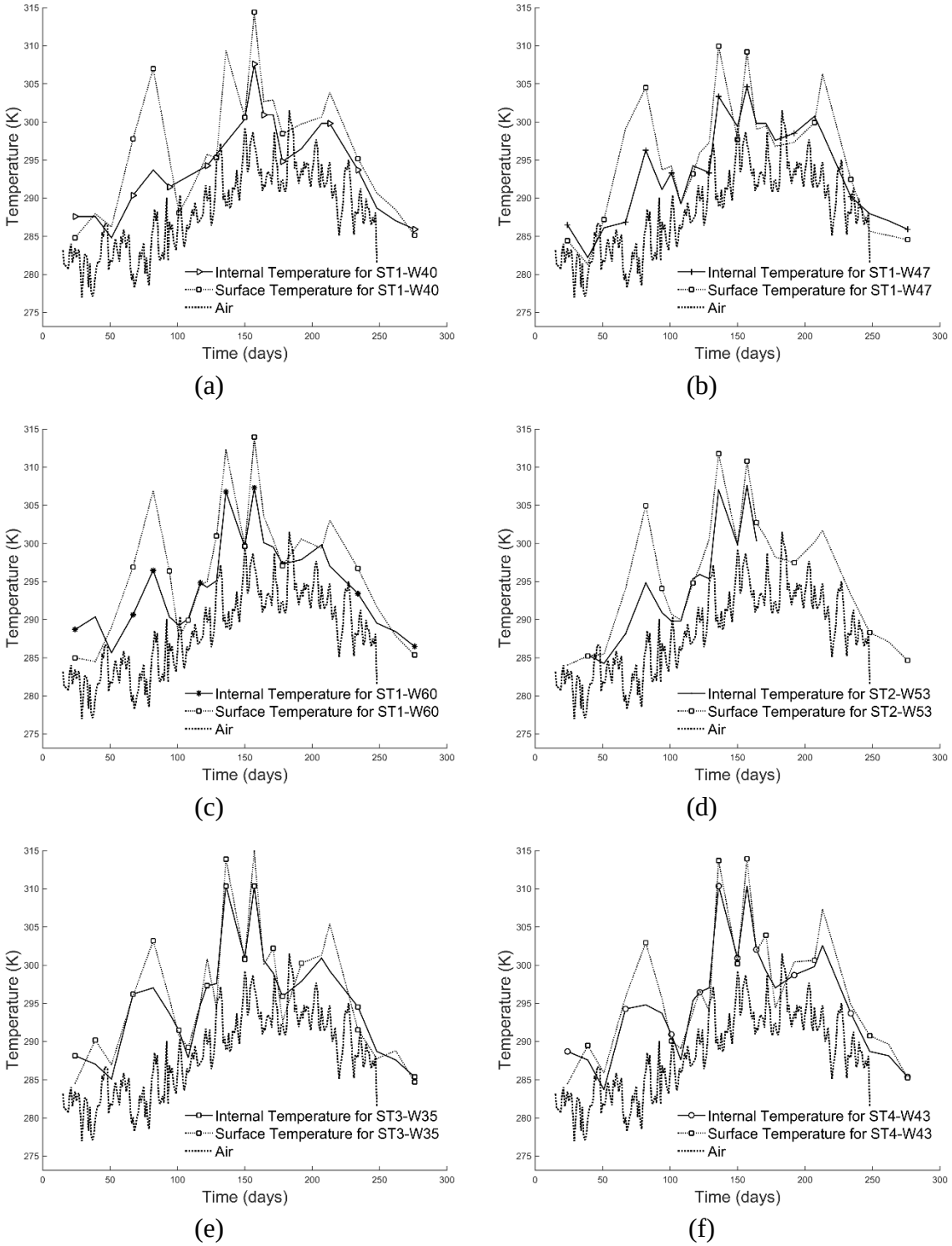

Figure 2.5 - Air, surface and internal temperature for concrete slabs over the 10 months of chloride testing: (a) ST1-A, (b) ST1-B, (c) ST1-C, (d) is ST2, (e) ST3, and (f) ST4.

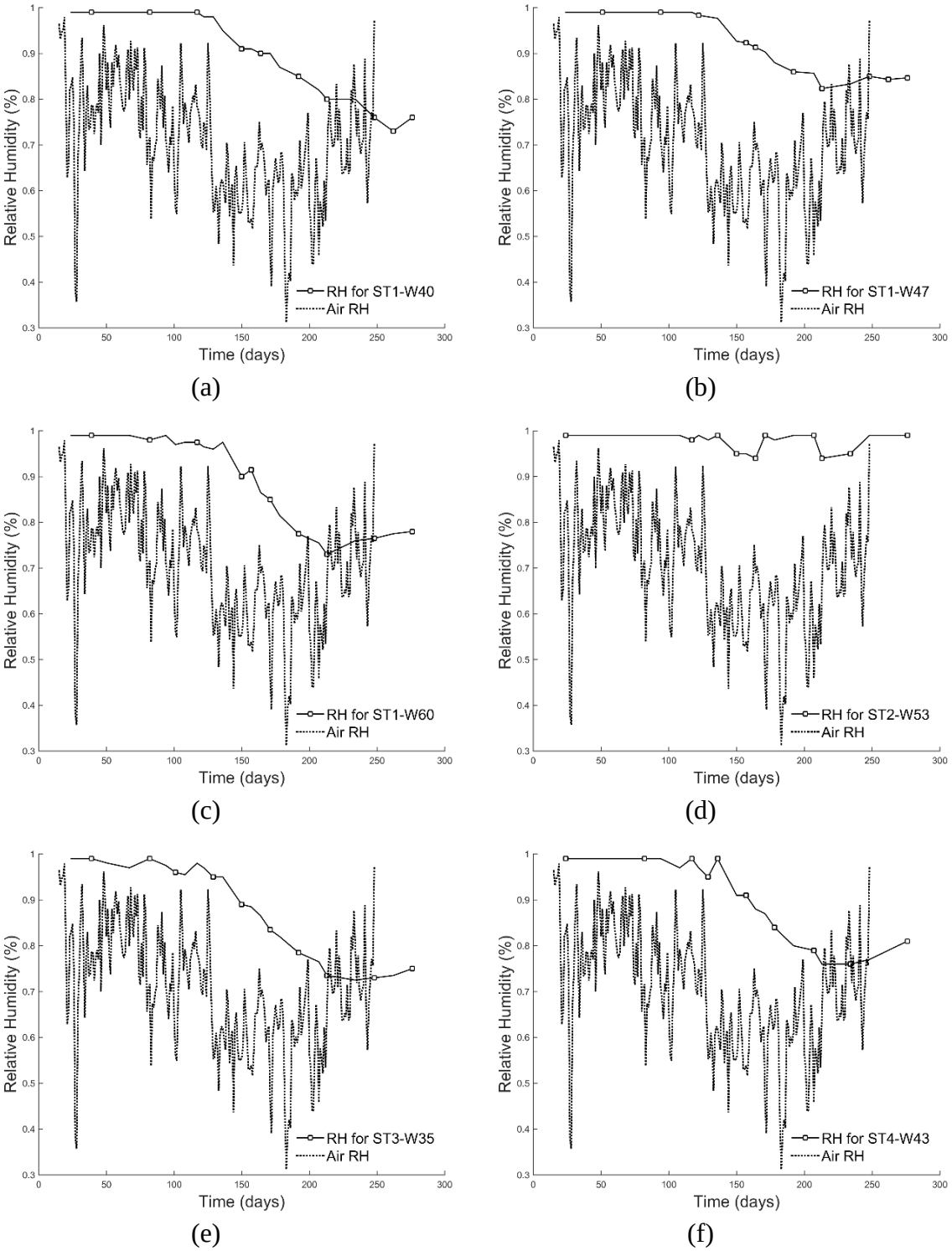

Figure 2.6 - Environmental and internal relative humidity for de-icing solution-ponded concrete slabs over the 10 months of chloride testing: (a) ST1-A, (b) ST1-B, (c) ST1-C, (d) is ST2, (e) ST3, and (f) ST4.

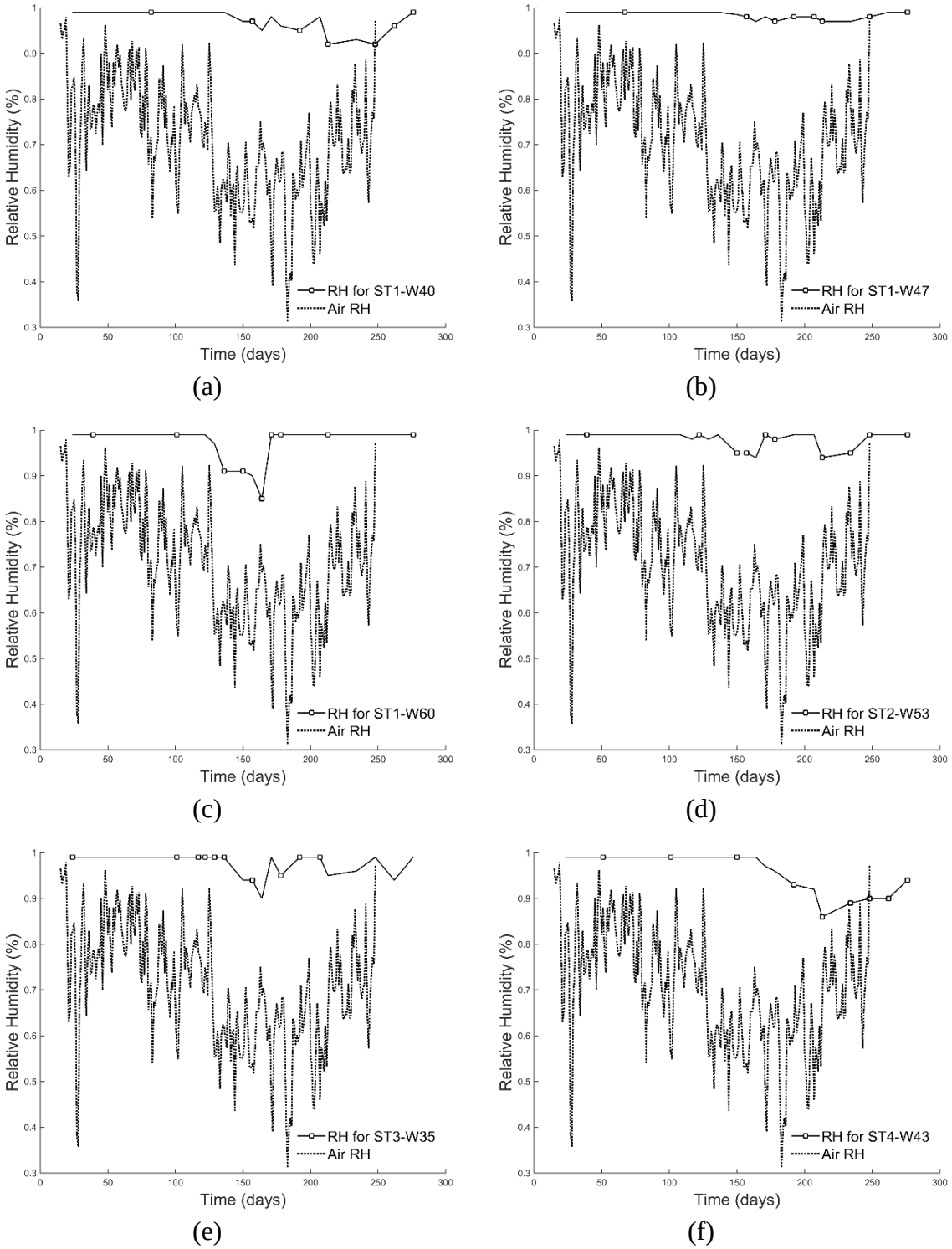

Figure 2.7 - Environmental and internal relative humidity for water-ponded concrete slabs over the 10 months of chloride testing: (a) ST1-A, (b) ST1-B, (c) ST1-C, (d) is ST2, (e) ST3, and (f) ST4.

2.3.4. Surface Resistivity

As mentioned in the testing methods, the surface resistivity was measured every week or bi-weekly throughout this study. The measurements were taken on both slabs that were ponded with the de-icing solution and the control slabs that were ponded with water to assess the effect of chloride ingress on surface resistivity measurements. The surface resistivity measurements were taken on un-reinforced sections and reinforced sections of the slabs. Since surface resistivity measurements are influenced greatly by temperature, all measurements were normalized by a temperature of 77°F (25 °C) using Hinrichsen-Rasch law (Hope 1987) which is given by equation 2.1.

$$\rho_2 = \rho_1 * exp\left[2900\left(\frac{1}{T_1} - \frac{1}{T_2}\right)\right] \quad (2.1)$$

where ρ_1 is the measured resistivity, ρ_2 is the normalized resistivity, T_1 (K) is the temperature of the concrete during the measurement, and T_2, is the normalized temperature. Figure 2.8 shows a comparison of SR measurements taken over the reinforcement and the unreinforced section on both the control slabs and the de-icing solution ponded slabs. Figure 2.8e contains no error bars because only one slab was ponded with de-icing solution and the other slab was ponded with water.

As noted, the measurements between the unreinforced and reinforced are nearly identical and fall well within the error bars, validating the techniques used to measure surface resistivity over the concrete reinforcement.

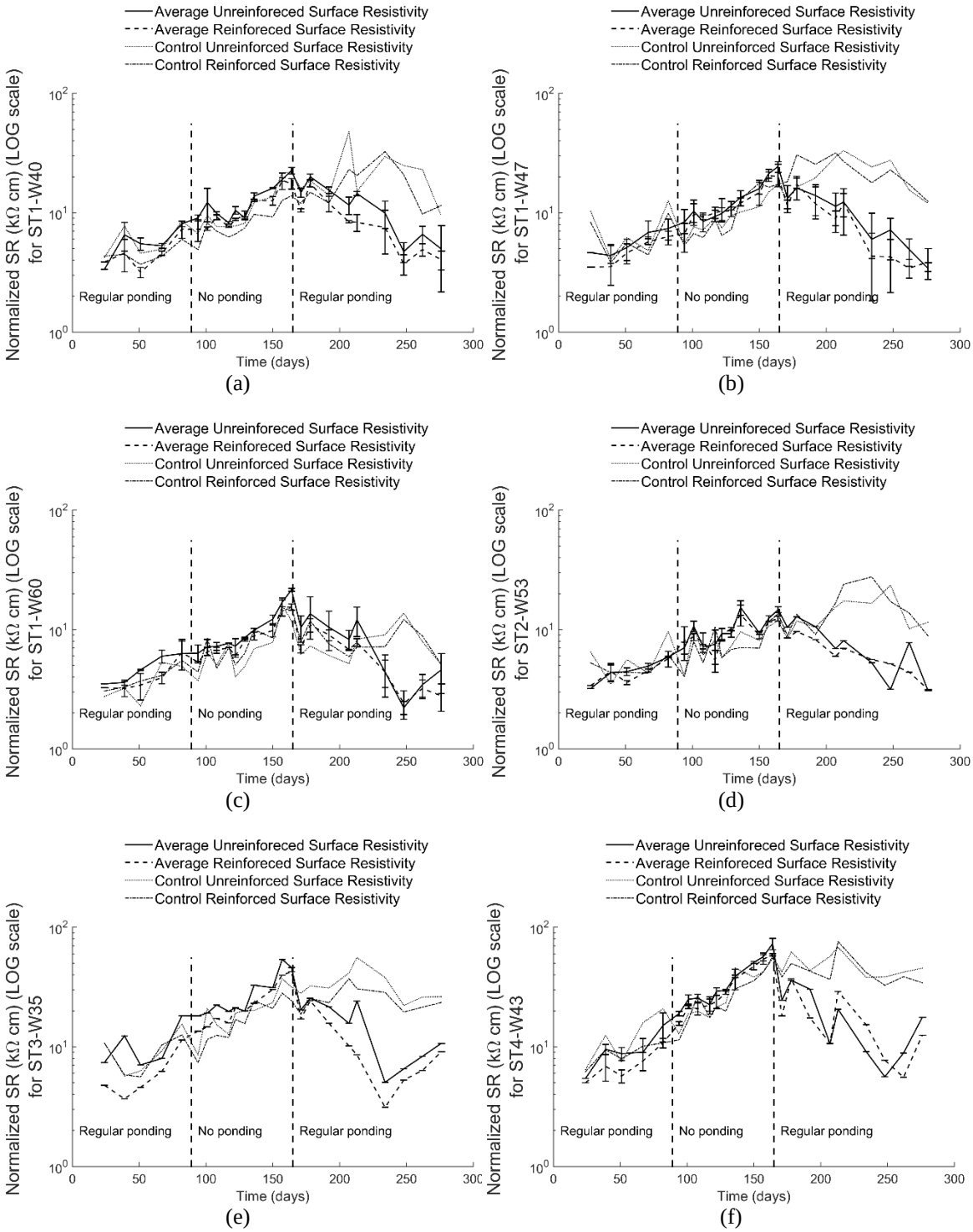

Figure 2.8 - Surface resistivity measurements taken over the unreinforced section of the control slabs and the de-icing solution ponded slabs. (a) is ST1 with w/c ratio of 0.40, (b) is ST1 with w/c ratio of 0.47, (c) is ST1 with w/c ratio of 0.60, (d) is ST2 with w/c ratio of 0.53, (e) is ST3 with w/c ratio of 0.35 and (f) is ST4 with w/c ratio of 0.43.

Avoiding early corrosion initiation was imperative in this study so that the relationship between SR and chloride ingress could be monitored for an extended period, hence the ponding cycles stopped after 7 cycles due to the high concentration of chlorides in the system. Figure 2.8 shows the section in which ponding cycles did not occur. Before the ponding cycles stopped, the surface resistivity was increasing in all the concrete types. The type of concrete influenced the SR measurements greatly. Figure 2.8a, b, c and d all started with SR values much lower than e and f which contained SCMs thus being less permeable. As time progressed, the SR measurements increased in all cases even after ponding stopped. This increase in resistivity can be accredited to curing. As the concrete slabs cured over time, the voids in the concrete closed up making the concrete more resistant, thus an increase in SR measurements. From Figure 2.8 it is clear that the water-ponded slabs also had an increase of SR measurements from the beginning of the study. This suggests that the curing process governed the SR measurements since the presence or chlorides or no chlorides did not seem to be as significant in the effect of SR measurements during the first half of the ponding cycles. As time progressed, as shown in Figure 2.4, the concentration of bound chlorides in the matrix began to increase as well. This can affect the SR measurements if the formation of Friedel's salts can increase enough to create a barrier which can alter the current flow through the pore structure. A study performed by Basheer et al. (Basheer et al. 2002) monitored electrical resistivity of various types of concrete that went through ponding cycles to assess their resistance to chloride ingress, and found that the electrical resistivity increased with time during the ponding cycles, which partly follows the trend seen in this study. Their explanation was that this trend was due to chloride binding or formation of chloro-aluminates, or both. A

separate study performed by Morales (2015) showed parallel results, indicating that an increase in SR measurements were due to chloride binding. The increase in SR values can also be attributed to the relative humidity inside the concrete which decreased after about 100 days. As seen in Figure 2.6, the RH began to decrease during the section of time that no ponding occurred. Since the RH decreased, it was expected that the SR values would increase. Once the cyclic ponding continued, the SR measurements taken on the slabs that had the de-icing solution began to decrease immediately while the SR measurements of the control slabs seem to have plateaued. This section seems to show the effect of chlorides in the system. When the chlorides were introduced once again into the system, the electrical conductivity of the concrete increased, thus lowering the electrical resistivity.

In order to provide additional support for the results that are presented in Figure 2.8, thermodynamic modeling, in the form of Gibbs Free Energy Minimization (GEMS), was used to study chloride binding in hydrated phase of concrete. The details of the GEMS algorithm and its validation to study hydrated cement phases are not presented here, but can be found in the literature (Wagner et al. 2012, Kulik et al. 2013, Paul Scherrer Institute 2013). The Friedel's salts and free chloride percentages for each concrete system were modeled assuming 100% hydration of the system, and the results are provided in Figure 2.9. It is important to note that the plots in Figure 2.9 models an idealized system, where the salt is added to the cement (without aggregate) during mixing (i.e., the binding is expected to be significantly larger than the case for which the chlorides are transported in hydrated concrete) and does not take into account physical binding, chlorides in the aggregates and temperature change effect. From these plots, it is

observed that Friedel's salts increase rapidly with a small addition of total chlorides for all cases and once it reaches a certain concentration, they start decreasing. This suggests that bound chlorides begin controlling the system when chlorides are first introduced, possibly contributing to the increasing SR measurements. All modeled concrete mixtures suggest that the free chlorides do not increase immediately after exposure, but eventually increases while bound chloride concentration decrease, possibly contributing the decrease in SR measurements. This also explains why the SR measurements for control slabs, that were only ponded with water, did not decrease at the same rate as the slabs saturated with chlorides.

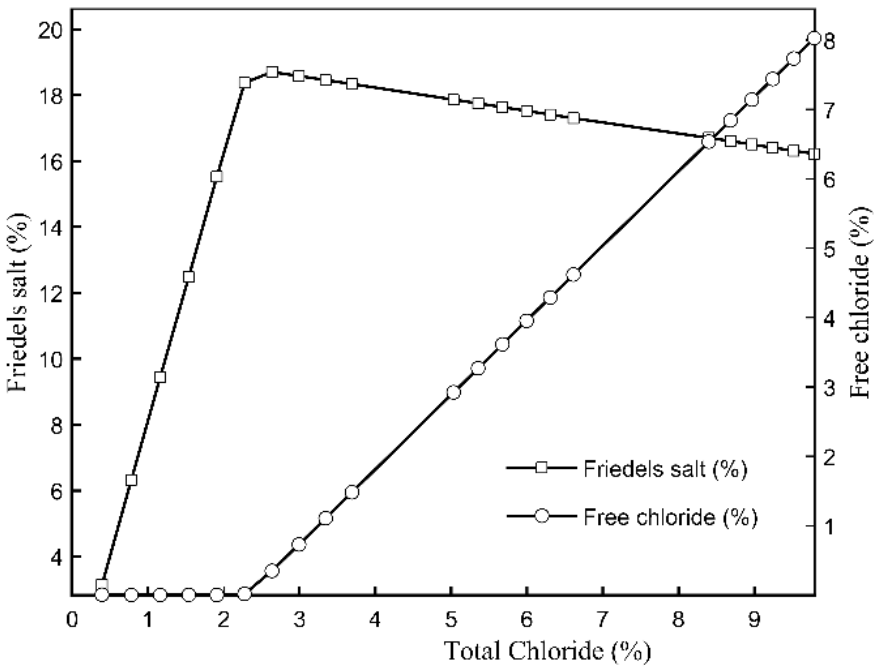

(a) ST1-W40

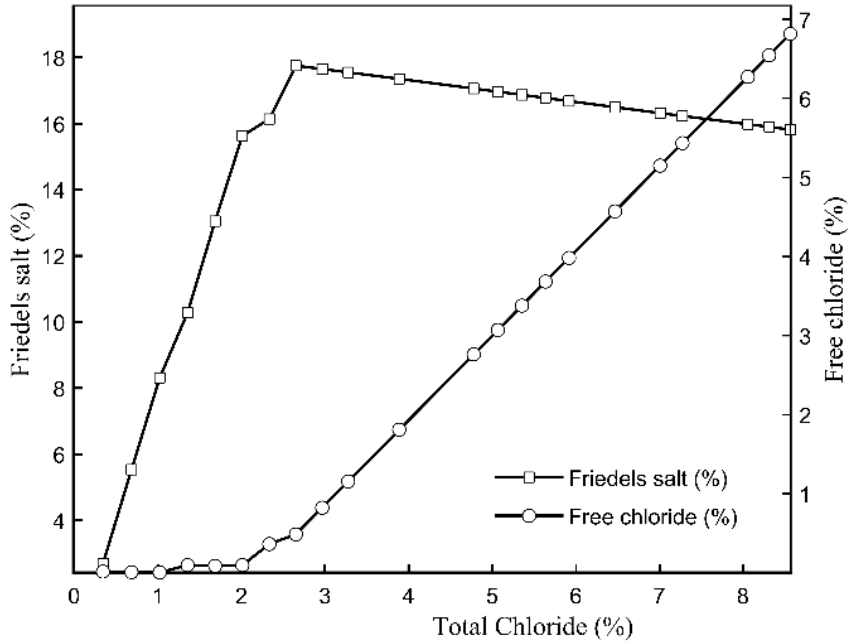

(b) ST1-W47

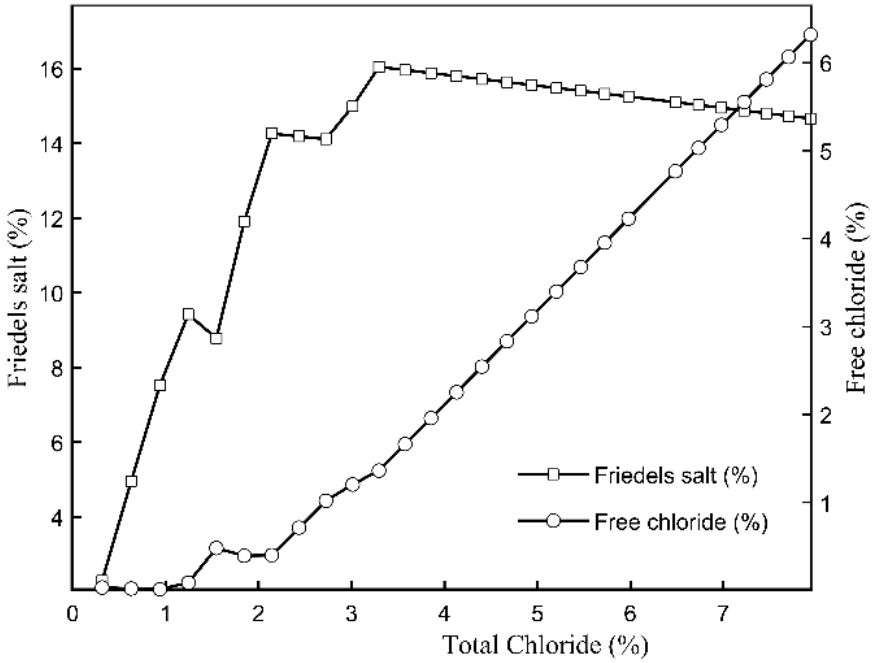

(c) ST1-W60

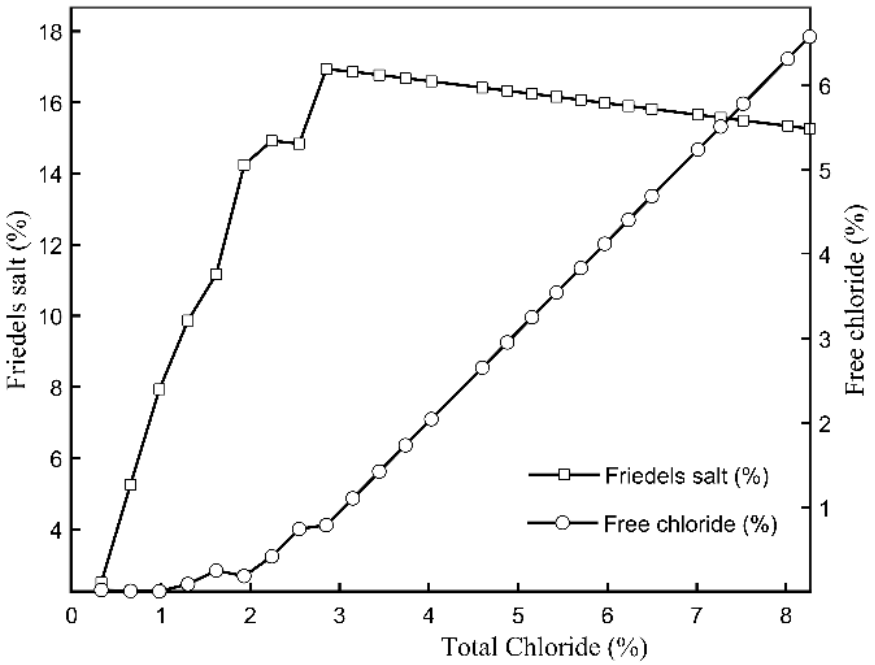

(d) ST2-W53

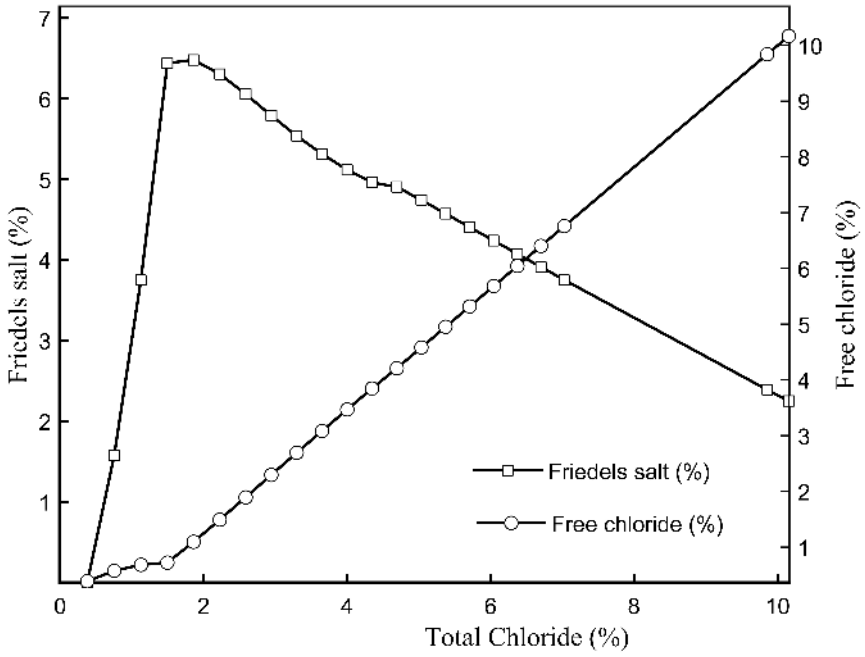

(e) ST3-W35

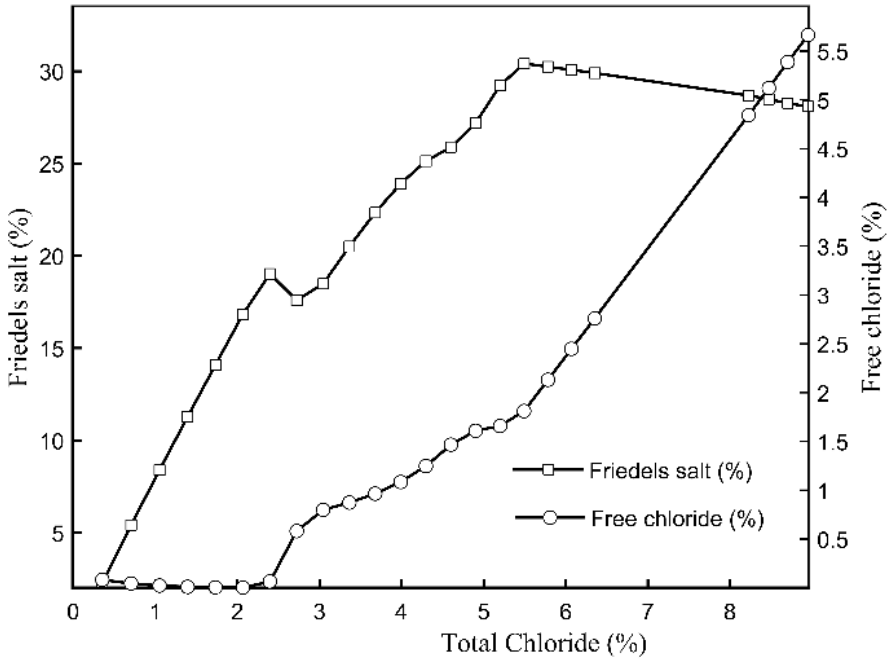

(f) ST4-W43

Figure 2.9 – The Friedel's salt and free chloride percentages from the thermodynamic modeling for different slabs after full hydration. (a) is ST1 with w/c ratio of 0.40, (b) is ST1 with w/c ratio of 0.47, (c) is ST1 with w/c ratio of 0.60, (d) is ST2 with w/c ratio of 0.53, (e) is ST3 with w/c ratio of 0.35 and (f) is ST4 with w/c ratio of 0.43.

2.4. Conclusions

In this study, surface resistivity measurements taken on concrete slabs that were saturated with chlorides from commercially available magnesium chloride de-icing solution that contained a corrosion inhibitor. Surface resistivity measurements were taken using a four-point Wenner probe at various locations on the slab surface that went through ponding cycles of a de-icer solution used in the state of Oregon by the DOT. From this study, the following was concluded.

- The difference in moisture content in concrete between the two extracting methods (wet vs. dry) was negligible.

- From the experiments, it was evident that the higher the w/cm, the greater the chloride ingress. The use of SCMs provide superior resistance to the transport of chlorides.
- The amount of bound chlorides increased over time, however, this increase was minimal compared to the amount of free chlorides that were retained at a specific depth in the concrete.
- At early age, surface resistivity was affected by the curing process of concrete.
- Surface resistivity values decreased for the chloride exposed concrete half way through the study whereas the water exposed concrete did not change significantly, suggesting that SR measurements could identify chloride ingress. Additional data collection and modeling are required to investigate this relationship further in detail.
- The increase in free chloride concentrations may be the reason in part for the SR measurements to have decreased, and this observation was also confirmed by thermodynamic modeling, however, it is recommended to study this further.

2.5. References

ACI Committee 222R-01: (2001), Protection of Metals in Concrete Against Corrosion. Reapproved 2010.

ASTM A615-15a Standard Specification for Deformed and Plain Carbon-Steel Bars for Concrete Reinforcement. (2015). ASTM International, West Conshohocken, PA.

ASTM C1152-12 Standard test method for acid-soluble chloride in mortar and concrete. (2012). ASTM International, West Conshohocken, PA.

ASTM C1218/C1218M-15 Standard Test Method for Water-Soluble Chloride in Mortar and Concrete. (2015). ASTM International, West Conshohocken, PA.

ASTM C1556-11a Standard test method for determining the apparent chloride diffusion coefficient of cementitious mixtures by bulk design. (2012). ASTM International, West Conshohocken, PA.

ASTM C39-15 Standard Test Method for Compressive Strength of Cylindrical Concrete Specimens. (2015). ASTM International, West Conshohocken, PA.

ASTM WK37880 New Test Method for Measuring the Surfae Resistivity of Hardened Concrete Using the Wenner Four-Electrode Method. (2014). ASTM International, West Conshohocken, PA.

Standard method of test for surface resistivity indication of concrete's ability to resist chloride ion penetration. (2011). American Association of State Highway and Transportation Officials, Washington DC.

Alonso, C., C. Andrade, J. A. González. (1988). "Relation between resistivity and corrosion rate of reinforcements in carbonated mortar made with several cement types." Cement and Concrete Research 18(5): 687-698.

Andrade, C., C. Alonso (2004). "Test methods for on-site corrosion rate measurement of steel reinforcement in concrete by means of the polarization resistance method." Materials and Structures 37(9): 623-643.

Basheer, P., P. Gilleece, A. Long, W. Mc Carter. (2002). "Monitoring electrical resistance of concretes containing alternative cementitious materials to assess their resistance to chloride penetration." Cement and Concrete Composites 24(5): 437-449.

Concrete materials and methods of concrete construction/Test methods and standard practices for concrete. (2009). Canadian Standards Association, Toronto, ON.

Florida method of test for concrete resistivity as an electrical indicator of its permeability. (2004). Department of Transportation Florida, FL, USA.

Gowers, K., S. Millard. (1999). "Measurement of concrete resistivity for assessment of corrosion severity of steel using Wenner technique." ACI Materials Journal 96(5): 536-541.

Hamilton, H., A. J. Boyd, E. Vivas, M. Bergin. (2007). Permeability of concrete - comparison on conductivity and diffusion methods. No. 00026899. Gainesville, FL, University of Florida.

Hong, K. (1999). Cyclic wetting and drying and its effects on chloride ingress in concrete. National Library of Canada, Ottawa, ON.

Hooton, R.D., A. Shahroodi, E. Karkar. (2012). Evaluating concretes using rapid test methods for fluid penetration resistance, ACI Fall Convention in Toronto, presented in the Emerging Technologies (Part 2); available at aci-int.org.

Hope, B., A. Ip. (1987). "Chloride Corrosion Threshold in Concrete." Materials Journal 84(4): 306-314.

Hussain, S., E. Rasheeduzzafar, A. Al-Musallam, A. Al-Gahtani. (1995). "Factors affecting threshold chloride for reinforcement corrosion in concrete." Cement and Concrete Research 25(7): 1543-1555.

Jackson, L. (2013). "Surface resistivity test evaluation as an Indicator of the Chloride Permeability of Concrete." Tech brief. Publication no. FHWA-HRT-13-024, McLean, VA.

Jaegermann, C. (1990). "Effect of Water-Cement Ratio and Curing on Chloride Penetration into Concrete Exposed to Mediterranean Sea Climate." Materials Journal 87(4): 333-339.

Kessler, R., R. Powers, M. Paredes. (2005). Resistivity measurements of water saturated concrete as an indicator of permeability. NACE International.

Kulik, D., T. Wagner, S.Dmytrieva, G. Kosakowski, F. Hingerl, K. Chudnenko, U. Berner. (2013). "GEM-Selektor geochemical modeling package: revised algorithm and GEMS3K numerical kernel for coupled simulation codes." Computational Geosciences 17(1): 1-24.

López, W., J. A. González (1993). "Influence of the degree of pore saturation on the resistivity of concrete and the corrosion rate of steel reinforcement." Cement and Concrete Research 23(2): 368-376.

Martin-Perez, B. (1999). "Service life modelling of R.C. highway structures exposed to chlorides." Ph.D. thesis: 168 pp.

Morales, M. T. (2015). Experimental investigation of the effects of embedded rebar, cracks, chloride ingress and corrosion on electrical resistivity measurements of reinforced concrete: 174 pp.

Morris, W., A. Vico, M. Vázquez. (2004). "Chloride induced corrosion of reinforcing steel evaluated by concrete resistivity measurements." Electrochimica Acta 49(25): 4447-4453.

Method of test for determination of electrical resistivity of concrete. (2013). Ministry of Transportation Ontario, Toronto, ON.

Neville, A. M. (1981). Properties of Concrete. Pitman Publising Limited, London, United Kingdon.

Paul Scherrer Institute. (2013). "GEMS: Gibbs Energy Minimization Software for Geochemical Modeling." From http://gems.web.psi.ch.

Presuel-Moreno, F.,Y. Liu, M. Paredes. (2009). Understanding the effect of rebar presence and/or multilayered concrete resistivity on the apparent surface resistivity measured via the four-point wenner method. Corrosion Conference 2009. NACE International, Atlanta, GA.

Qiang, Y., A. Katrien, S. Caijun, S. Geert De. (2008). Effect of temperature on transport of chloride ions in concrete. Concrete Repair, Rehabilitation and Retrofitting II, CRC Press: 159-160.

Rupnow, T., I Patrick. (2011). Evaluation of surface resistivity measurements as an alternative to the rapid chloride permeability test for quality assurance and acceptance, Louisiana Transportation Research Center: 68 pp.

Salehi, M. (2013). Numerical investigation of the effects of cracking and embedded reinforcement on surface concrete resistivity measurements using Wenner probe. Civil and Environmental Engineering. Ottawa, Ontario, Carleton University. Master of Applied Science in Civil Engineering: 155 pp.

Sengul, O., O. E. Gjorv. (2008). "Electrical resistivity measurements for quality control during concrete construction." ACI Materials Journal 105(6): 541-547.

Sengul, O., O. E. Gjorv. (2009). "Effect of embedded steel on electrical resistivity measurements on concrete structures." ACI Materials Journal 106-M02 (January/February 2009): 11-18.

Song, H., V. Saraswathy. (2007). "Corrosion monitoring of reinforced concrete structures - a review." International Journal of Electrochemical Science 2(2007):1-28.

Wagner, T., D. A. Kulik ,F. F. Hingerl, S. V. Dmytrieva. (2012). "Gem-Selektor geochemical modeling package: TSolmod library and data interface for multicomponent phase models." Canadian Mineralogist 50(5): 1173-1195.

Weydert, R., C. Gehlen. (1999). "Electrolytic resistivity of cover concrete: Relevance, measurement and interpretation." Proceedings of the 8th International Conference on Durability of Building Materials and Components. 409-419. NRC Research Press, Vancouver, Canada.

3 Second Manuscript

The Effect of Freeze-Thaw Action on Electrical Resistivity Measurements Taken on Concrete Saturated with Magnesium Chloride De-Icing Solution

David Esteban Rodriguez Matiz, Vahid J. Azad, David Trejo,
O. Burkan Isgor, Jason H. Ideker

Abstract: Developing a method in which surface resistivity can provide accurate information about the amount of chlorides in a concrete system after exposure to de-icing chemicals, and understanding the behavior of chloride ingress in concrete that underwent freeze-thaw action, would create the opportunity to service structures earlier. This would result in saving resources and time and giving the structure a longer service life. To this end, this study provides a deeper understanding of the effect of freeze-thaw cycles on chloride ingress and surface resistivity measurements taken on concrete slabs previously exposed to a de-icing solution. Electrical resistivity measurements were taken at various locations on slab surfaces as well as companion concrete cylinders subjected to freeze-thaw cycling. The results from the surface resistivity measurements that underwent freeze-thaw action are not clear. However, it is evident that freeze-thaw action has a significant negative impact on the rate of chloride ingress on the slabs. The chloride profiles strongly indicate that chloride penetrability of the ordinary portland cement (OPC) mixtures increased compared to a similar slab that did not go through freeze-thaw action. An increase in penetrability is not apparent for the high performance concrete (HPC) mixture and cannot be seen in the chloride profiles.

3.1. Introduction

The purpose of this study was to develop a better understanding of the electrical resistivity of concrete when reinforced concrete slabs are saturated with de-icer solution underwent freeze-thaw cycles. The de-icing solution selected is the commercial product used by the Oregon Department of Transportation (ODOT) and is composed of a 30% magnesium chloride solution with a corrosion inhibitor. While de-icing chemicals are effective at reducing freezing points, they are also known to damage the concrete bridge decks. It is well known that the use of de-icing chemicals containing chlorides can lead to corrosion of the reinforcing steel (Backus et al. , Shi. et al. 2013). As a result of this concern it is common to use deicing chemicals that contain corrosion inhibitors (Shi 2010, Shi 2011). According to Shi (2010, 2011), the corrosion inhibitors helped maintain the strength of the concrete and slowed the chloride ingress, however, when chlorides reach the reinforcing steel, corrosion can initiate if a certain chloride concentration threshold is reached. Studies have also shown that the use of de-icers deteriorate the concrete as well (Julio-Betancourt 2009). A study done by the Michigan Tech Transport Institute (2008), determined that the use of magnesium chloride and calcium chloride de-icer solutions cause expansive cracking, increase in permeability, and loss of strength. A report by the Oregon Department of Transportation (ODOT) also showed that the use of magnesium chloride de-icer decreased the strength of concrete. Hardened air void analysis were performed on the cores following ASTM C457, taken from twelve bridges in Oregon and showed that half of the cores had a spacing factor of over .008 in. (200 microns), proving to be inadequate for good freeze-thaw resistance. ODOT concluded that the magnesium chloride de-icing solution combined with freeze-thaw action

deteriorated the concrete both physically and chemically. Interestingly, a survey taken by ODOT indicated that their winter maintenance managers did not agree on the severity of the damage that their magnesium chloride de-icer solution had on their bridge decks. The report noted that some managers however, did believe that this solution caused a high level of risk to the structures so changes were made on concrete mixture designs and rehabilitation practices to address this risk (Huang 2014).

Electrical resistivity has proven to be a good indicator for the progression of deterioration in reinforced concrete (Alonso et al. 1988, López et al. 1993, Gowers et al. 1999). There are various methods for measuring the resistivity of concrete. There are some limitations to the testing methods, however. Bulk resistivity entails taking cylinders or cores from structures to be able to perform the test. This destructive technique is not always feasible. Surface resistivity on the other hand can be done in-situ in a non-destructive manner. However, it is influenced by rebar location, moisture, relative humidity (RH) and depth of steel as reported studies done by Sengul and Gjorv, and Morales (Sengul et al. 2009, Morales 2015). Studies have been conducted on the changes in moisture and internal RH of concrete (Ryu et al. 2011, Jiang 2013), however, no study has provided a correction factor based on moisture and RH for surface resistivity (SR) measurements. There is also little existing information on relating SR with freeze-thaw action. One study was able to use electrical resistivity to assess frost damage (Zhendi Wang 2015). Wang showed that as temperature decreases, electrical resistivity increases, and as F-T cycles continued, the resistivity continued to increase, which indicated that freeze-thaw related damage was progressively increasing. Frost damage was also proven by the loss of strength and visible cracks on their specimens. No literature was found on relating SR values with

chloride ingress and F-T action, which is of great concern since de-icing chemicals are used only in environments in which F-T occurs.

This study describes an investigation into the potential for electrical resistivity to provide a non-destructive evaluation tool to assess the deterioration of concrete due to F-T and chloride ingress. The effect that F-T action had on chloride ingress was also investigated and reported herein.

3.2. Research Significance

Corrosion of the reinforcing steel is the most expensive reoccurring problem when it comes to the U.S infrastructure (Koch et al. 2002). Once corrosion initiates, the costs of repairs are substantially greater than the cost of slowing the ingress of chlorides prior to corrosion. Being able to understand and predict the amount of chlorides in a system accurately would benefit the DOTs greatly. The destructive and expensive nature of the testing for chloride ingress, however, makes it an undesirable task. The use of surface resistivity (SR) meters can provide the opportunity for researchers to discover new methods of predicting deterioration of concrete. However, caution is required when SR is used, due to limitations. This study investigated limitations of the SR measurements, as well as to help close the gaps in literature in relation to electrical resistivity and the effects that F-T cycles have on concrete slabs saturated with chlorides. Developing a method in which SR could provide accurate information about the amount of chlorides in a system after de-icing chemicals have been used, or understanding the behavior of chloride ingress in concrete that underwent F-T cycles, could provide the opportunity to

service structures at earlier age, saving resources and time, while providing a longer service life of the structure.

3.3. Experimental Procedure

3.3.1. General Information

The experimental study involved monitoring of surface resistivity measurements, temperature, relative humidity and chloride ingress to examine the effect of freeze-thaw action on reinforced concrete slabs that were cast at an outdoor exposure site. The slabs represent bridge decks commonly used in Oregon from the 1960s to the present. The slabs were cast based on concrete mixture designs from their respective periods of time. Slab Type A (STA), composed of air-entrained slabs designed per 1960s specifications, Slab Type B (STB) consisted of non-air-entrained slabs designed per 1960s specifications, and Slab Type C (STC) were air-entrained slabs designed per current specifications.

3.3.2. Materials

3.3.2.1. Concrete

The concrete mixtures were ordered from a local ready-mix concrete plant. Three mixtures were selected to represent the most common types of concrete used in Oregon bridge decks. The concrete mixtures span an approximate 55-year age range.

3.3.2.2. Specimens

Three slab types were selected to investigate the effect of freeze-thaw action on SR measurements. The mixture proportions for each slab are included in Table 3.1.

Table 3.1 - Fresh properties and three mixture designs used in this study.

	STA	STB	STC
w/cm ratio	0.47	0.53	0.43
Measured slump, in. (cm)	6.25 (15.9)	5.5 (14.0)	3.5 (8.9)
Measured air (%)	5	1	2.5
Measured unit Weight, lb/ft^3 (kg/m^3).	142.16 (2277.2)	148 (2370.7)	145.88 (2336.8)
Cement, lbs. (kg)	512 (232.2)	515 (233.6)	461 (209.1)
Flyash, lbs. (kg)	0	0	204 (92.5)
Silica Fume, lbs. (kg)	0	0	25 (11.3)
Water, lbs. (kg)	240 (108.9)	275 (124.7)	300 (136.1)
3/4" - No.4, lbs. (19.1mm – 4.76mm (kg)	1690 (766.6)	1693 (767.9)	1714 (777.5)
Sand, lbs. (kg)	1196 (542.5)	1401 (635.5)	617 (279.9)
Total, lbs. (kg)	3638 (1750.2)	3884 (1761.8)	3321 (1506.4)

Slab type A (STA), and slab type B (STB) were slabs designed from 1960's specifications, which used ordinary portland cement (OPC) concrete with no supplementary cementitious materials. STB was not air-entrained. Slab type C (STC) was

a modern air-entrained high performance (HPC) mixture with class F fly ash with a CaO content of 13.94% and silica fume at a 30% and 4% replacement of portland cement, respectively. Mixtures STA and STC did not meet the target air-content that was specified, which was 6 percent. Mixture STC was dosed with increasing amounts of air entraining admixture with minimal increase in air content. A previous mixture also proved difficult to achieve an adequate air content and after the final dosage the air content dramatically increased to 9%. In an effort to avoid that happening mixture STC was used despite not meeting the target air percentage. Fifteen 4-inch by 8-inch (10.16 cm by 20.32 cm) cylinders were cast from each one of the different mixture types. These cylinders were used for additional mechanical property and performance testing.

3.3.2.3. Reinforcement

All slabs were reinforced with #5 (5/8 in., 16mm) ASTM A615 carbon steel rebar. Historical data on bridge decks show that most decks in Oregon are reinforced with #5 (5/8 in., 16mm) rebar. Although #4 rebar is also common, previous studies showed that the difference between these two bar sizes does not affect resistivity measurements (Salehi 2013). The slabs were reinforced with orthogonal rebar with 8-inch (10.16 cm) center-to-center spacing. All slabs had a concrete cover thickness of 2.5 inches (6.35 cm) congruent with historical data of a significant number of Oregon bridge decks. A schematic of the slabs is provided in Figure 3.1.

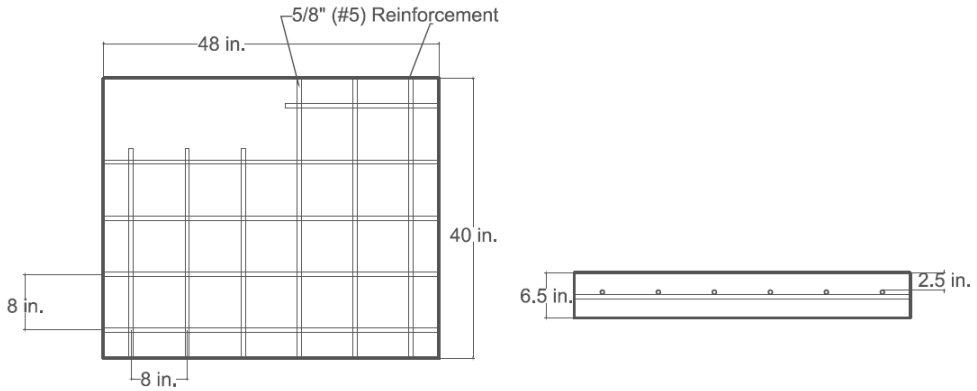

Figure 3.1 - illustrates the slab dimensions and the placement of the reinforcing steel. The section that is unreinforced was used to take measurements and to extract cores for additional testing.

3.3.3. Exposure Regime

3.3.3.1. Initial Curing

The slabs and the cylinders were each cured under wet burlap for 28 days after casting. Compressive strength testing according to ASTM C39 was performed at 28 and 90 days.

3.3.3.2. Ponding

After 28 days of wet curing, the slabs were exposed to commercially available 30% magnesium chloride ($MgCl_2$) solution that contained a corrosion inhibitor in alternating wet/dry cycles. This was done to increase chloride ingress rates. This is the same deicing solution used by ODOT. In each cycle, the slabs were ponded with the $MgCl_2$ solution for 96 hours. After 96 hours, the $MgCl_2$ solution was removed by vacuum, then the slabs were exposed to ambient conditions for a 10-day period. The duration of each cycle was decided based on the needs of the project in addition to previous studies that showed this cycling approach increased chloride ingress but still represented field exposure (Hong 1999). The chloride ingress was checked using a profile grinder after every two cycles.

After 7 cycles the ingress was determined to be occurring too rapidly, so the cycles were postponed for ten weeks and were then exposed to the magnesium chloride solution once again continuing the ponding regime.

3.3.3.3. Internal and Atmospheric Conditions

In-situ Wagner Rapid RH® probes were installed at various depths inside the slabs. These probes measured temperature and relative humidity inside the concrete at the time that SR measurements were taken. The probes were installed at one inch (2.54 cm) and at two and a half inches (6.35 cm) from the surface of the slabs. The depths of the probes were chosen based on practicality. At one inch (2.54cm), it decreased the chance of cracks near the surface and at two and a half inches (6.35 cm) it provided information regarding the change in temperature and relative humidity compared to the one inch (2.54cm) probe. Surface temperature was measured with an infrared temperature gun. In addition to these measurements, a weather station continuously collected weather data onsite. This included relative humidity, wind speed, wind direction, precipitation, barometric pressure, etc. The data were used to calibrate measurements and provide additional information for the companion modeling study.

3.3.3.4. Freeze-Thaw Cyclic Testing

Three slabs were exposed to F-T cycling. These slabs went through 8 de-icing solution ponding cycles before they were exposed to F-T. The concrete slabs were exposed to 300 freeze-thaw cycles commensurate with ASTM C666-15 Procedure B. The cycles were divided into five segments of 60 cycles per each segment. Each F-T cycle involved 1 hour of freezing at 3.2^{o}F (-16^{o}C) and 1 hour of thawing at 60.8^{o}F (+16^{o}C) with a 30-

minute temperature increase or decrease in between. The goal of this regime was to achieve an approximate cycling range of 14°F/+50°F (-10°C/+10°C) at 1.5-inch (3.81cm) depth. Each F-T exposure period started at the end of a de-icing ponding cycle and lasted eight days before the slabs were placed back into ambient conditions where they underwent three additional ponding cycles in between each F-T exposure. Concrete cylinders, made from the same concrete as the slabs, were subjected to F-T cycles following ASTM C666 in a Scientempt F-T chamber for 300 cycles and were compared to additional cylinders that were placed in the F-T environmental chamber with the slabs. ASTM C666 standard provides two procedures for testing. Procedure A requires that the specimens undergo freezing and thawing submerged in water. Procedure B requires specimens to undergo freezing in air and thawing in water. To keep the environment consistent between the slabs and the cylinders, the cylinders followed the ASTM C666 went through a wet thawing and dry freezing exposure (Procedure B). The cylinders were conditioned by saturating them in a fog room until their saturated surface dry mass stopped increasing.

3.3.4. Testing Methods

The concrete slabs, cylinders, and cores that were extracted from the unreinforced zone of the slabs went through various tests throughout the duration of the project. The tests that were performed on concrete slabs, cylinders, and cores are described in the following sections.

3.3.4.1. Chloride Profiling

Chloride profiling was performed on each slab at various ages using a field profile grinder; there are nine possible chloride profiling sites on each slab due to the location of rebar and the unreinforced zone. Collected powders were analyzed for acid-soluble chloride content following ASTM C1152. These profiles were generated for determination of chloride transport properties per ASTM C1556 to discern the effects of both chloride ingress and F-T action on chloride ingress. After each chloride profile was taken, the area where the grinding occurred was sealed with a commercial self-consolidating, shrinkage-compensating concrete repair material.

3.3.4.2. Four Point Probe Surface Resistivity

SR measurements were taken using a four-point Wenner probe at various locations on the slab surface. When taking SR measurements in sections where rebar was present, the probe was oriented perpendicular to the topmost rebar and parallel to the bottommost rebar. The orientation of the probe and procedure was decided following an extensive study performed on probe orientation by Morales (2015). Measurements were rapid, they were performed weekly or bi-weekly, depending on the ponding cycles. SR measurements were taken during the 8-day period of freeze-thaw cycles on concrete slabs at the same point in time during a thawing cycle. SR was measured every 36 cycles on the cylinders undergoing freeze-thaw cycles as well. The procedure for measuring SR measurements followed the draft standard method created by AASHTO (AASHTO Designation: T XXX-08). However, the procedure used in this research deviated from the draft by taking five measurements every 90 degrees instead of two, and the median value

of the five was used instead of the average. This deviation was done to follow the same measurements techniques as the ones taken on the concrete slabs.

3.3.4.3. Bulk Electrical Conductivity/Resistivity ASTM C1760

Bulk resistivity was measured after every 36 cycles on the cylinders undergoing F-T cycles following ASTM C666. The values obtained from bulk resistivity measurements were used to validate and compare the SR measurements of the cylinders. Bulk resistivity was done using the Giatec RCON electrical resistivity meter and manufacturer's recommendations were followed when testing concrete cylinders.

3.3.4.4. Resonant Frequency Test ASTM C215

Resonant frequency, using the transverse method, was measured every 36 cycles on cylinders undergoing F-T cycles per ASTM C666. Concrete's resonant frequency is directly related to the dynamic modulus of elasticity which can decrease if there is degradation of the concrete during F-T testing.

3.4. Experimental Results and Discussion

3.4.1. Compressive Strength

Compressive strength of cylindrical concrete specimens was measured 28 and 90 days after casting following ASTM C39 and are shown in Table 3.2.

Table 3.2 - Compressive strengths of the concrete at 28 days and 90 days in MPa.

	STA	STB	STC
28 Day, MPa (psi)	20.9 (3031.3)	28.3 (4104.6)	24.6 (3567.9)
90 Day, MPa (psi)	28.3 (4104.6)	37.3 (5409.9)	33.1 (4800.7)

Table 2.3 shows the compressive strengths of the concrete used in this study. STB specimen had over all the highest strength both at 28 days and at 90 days. STB specimen contained no air-entrainment and no supplementary cementitious materials, which were the two main factors that resulted in greater strengths than the other two concrete types. Mixture STC, contained fly ash and will take a longer period of time to mature, and therefore it is expected that the maximum strength will surpass the strength of the rest of the concretes at later ages. Overall, the compressive strengths of all the mixtures was lower than the design strengths. A reason for this can be attributed to the low temperature at the time of casting. The temperature was 45°F (7.2 °C) and the temperature fluctuated near these lower levels over the wet curing duration since the slabs were cast outside and the cylinders were cured in the same environment.

3.4.2. Concrete Cylinders Undergoing Freeze-Thaw in Scientempt F-T chamber

Surface and Bulk electrical resistivity of concrete cylinders that underwent 300 F-T cycles following ASTM C666 Procedure B in a Scientemp F-T chamber were compared to additional cylinders that were placed in the F-T environmental chamber with the slabs. Since SR measurements are influenced greatly by temperature, all measurements were normalized to a temperature of 25 °C using the Hinrichsen-Rasch law which is given by equation 3.1.

$$\rho_2 = \rho_1 * exp\left[2900\left(\frac{1}{T_1} - \frac{1}{T_2}\right)\right] \quad (3.1)$$

Where ρ_1 is the measured resistivity, ρ_2 is the normalized resistivity, T_1 (K) is the temperature of the concrete during the measurement, and T_2, is the normalized

temperature. The SR and the bulk resistivity of the cylinders are found in Figures 3.2 and 3.3, respectively.

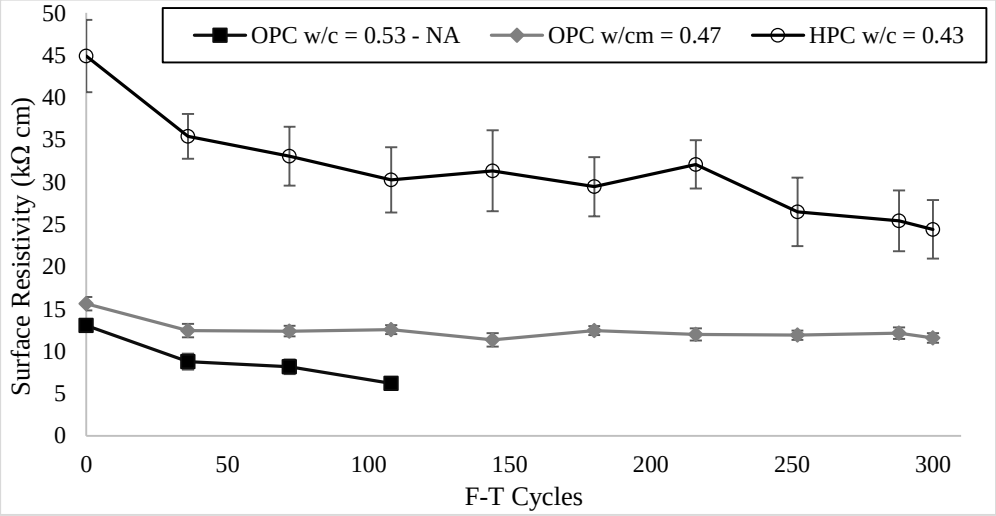

Figure 3.2 - Surface resistivity taken on cylinders that underwent 300 F-T cycles according to ASTM C666 Procedure B. Three types of concrete were tested: 1) OPC concrete with w/c ratio of 0.53 and no air-entrainment, 2) an OPC concrete w/cm ratio of 0.47 with air-entrainment and 3) a HPC with a w/cm ratio of 0.43 that contained silica fume, fly ash and air-entrainment.

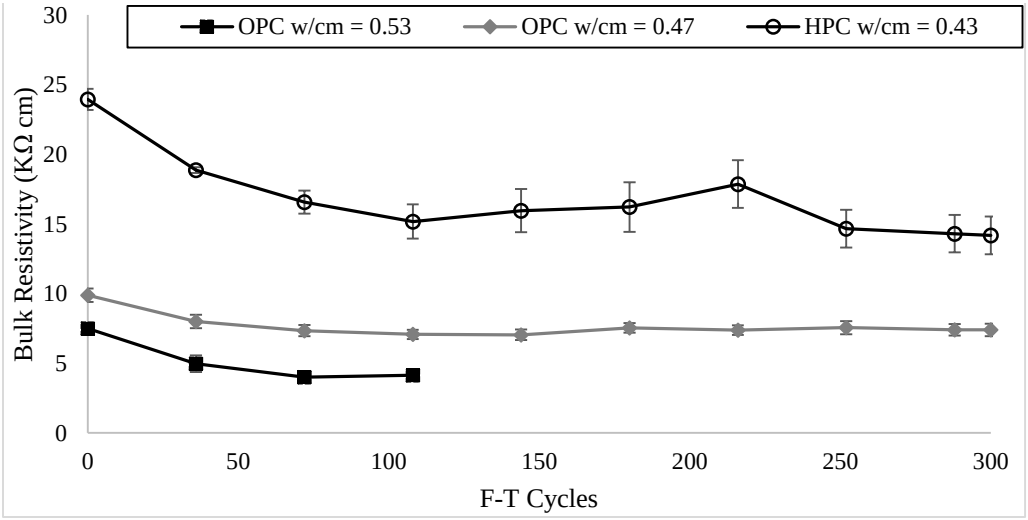

Figure 3.3 - Bulk electrical resistivity on concrete cylinders that underwent 300 F-T T cycles according to ASTM C666 Procedure B. Three types of concrete were tested: 1) OPC concrete with w/c ratio of 0.53 and no air-entrainment, 2) an OPC concrete w/cm ratio of 0.47 with air-entrainment and 3) a HPC with a w/cm ratio of 0.43 that contained silica fume, fly ash and air-entrainment.

Figures 3.2 and 3.3 show the resistivity of the three concrete types over 300 cycles following ASTM C666 Procedure B. The lower the electrical resistivity, the generally the

lower the concrete quality or maturity and this typically the more prone the concrete is to various durability problems. The lowest resistivity is of OPC with w/cm ratio of 0.53, which contained no air entrainment. These concrete cylinders did not perform well under freeze-thaw, as expected. All cylinders from this type of concrete began to deteriorate at about 72 F-T cycles and deteriorated by spalling at 108 F-T cycles. The surface of the entire cylinder came off in chunks and only the core of the cylinder remained exposing the aggregates. The figure shows the resistivity decreasing rapidly as the specimens deteriorated until the SR measurements could not be taken any more. The performance of the remaining concrete mixtures was significantly better when compared to the mixture with no air-entrainment. Based on SR measurements alone, it can be said that SR can be an indicator of F-T deterioration since the values decreased for the specimens that deteriorated below 5 kΩ cm, however, SR measurements should be combined with other tests to verify the extent of deterioration. From visual inspection, the specimens did not have any spalling or pop-outs. Table 3.1 Table shows the air content of the concrete mixtures, having 5% and 2.5% for OPC with w/cm ratio of 0.47 and HPC with w/cm ratio of 0.43 respectively. It was expected that the HPC concrete would deteriorate at a faster rate than the OPC mixture due to a low percent of air content, however the specimens did not show any visual signs of deterioration. Running an air void analysis following ASTM C457 would help determine the true percent of air entrained in the matrix. This would help develop a better understanding of why this concrete mixture performed well.

The surface resistivity of the OPC mixture with w/cm ratio of 0.47 had a minimal change throughout the duration of the test. The SR measurements decreased by about 2 kΩ cm, where the SR of the HPC mixture decreased by over 15 kΩ cm throughout the duration of the test. The bulk resistivity of the OPC and HPC mixtures also decreased by about 2 and 10 kΩ cm respectively. The general trend for all measurements in both, bulk and surface resistivity seem to decrease over time. This is contrary to what it is expected. Resistivity should increase due to the micro-cracks that may form through F-T cycles when expansion of water molecules freeze inside the pores of the concrete matrix and create internal tensile forces. These micro cracks reduce the conductivity of the current flowing through the matrix, thus increasing resistivity. Because both figures follow the same trend for all three types of concrete and since electrical resistivity has been used in the concrete industry as an aid for durability related studies, a comparison between the two methods was made to validate the results obtained. This comparison is important to establish since the use of bulk resistivity test may not always be the most convenient since it requires taking cores or cylinders from a structure and this may not always be an option. Bulk and surface resistivity were plotted against each other and can be seen in Figure 3.4.

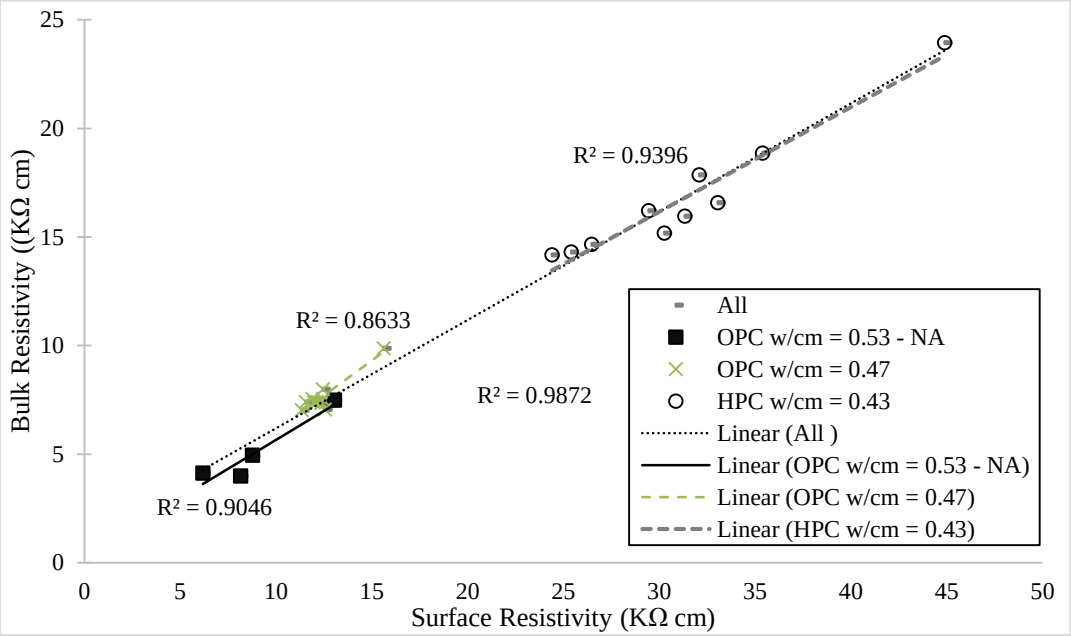

Figure 3.4 - Linear regression relationship between surface resistivity and bulk resistivity taken on cylinders for each type of concrete.

Figure 3.4 shows the linear correlation coefficients (R^2) between bulk resistivity and surface resistivity. The coefficients are shown for each set of concrete samples as well as the overall group. The coefficient for the concrete mixtures with w/cm ratio of 0.47, 0.53 and 0.43 are 0.863, 0.905 and 0.940 respectively. The correlation coefficient for the overall set of points is 0.987. These coefficients support a strong correlation between bulk and surface resistivity and indicate that surface resistivity alone will provide accurate information. The ratio of the theoretical bulk resistivity to the surface resistivity of the data collected was calculated to be 0.576. A separate study done on the relationship between bulk and surface resistivity supports this finding. Ghosh and Tran showed that the two techniques were well correlated for different types of OPC, HPC and control mixtures over longer periods of time (Ghosh et al. 2015).

To further investigate the behavior of the cylinders going through F-T cycles and to better understand the results obtained from the electrical resistivity measurements, the mass over time and the relative dynamic modulus of the cylinders were monitored and it can be seen in Figure 3.5 and Figure 3.6 respectively.

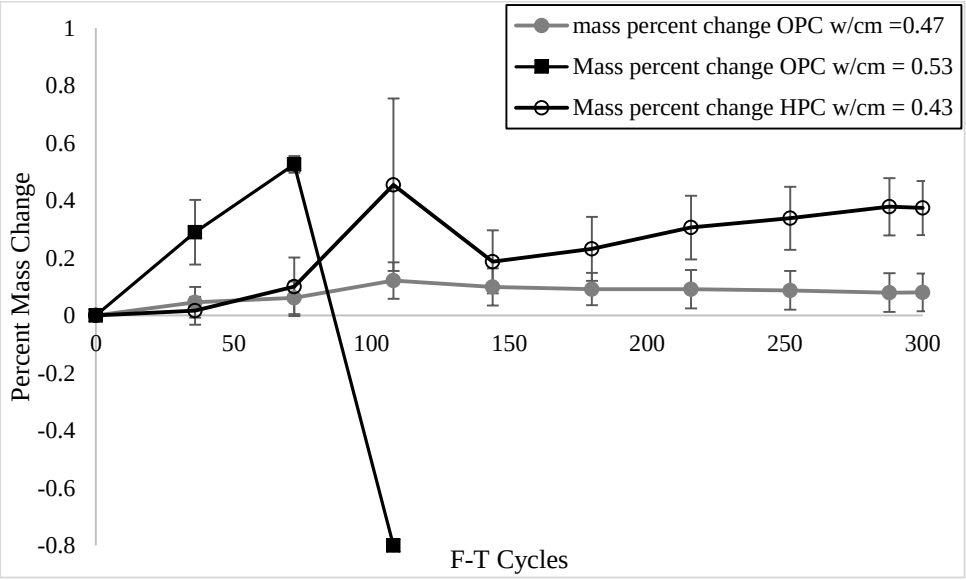

Figure 3.5 – Percent mass change over time on cylinders that underwent 300 F-T cycles in the Scientempt chamber. Three types of concrete were tested: 1) OPC concrete with w/c ratio of 0.53 and no air-entrainment, 2) an OPC concrete w/cm ratio of 0.47 with air-entrainment and 3) a HPC with a w/cm ratio of 0.43 that contained silica fume, fly ash and air-entrainment.

Figure 3.5 shows that the three types of concrete increased in mass throughout the duration of the F-T cycles. The concrete mixture with no air (OPC w/cm = 0.53), while had a steep increase in mass compared to the other two mixtures, deteriorated under freeze-thaw cycles rather rapidly due to spalling. This gain in mass could be explained by an increase in water content in the concrete matrix which caused expansion when the water froze to the point that it created the surface to spall off and separate from the aggregates. Literature shows contrary results when it comes to mass gain throughout the

F-T cycles(Zhendi Wang 2015). In these freeze-thaw studies, the concrete decreases in mass. This is attributed to the paste on the surface separating from the aggregate due to the expansion of water when frozen. However, most studies rely on procedure A from ASTM C666 standard. Procedure A requires that the specimens undergo freezing and thawing submerged in water. Procedure B was used in this study, because it mimics the F-T cycles that the concrete slabs underwent. This provides a better understanding of what could be happening in the concrete matrix. While the F-T action is providing some damage to the microstructure of the concrete, the continuous cycles may also be driving water in the concrete further into the matrix during thawing phase, which is submerged in water, allowing for more water to be absorbed by the cracks that are newly developed. Since Procedure A of the standard requires full submersion of the samples, it does not provide the concrete surface to go through a wet and dry period, and it is well understood that wet and dry cycles provide an increase of moisture ingress into the concrete matrix. This gain in moisture also helps understand why the electrical resistivity is decreasing over time. The conductivity will increase with an increase in water available in the system. The relative dynamic modulus RDM of the cylinders was also monitored in this study and can be found in Figure 3.6.

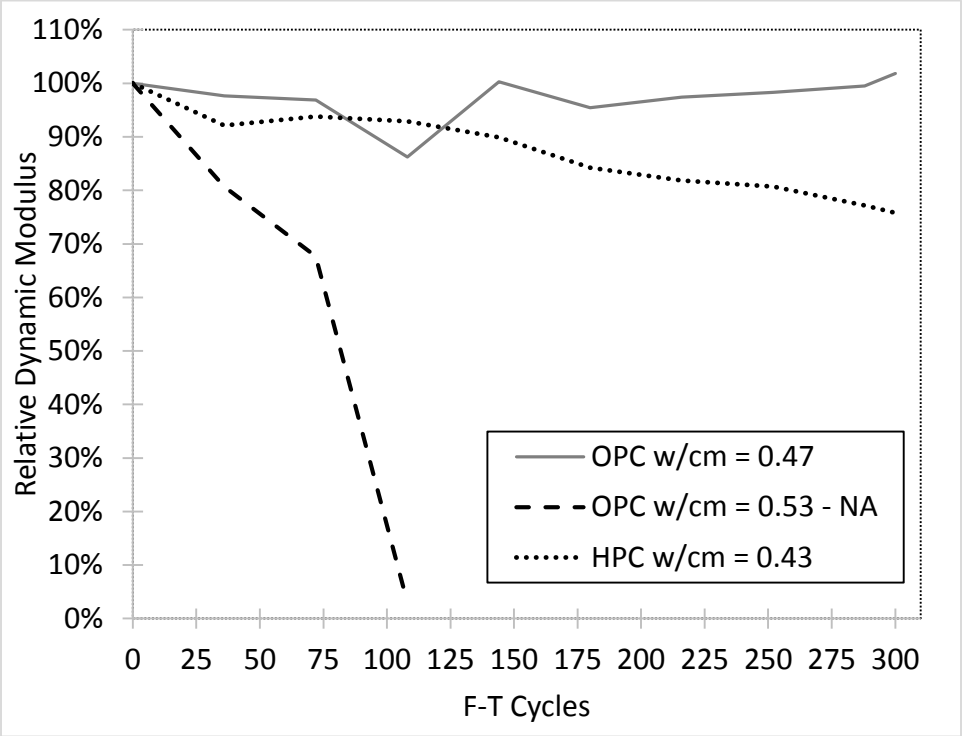

Figure 3.6 - Relative dynamic modulus of elasticity on concrete cylinders after 300 F-T cycles in the in the Scientempt chamber.

The RDM of the air entrained specimens essentially experiences no decrease and indicates that these mixtures contain a properly air-entrained system and should be expected to have excellent freeze-thaw resistance in the field. This further underscores the disconnect between the measured air content of the 0.43 mixture and the high dosage rate, which further supports the need to evaluate the samples for hardened air void analysis. The non-air entrained mixture on the other hand performed poorly as was expected. The mixture experienced a very rapid decrease in RDM from the beginning and it was recorded in the first 36 cycles. After 108 cycles the mixture was completely disintegrated due to effects of freeze-thaw action.

3.4.3. Concrete Slabs

Surface resistivity measurements were taken on reinforced concrete slabs that went through 14 ponding cycles of de-icer that contained 30% $MgCl_2$ solution with a corrosion inhibitor. The concrete slabs underwent three sets of 60 freeze-thaw cycles in the second half of the ponding cycles (e.g. after 7 ponding cycles). Figure 3.7shows the surface resistivity measurements taken on the reinforced and unreinforced section of the slabs. SR measurements were also taken on the control slabs, which were only ponded with water. The control slabs did not go through F-T action. Each set of 60 F-T cycles are also illustrated with vertical dotted lines labeled FT1, FT2 and FT3. All surface resistivity measurements are corrected for temperature and normalized to a 25°C reference temperature so that it did not have an effect on the measurements. Avoiding corrosion initiation was imperative in this study, so to prevent chlorides from reaching the reinforcement at an early age, the ponding cycles stopped after 7 cycles due to the high concentration of chloride ions in the system. Figure 3.7 shows the section in which ponding cycles did not occur.

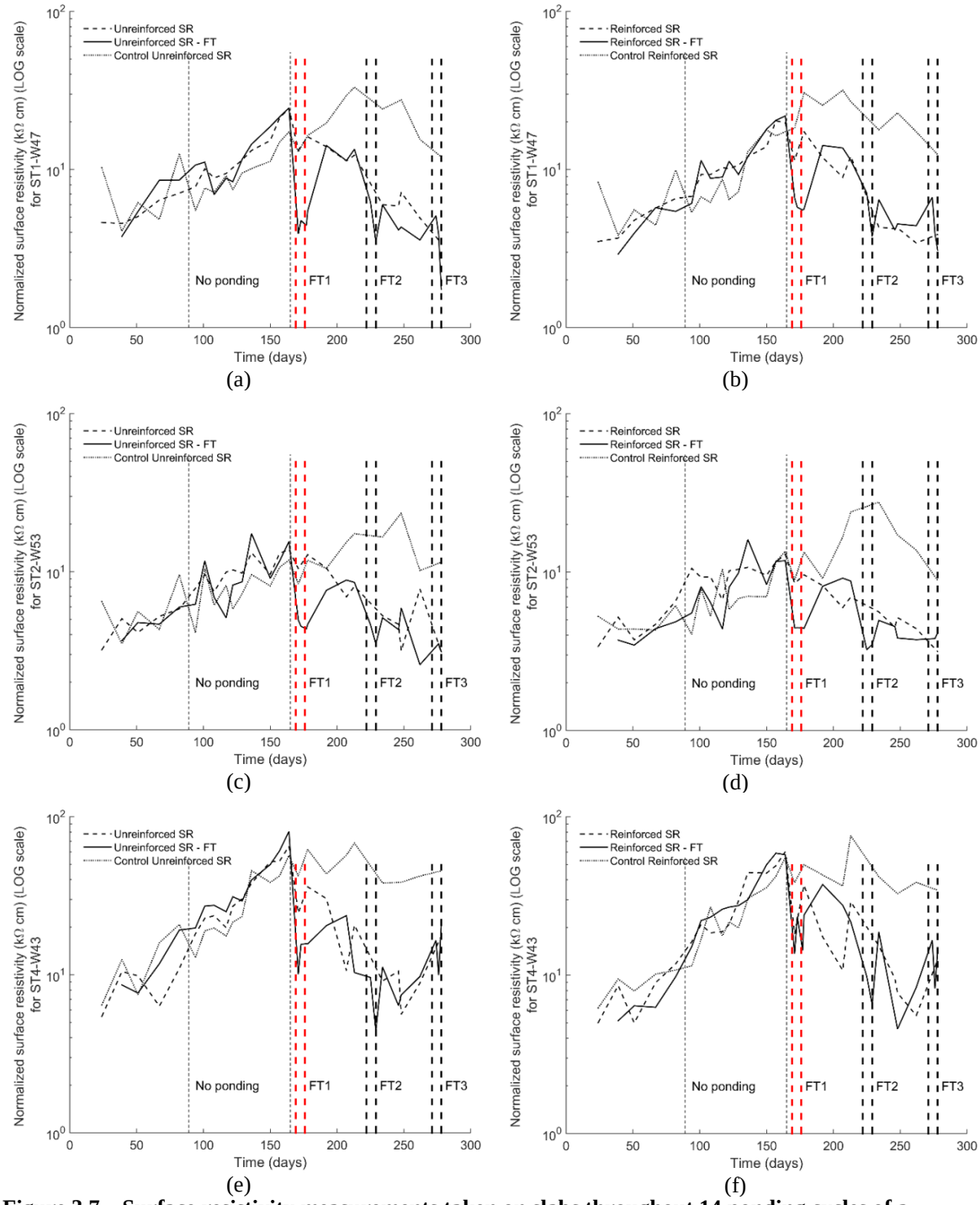

Figure 3.7 – Surface resistivity measurements taken on slabs throughout 14 ponding cycles of a magnesium chloride de-icing solution. Comparison between slabs that underwent 180 F-T cycles divided in three-60 F-T cycle sections from control slabs ponded with water that that did not go through F-T cycles are shown in the figure. Each section is shown with vertical doted lines labeled FT1, FT2 and FT3. Figure (a), (c), (e) and (b), (d) and (f) show the SR measurements taken on the unreinforced and reinforced section of the slabs respectively. Figures include SR measurements of the control slabs (water-ponded).

Before the ponding cycles stopped, the surface resistivity was increasing in all the concrete types. The type of concrete influenced the SR measurements greatly. The denser the concrete, the greater the SR measurements mainly due to a reduction in permeability. As time progressed, the SR measurements increased in all cases even after ponding stopped. This increase in resistivity can be accredited to curing. As the concrete slabs matured over time, the voids in the concrete became smaller and less well connected thus, increasing resistivity. However, as time progressed, the concentration of bound chlorides in the matrix began to increase as well. This can affect the SR measurements if the formation of Friedel's salts can increase enough to create a barrier which can alter the current flow through the pore structure. A study performed by Basheer (Basheer et al. 2002) monitored electrical resistivity of various types of concrete that went through ponding cycles to assess their resistance to chloride ingress, and found that the electrical resistivity increased with time during the ponding cycles, which partly follows the trend seen in this study. Their explanation was that this trend was due to chloride binding or formation of chloro-aluminates, or both. However, it is clear that the water-ponded slabs also had an increase of SR measurements from the beginning of the study. The increase in SR values can also be attributed to the relative humidity inside the concrete since the RH began to decrease during the summer months. Since the RH decreased, it was expected that the SR values would increase. Once the cyclic ponding continued, the SR measurements taken on the slabs that had the de-icing solution began to decrease immediately while the SR measurements of the control slabs seem to have plateaued. This section seems to show the effect of chlorides in the system. When the chlorides were introduced once again into the system, the electrical conductivity of the concrete

increased, thus lowering the electrical resistivity. As noted, the measurements between the unreinforced and reinforced section are nearly identical, validating the techniques used to measure surface resistivity over the concrete reinforcement. Figure 3.8 shows a focus or close up view of the surface resistivity measurements. Starting from when the ponding cycles began once again.

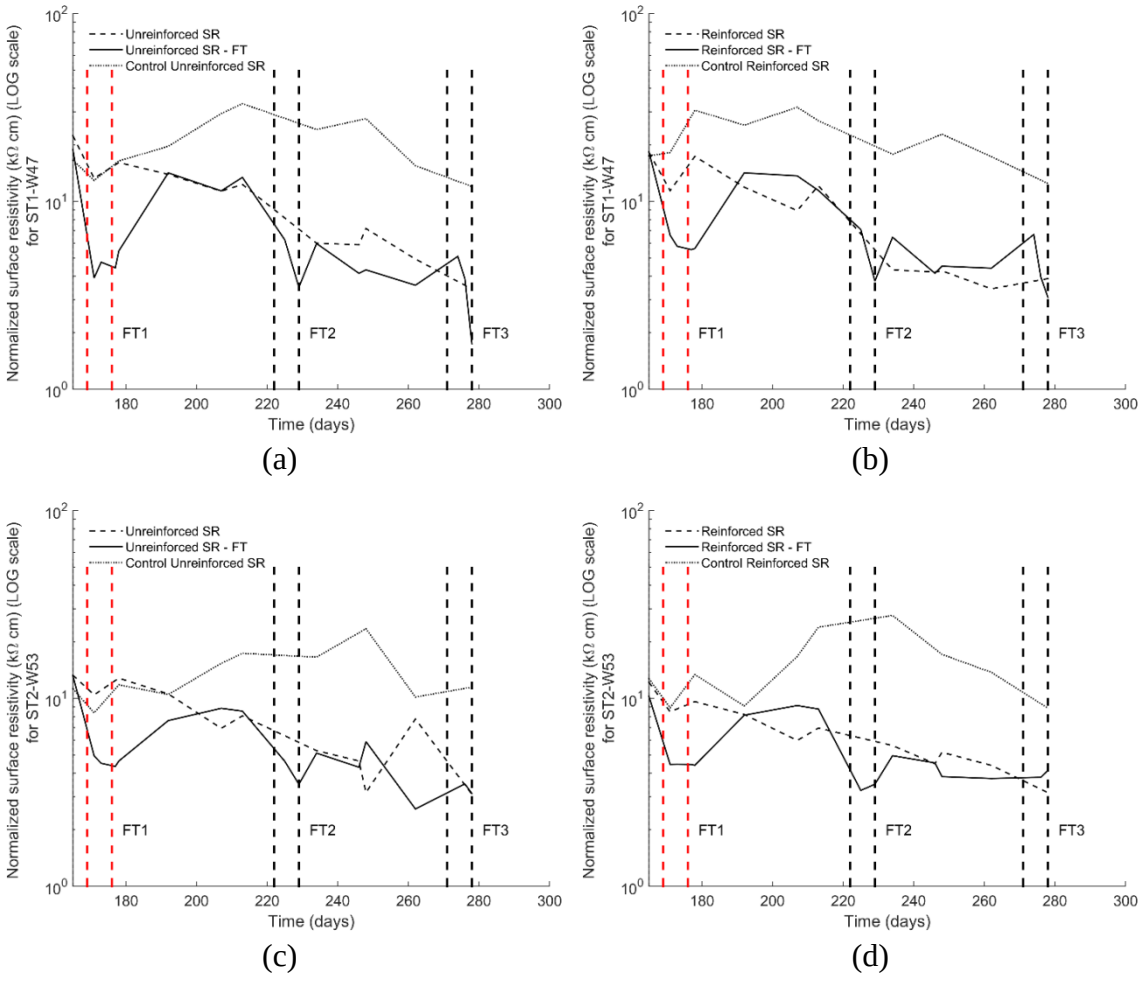

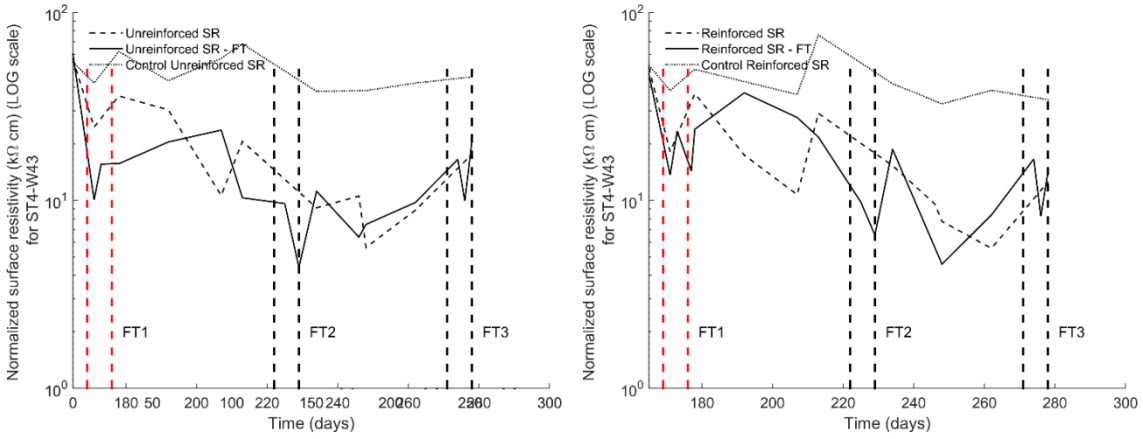

Figure 3.8 - Surface resistivity measurements taken on slabs throughout the last seven ponding cycles of a magnesium chloride de-icing solution. Comparison between slabs that underwent 180 F-T cycles divided in three-60 F-T cycle sections from ones that did not go through F-T cycles are shown in the figure. Each section is shown with vertical doted lines labeled FT1, FT2 and FT3. Figure (a), (c), (e) and (b), (d) and (f) show the SR measurements taken on the unreinforced and reinforced section of the slabs respectively. Figures include SR measurements of the control slabs (water-ponded).

Figure 3.8 shows the section in which the F-T cycles occurred. The slab with no air entrainment had severe deterioration on the surface of the concrete after the initial 60 F-T cycles. The surface of the concrete had pop-outs and concrete paste particles on the surface had begun to separate from the slab. An image of the deterioration can be found in the Appendix. From Figure 3.8 It is evident that SR measurements are affected by the F-T cycles. The measurements decreased significantly while the slabs underwent F-T cycles. The measurements take a steep decrease commensurate with F-T, however, the measurements recovered once the F-T action ended and then followed the trend of the slabs that did not go through F-T action. It indicates that the microstructure may experience some level of recovery after F-T. Another possibility is that the internal temperature decreases low enough that the correction factor for temperature may not appropriately normalize the readings taken. In all three sets of F-T cycles, regardless of the type of concrete, the SR measurements decreased and once the cycles stopped, the

measurements increased once again suggesting that taking SR measurements during F-T action may not be representative of the true resistivity. Since the behavior observed is not clear, it is suggested that additional F-T cycles continue in this study, especially until the concrete with no air-entrainment starts to fail to see how the SR values are impacted by the deterioration and to see if the decrease in surface resistivity ever remains a permanent feature or if a different trend is observed once more widespread failure occurs.

Figure 3.9 shows the SR measurements that were taken while the cylinders went through F-T cycles with the concrete slabs. The figure shows an increase in SR measurements in the two types of concrete that had air entrainment, which is the opposite behavior of the measurements from the cylinders that followed ASTM C666 in a Scientempt F-T chamber. This can be attributed to the fact that the cylinders were never fully submerged under water like the ones in the Scientempt F-T chamber. The increase in SR could indicate microstructural damage due to F-T action, however, it may be too early to tell until the cylinders undergo the full 300 cycles. The measurements on the concrete cylinders with no air entrainment seem to be consistent but once again, it is too early in the F-T cycle test to conclude anything.

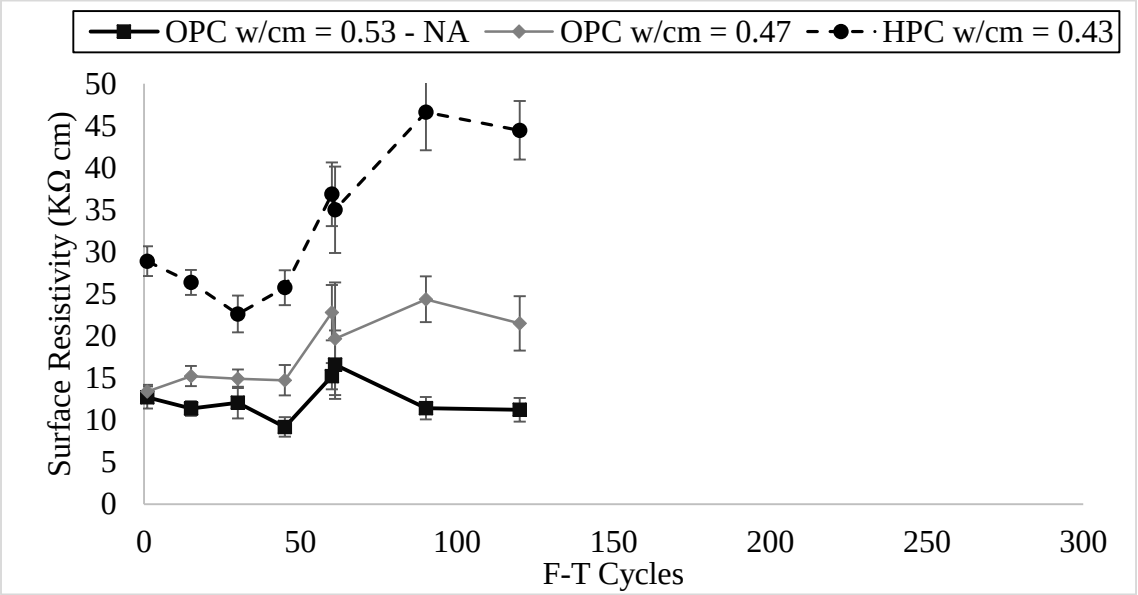

Figure 3.9 - Surface resistivity taken on cylinders that underwent two sets of 60 F-T cycles in a controlled environmental chamber. An OPC concrete with w/c ratio of 0.53 and no air-entrainment, an OPC concrete w/cm ratio of 0.47 with air-entrainment and a HPC with a w/cm ratio of 0.43 that contained silica fume, fly ash and air-entrainment.

Figure 3.9 shows four chloride profiles for each type of concrete. The control slab, which is the slab that did not go through F-T action, is shown with a solid black line. After three ponding cycles, chloride profiles were taken and are depicted with a grey solid line. This shows the amount of chloride ingress after three ponding cycles. The same procedure was repeated for the slabs that underwent F-T action. These slabs underwent 60 F-T cycles, and were then ponded for three cycles. Chloride profiles were taken before any F-T action occurred and after the three ponding cycles had ended. These slabs are represented with a dotted line and are labeled FT in the legend.

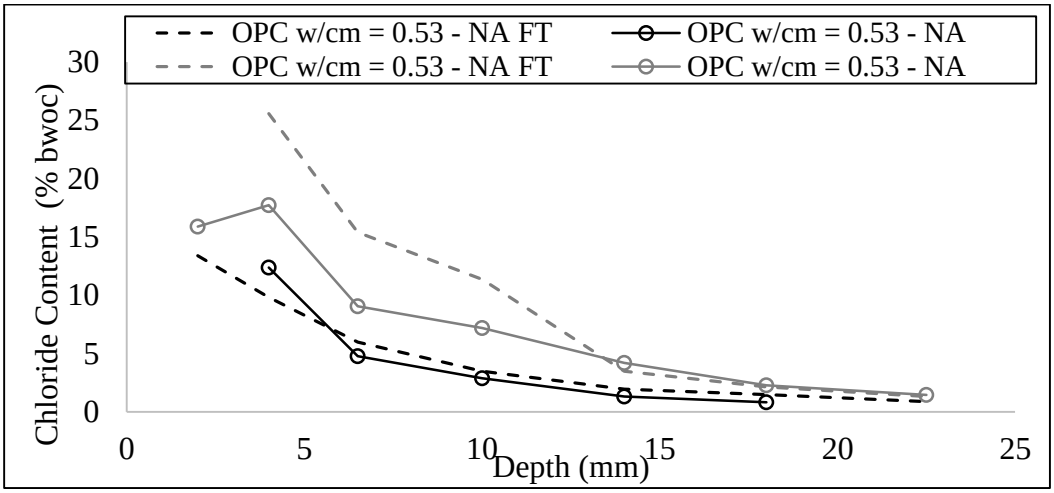

(a)

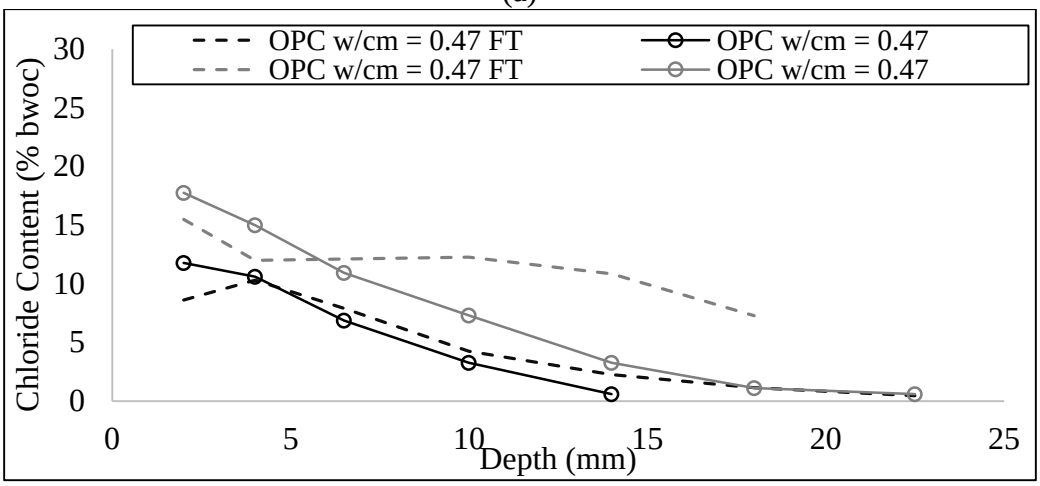

(b)

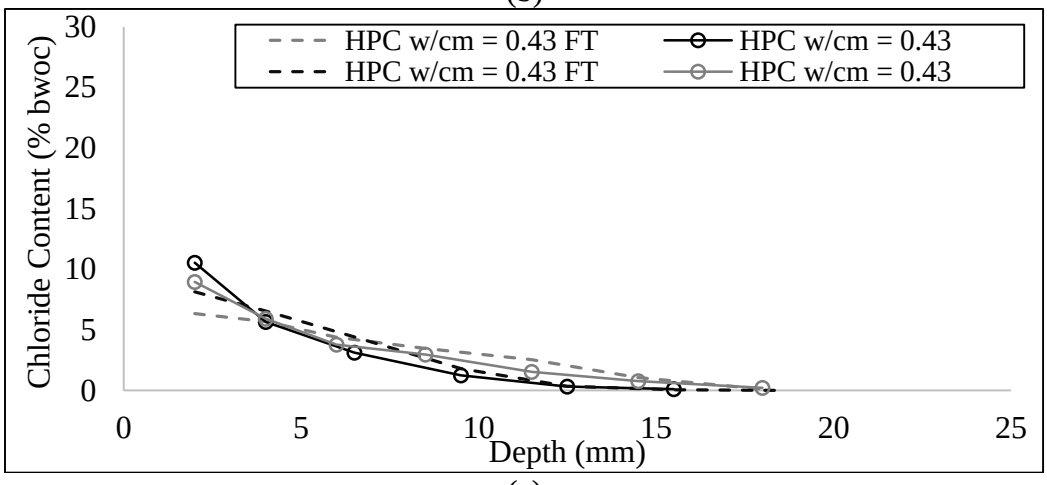

(c)

Figure 3.10 – Two chloride profiles for three types of concrete are showing the effect of F-T action on chloride ingress. An OPC concrete with w/c ratio of 0.53 and no air-entrainment, an OPC concrete w/cm ratio of 0.47 with air-entrainment and a HPC with a w/cm ratio of 0.43.

From Figure 3.10 it is clear that F-T action has a significant impact in the amount of chlorides penetrating the concrete. The slab with no air entrainment had severe deterioration on the surface of the concrete after the initial 60 F-T cycles. It also allowed for substantial chloride ingress within only three ponding cycles. The OPC mixture with air-entrainment also showed signs of deterioration with spalling and pop-outs on the surface of the slab. Although the slabs did not appear to be as deteriorated compared to the slab with no air-entrainment, the chloride profiles clearly indicate that the penetrability of the slab increased compared to the same slab that did not go through F-T action. The HPC slab, even though it had such a low air content according to the measured fresh air content, still outperformed the other slabs. Due to the use of SCMs, the HPC concrete has very low penetrability and this is evident when comparing the chloride profiles.

3.5. Conclusions

This study provided a better understanding of the effect that freeze-thaw cycles had on surface resistivity measurements taken on concrete slabs that were exposed to a commercially available magnesium chloride de-icing solution that contained a corrosion inhibitor. The concrete was produced at a ready-mix concrete facility and delivered to an outdoor exposure site in Corvallis, Oregon to provide a consistent mixture for the number of slabs included in this study. The slabs were alternated between ambient environmental exposure, where the deicing solution was ponded on the top surface, and exposure to freeze-thaw cycling in an environmental chamber. In this manuscript data for up to 180 freeze-thaw cycles is reported. The slabs will ultimately undergo 300 freeze-thaw cycles

commensurate with ASTM C666. Routine surface resistivity measurements were taken using a four-point Wenner probe at various locations on the surface of the slabs. Companion concrete cylinders were subjected to freeze-thaw cycling in the same chamber with the slabs as well as cylinders that were subjected to freeze-thaw cycling in accordance with ASTM C666 Procedure B. Cylinders were measured using bulk and surface resistivity techniques.

- Based on this study, it is recommended that the surface resistivity measurements not be taken when the concrete is at or below freezing temperatures (e.g. T > 5 C).
- Since the behavior of the surface resistivity measurements observed was not clear, it is suggested that additional F-T cycles continue in this study, especially until the concrete with no air-entrainment starts to fail to see how surface resistivity is impacted by the deterioration and to see if the damage stays permanently.
- It is recommended that if bulk or surface resistivity are to be used congruently with ASTM C666, to use Procedure A in the standard, so as to eliminate the effects that wet and dry exposure conditions used in Procedure B may have on the specimens and measurements.
- Bulk and SR resistivity measurements taken on the cylinders showed a linear relationship which is in line with previous studies that compared the two testing methods.
- F-T action had a significant negative impact on the rate of chloride ingress on the slabs. The concrete slab with no air entrainment had severe deterioration and allowed for substantial chloride ingress within only three ponding cycles after F-T action.

- Although the OPC mixture with air-entrainment visually did not appear to be as deteriorated compared to the slab with no air-entrainment, the chloride profiles clearly indicate that the penetrability of the slab increased compared to the same slab that did not go through F-T action.
- The HPC mixture performed well under F-T action. An increase in transport of chlorides was not evident and cannot be seen in the chloride profiles, however, it would be beneficial in this study to do a hardened air void analysis on this mixture to verify the air void content since the excellent performance of this mixture under F-T action was not expected due to the low fresh concrete air content measured.

3.6. References

Alonso, C., C. Andrade, J. A. González. (1988). "Relation between resistivity and corrosion rate of reinforcements in carbonated mortar made with several cement types." Cement and Concrete Research 18(5): 687-698.

ASTM C39-15 Standard Test Method for Compressive Strength of Cylindrical Concrete Specimens. (2015). ASTM International, West Conshohocken, PA.

ASTM C457-12 Standard Test Method for Microscopical Determination of Parameters of the Air-Void System in Hardened Concrete. (2012). ASTM International, West Conshohocken, PA.

ASTM C666/C666M-15 Standard Test Method for Resistance of Concrete to Rapid Freezing and Thawing. (2015). ASTM International, West Conshohocken, PA.

ASTM C1152 Standard test method for acid-soluble chloride in mortar and concrete. (2012). ASTM International, West Conshohocken, PA.

ASTM C1556-11a Standard test method for determining the apparent chloride diffusion coefficient of cementitious mixtures by bulk design. (2012). ASTM International, West Conshohocken, PA.

ASTM C215-08 Standard Test Method for Fundamental Transverse, Longitudinal, and Torsional Resonant Frequencies of Concrete Specimens. (2014). ASTM International, West Conshohocken, PA.

Backus, J., D. McPolin, A. Long, M. Basheer, N. Holmes. (2013). "Exposure of mortars to cyclic chloride ingress and carbonation." Advances in Cement Research 25(1): 3-11.

Basheer, P. A. M., P. R. V. Gilleece, A. E. Long, W. J. Mc Carter. (2002). "Monitoring electrical resistance of concretes containing alternative cementitious materials to assess their resistance to chloride penetration." Cement and Concrete Composites 24(5): 437-449.

Koch, G., M. Brongers, N. Thompson, Y. Virmani, J.H. Payer. (2002). "Corrosion Costs and Preventive Strategies in the United States." FHWA-RD-01-156(Final Report): 773 pp.

Ghosh, P., Q. Tran. (2015). "Correlation Between Bulk and Surface Resistivity of Concrete." International Journal of Concrete Structures and Materials 9(1): 119-132.

Gowers, K. R., S. G. Millard. (1999). "Measurement of concrete resistivity for assessment of corrosion severity of steel using Wenner technique." ACI Materials Journal 96(5): 536-541.

Hong, K. (1999). Cyclic wetting and drying and its effects on chloride ingress in concrete. National Library of Canada, Ottawa, ON.

Huang, J., W. Shaowei, J. Chaudhari, S. Soltesz, X. Shi. (2014). Deicer effect on concrete bridge decks: practitioners perspective and a method of developing exposure maps. Transportation Research Board Annual Meeting: 1-13, Washington DC.

Jiang, J. H. (2013). "Relationship of moisture content with temperature and relative humidity in concrete." Magazine of Concrete Research 65(11): 685-692.

Julio-Betancourt, J. A. (2009). Effect of de-icer and anti-icer chemicals on the durability microstructure, and properties of cement-based materials. Graduate of Civil Engineering. Toronto, Canada, University of Toronto. Doctor of Philosophy: 854 pp.

López, W., J. A. González (1993). "Influence of the degree of pore saturation on the resistivity of concrete and the corrosion rate of steel reinforcement." Cement and Concrete Research 23(2): 368-376.

Morales, M. T. (2015). Experimental investigation of the effects of embedded rebar, cracks, chloride ingress and corrosion on electrical resistivity measurements of reinforced concrete: 174 pp.

ODOT. (2008). Oregon Standard and Specifications for Construction, Oregon Department of Transportation: 814 pp.

Ryu, D, W. Ko, T. Noguchi. (2011). "Effects of simulated environmental conditions on the internal relative humidity and relative moisture content distribution of exposed concrete." Cement and Concrete Composites 33(1): 142-153.

Salehi, M. (2013). Numerical investigation of the effects of cracking and embedded reinforcement on surface concrete resistivity measurements using Wenner probe. Civil and Environmental Engineering. Carleton University. Master of Applied Science in Civil Engineering: 155 pp., Ottawa, ON.

Sengul, O., O. E. Gjorv (2009). "Effect of embedded steel on electrical resistivity measurements on concrete structures." ACI Materials Journal 106-M02 (January/February 2009): 11-18.

Shi, X. (2011). Understanding and mitigating effects of chloride deicer exposure on concrete. Western Transportation Institute. Bozeman, MT, Montana State Univerity.

Shi, X., L. Yajun, M. Mooney, M. Berry, L. Fay, A. B. Leonard. (2010). Effect of chloride-based deicers on reinforced concrete structures. Bozeman, MT, Montana State University: 1-74.

Shi, X., Y. Li., S. Jungwirth, Y. Fang, N. Seeley, E. Jackson. (2013). "Identification and laboratory assessment if best practices to protect DOT equipment from the corrosive effect of chemical deicers." 217 pp.

Sutter, L., K Peterson, G. Julio-Betancourt, D. Hooton, T. V. Dam, k. Smith. The Deleterious Chemical Effects of Concentrated Deicing Solutions on Portland Cement Concrete. (2008). SD2002-01. Federal Highway Administration: 1-198, Houghton, MI.

Wang, Zhendi, , L. Wang, Y. Yao, K. Li. (2015). "Electrical resistivity of cement pastes undergoing cyclic freeze-thaw action." Journal of Materials in Civil Engineering 27(1) 1-8.

4 General Conclusions

Experimental procedures were performed through the use of electrical resistivity to develop a better understanding of the chloride ingress due to de-icer solution exposure and freeze-thaw action on reinforced concrete. The experimental investigations evaluated selected reinforced concrete properties, such as concrete cover depth, the use of SCMs, varying air content and a range of water-to-cement ratios. Deterioration means, such as chloride ingress and freeze-thaw attack were evaluated in concurrence with electrical resistivity measurements to establish a correlation.

The first manuscript titled “Evaluation of the Effect of Chloride Ingress in Reinforced Concrete on Surface Resistivity Measurements” investigates the potential for surface resistivity, using the four-point Wenner probe technique, to be used as a non-destructive evaluation tool to assess the deterioration of concrete due to chloride ingress. The main conclusions drawn from this study are:

- Surface resistivity values decreased for the chloride-saturated concrete once ponding was initiated half way through the study, and water-saturated concrete did not change as much, suggesting that SR measurements could identify chloride ingress. Additional data collection and modeling are required to investigate this relationship in further detail.

- Over time, the amount of bound chlorides in the system increased; however, this increase was dominated by the amount of free chlorides that were retained at a specific depth in the concrete.
- The increase in free chloride concentrations may be a contributing factor to the decrease in SR measurements. This observation was also confirmed by thermodynamic modeling, however this relationship needs to be studied further.

The second manuscript titled "The Effect of Freeze-Thaw Action on Electrical Resistivity Measurements Taken on Concrete Saturated with Magnesium Chloride De-Icing Solution" investigates the effect that freeze-thaw cycles have on electrical resistivity measurements taken on concrete cylinders as well as concrete slabs that were exposed to a magnesium chloride de-icing solution. The ability for chloride to ingress concrete after freeze-thaw exposure was also investigated.

- It is too early in the study to understand the behavior of the surface resistivity measurements observed. It is suggested that additional F-T cycles continue in this study, especially until the concrete with no air-entrainment starts to fail to see how surface resistivity is impacted by the deterioration and to see if the damage stays permanently.
- It is clear that F-T action has a significant negative impact on the rate of chloride ingress on the OPC concrete slabs. The concrete slab with no air entrainment had severe deterioration and allowed for substantial chloride ingress. The chloride

profiles for the air-entrained OPC mixture clearly indicate that the penetrability of the slab increased compared to the same slab that did not go through F-T action.

- An increase in transport of chlorides for the HPC mixture is not evident and cannot be seen in the chloride profiles. However, it would be beneficial to do a hardened air void analysis on this mixture to verify the air void content because the excellent performance of this mixture under F-T action was not expected due to its low fresh concrete air content.

Bibliography

ACI Committee 222R-01: (2001), Protection of Metals in Concrete Against Corrosion. Reapproved 2010.

Alonso, C., C. Andrade, J. A. González. (1988). "Relation between resistivity and corrosion rate of reinforcements in carbonated mortar made with several cement types." Cement and Concrete Research 18(5): 687-698.

Andrade, C., C. Alonso (2004). "Test methods for on-site corrosion rate measurement of steel reinforcement in concrete by means of the polarization resistance method." Materials and Structures 37(9): 623-643.

Andrade, C., M. Prieto, P. Tanner, F. Tavares, R. d'Andrea. (2013). "Testing and modelling chloride penetration into concrete." Construction and Building Materials 39: 9-18.

ASTM C215-08 Standard Test Method for Fundamental Transverse, Longitudinal, and Torsional Resonant Frequencies of Concrete Specimens. (2014). ASTM International, West Conshohocken, PA.

ASTM A615-15a Standard Specification for Deformed and Plain Carbon-Steel Bars for Concrete Reinforcement. (2015). ASTM International, West Conshohocken, PA.

ASTM C1152-12 Standard test method for acid-soluble chloride in mortar and concrete. (2012). ASTM International, West Conshohocken, PA.

ASTM C1218/C1218M-15 Standard Test Method for Water-Soluble Chloride in Mortar and Concrete. (2015). ASTM International, West Conshohocken, PA.

ASTM C1556-11a Standard test method for determining the apparent chloride diffusion coefficient of cementitious mixtures by bulk design. (2012). ASTM International, West Conshohocken, PA.

ASTM C39-15 Standard Test Method for Compressive Strength of Cylindrical Concrete Specimens. (2015). ASTM International, West Conshohocken, PA.

ASTM C457-12 Standard Test Method for Microscopical Determination of Parameters of the Air-Void System in Hardened Concrete. (2012). ASTM International, West Conshohocken, PA.

ASTM C597-09 Standard test method for pulse velocity through concrete. (2010). ASTM International, West Conshohocken, PA .

ASTM C666/C666M-15 Standard test method for resistance of concrete to rapid freezing and thawing. (2015). ASTM International, West Conshohocken, PA.

ASTM WK37880 New Test Method for Measuring the Surfae Resistivity of Hardened Concrete Using the Wenner Four-Electrode Method. (2014). ASTM International, West Conshohocken, PA.

Backus, J., D. McPolin, A. Long, M. Basheer, N. Holmes. (2013). "Exposure of mortars to cyclic chloride ingress and carbonation." Advances in Cement Research 25(1): 3-11.

Basheer, P., P. Gilleece, A. Long, W. Mc Carter. (2002). "Monitoring electrical resistance of concretes containing alternative cementitious materials to assess their resistance to chloride penetration." Cement and Concrete Composites 24(5): 437-449.

Blackburn, R., D. Amsler, K. Bauer (2004). Snow removal and ice control technology. Sixth International Symposium on Snow Removal and Ice Control Technology, Transportation Research Board of the National Academies, Spokane, WA .

Brencich, A., G. Cassini, D. Pera, G. Riotto (2013). "Calibration and Reliability of the Rebound (Schmidt) Hammer Test." Civil Engineering and Architecture 1(3): 66-78.

Conciatori, D, H. Sadouki, E. Brühwiler. (2008). "Capillary suction and diffusion model for chloride ingress into concrete." Cement and Concrete Research 38(12): 1401-1408.

Concrete materials and methods of concrete construction/Test methods and standard practices for concrete. (2009). Canadian Standards Association, Toronto, ON.

Florida method of test for concrete resistivity as an electrical indicator of its permeability. (2004). Department of Transportation Florida, FL, USA.

Garzon, A. J., J. Sanchez, C. Andrade, N. Rebolledo, E. Menéndez, J. Fullea. (2014). "Modification of four point method to measure the concrete electrical resistivity in presence of reinforcing bars." Cement and Concrete Composites 53: 249-257.

Ghosh, P., Q. Tran. (2015). "Correlation Between Bulk and Surface Resistivity of Concrete." International Journal of Concrete Structures and Materials 9(1): 119-132.

Gowers, K. R., S. G. Millard. (1999). "Measurement of concrete resistivity for assessment of corrosion severity of steel using Wenner technique." ACI Materials Journal 96(5): 536-541.

Gowers, K., S. Millard. (1999). "Measurement of concrete resistivity for assessment of corrosion severity of steel using Wenner technique." ACI Materials Journal 96(5): 536-541.

Gucunski, N., I. Arezoo; F. Romero, S. Zanarian, D. Yuan, H. Wiggenhauser, P. Shokouhi, A. Taffe, D. Kutrubes. (2013). Nondestructive testing to identify concrete bridge deck deterioration. Transportation Research Board. Washington, D.C.

Hamilton, H., A. J. Boyd, E. Vivas, M. Bergin. (2007). Permeability of concrete - comparison on conductivity and diffusion methods. No. 00026899. Gainesville, FL, University of Florida.

Hong, K. (1999). Cyclic wetting and drying and its effects on chloride ingress in concrete. National Library of Canada, Ottawa, ON.

Hooton, R.D., A. Shahroodi, E. Karkar. (2012). Evaluating concretes using rapid test methods for fluid penetration resistance, ACI Fall Convention in Toronto, presented in the Emerging Technologies (Part 2); available at aci-int.org.

Hope, B., A. Ip. (1987). "Chloride Corrosion Threshold in Concrete." Materials Journal 84(4): 306-314.

Huang, J., W. Shaowei, J. Chaudhari, S. Soltesz, X. Shi. (2014). Deicer Effect on Concrete Bridge Decks: Practitioners Perspective and a Method of Developing Exposure Maps. Transportation Research Board Annual Meeting: 1-13. Washington, DC.

Hussain, R. R. (2011). "Effect of moisture variation on oxygen consumption rate of corroding steel in chloride contaminated concrete." Cement and Concrete Composites 33(1): 154-161.

Hussain, S., E.,Rasheeduzzafar, A. Almusallam, A. S. Algahtani. (1995). "Factors affecting threshold chloride for reinforcement corrosion in concrete." Cement and Concrete Research 25(7): 1543-1555.

Jackson, L. (2013). "Surface resistivity test evaluation as an Indicator of the Chloride Permeability of Concrete." Tech brief. Publication no. FHWA-HRT-13-024, McLean, VA.

Jaegermann, C. (1990). "Effect of water-cement ratio and curing on chloride penetration into concrete exposed to Mediterranean Sea climate." Materials Journal 87(4): 333-339.

Ji, Y., T. Zan, Y. Yuan. (2009). "Chloride Ion Ingress in Concrete Exposed to a Cyclic Wetting and Drying Environment." American Society of Agricultural and Biological Engineers 52(1): 239-245.

Jiang, J. H. (2013). "Relationship of moisture content with temperature and relative humidity in concrete." Magazine of Concrete Research 65(11): 685-692.

Jianhong, C., B. Dylan, J. Frank, H. Dryver. (2008). Concrete bridge deck condition assessment with automated multisensor techniques. Bridge Maintenance, Safety Management, Health Monitoring and Informatics. Burlington, VT, Taylor & Francis.

Julio-Betancourt, J. A. (2009). Effect of de-icer and anti-icer chemicals on the durability microstructure, and properties of cement-based materials. Graduate of Civil Engineering. Toronto, Canada, University of Toronto. Doctor of Philosophy: 854 pp.

Kessler, R., R. Powers, M. Paredes. (2005). Resistivity measurements of water saturated concrete as an indicator of permeability. NACE International.

Khalim, A. R., D. Sagar, M. D. Kumruzzaman, A. S. M. Z. Hasan. (2011). "Combination of nondestructive evaluations for reliable assessment of bridge deck." Facta universitatis - series: Architecture and Civil Engineering 9(1): 11-22.

Koch, G.H., M. Brongers, N. Thompson, Y. Virmani, J. Payer. (2002). "Corrosion Costs and Preventive Strategies in the United States." FHWA-RD-01-156 (Final Report): 773 pp.

Kosmatka, S. H., M. L. Wilson. (2011). "Design and Control of Concrete Mixtures." 15th Edition: 444, Portland Cement Association, Washington, D.C .

Kulik, D., T. Wagner, S.Dmytrieva, G. Kosakowski, F. Hingerl, K. Chudnenko, U. Berner. (2013). "GEM-Selektor geochemical modeling package: revised algorithm and GEMS3K numerical kernel for coupled simulation codes." Computational Geosciences 17(1): 1-24.

Lingen, R. T. (1998). "Concrete in coastal structures." 301. London, U.K., Thomas Telford Limited.

López, W., J. A. González. (1993). "Influence of the degree of pore saturation on the resistivity of concrete and the corrosion rate of steel reinforcement." Cement and Concrete Research 23(2): 368-376.

Lord, B. N. (1988). "Program to reduce deicing chemical usage." Federal Highway Administration: 13 pp. , McLean, VA.

Martin-Perez, B. (1999). "Service life modelling of R.C. highway structures exposed to chlorides." Ph.D. thesis: 168 pp.

Method of test for determination of electrical resistivity of concrete. (2013). Ministry of Transportation Ontario, Toronto, ON.

Morales, M. T. (2015). Experimental investigation of the effects of embedded rebar, cracks, chloride ingress and corrosion on electrical resistivity measurements of reinforced concrete: 174 pp.

Morris, W., A. Vico, M. Vázquez. (2004). "Chloride induced corrosion of reinforcing steel evaluated by concrete resistivity measurements." Electrochimica Acta 49(25): 4447-4453.

Mussato, B. T.,O. K. Gepraegs and G. Farnden (2004). "Relative effects of sodium chloride and magnesium chloride 0n reinforced concrete: state of the art." Transportation research record.(1866): 59-66.

Mutale, L. (2014). An investigation into the relationship between surface concrete resistivity and chloride conductivity tests: 105 pp.

Neville, A. M. (1981). Properties of Concrete. Pitman Publising Limited, London, United Kingdon.

Neville, A. M. (1996). Properties of Concrete: Fourth Edition. 844. Hoboken, NJ, Wiley.

ODOT. (2008). Oregon Standard and Specifications for Construction, Oregon Department of Transportation: 814 pp.

Paul Scherrer Institute. (2013). "GEMS: Gibbs Energy Minimization Software for Geochemical Modeling." From http://gems.web.psi.ch.

Presuel-Moreno, F., Y. Liu, M. Paredes (2009). Understanding The Effect Of Rebar Presence And/Or Multilayered Concrete Resistivity On The Apparent Surface Resistivity Measured Via The Four-Point Wenner Method. Corrosion Conference 2009. Atlanta, GA, NACE International.

Qiang, Y., A. Katrien, S. Caijun, S. Geert De. (2008). Effect of temperature on transport of chloride ions in concrete. Concrete Repair, Rehabilitation and Retrofitting II, CRC Press: 159-160.

Rupnow, T., I. Patrick. (2011). Evaluation of surface resistivity measurements as an alternative to the rapid chloride permeability test for quality assurance and acceptance. Louisiana Transportation Research Center: 68 pp.

Ryu, D,W. Ko, T. Noguchi. (2011). "Effects of simulated environmental conditions on the internal relative humidity and relative moisture content distribution of exposed concrete." Cement and Concrete Composites 33(1): 142-153.

Sadowski, L. (2013). "Methodology for assessing the probabilty of corrosion in concrete structures on the basis of half-cell potential and concrete resistivity measurements." Scientific World Journal. 2013: 8. Article ID 714501.

Salehi, M. (2013). Numerical investigation of the effects of cracking and embedded reinforcement on surface concrete resistivity measurements using Wenner probe. Civil

and Environmental Engineering. Ottawa, Ontario, Carleton University. Master of Applied Science in Civil Engineering: 155 pp.

Sengul, O., O. E. Gjorv (2009). "Effect of embedded steel on electrical resistivity measurements on concrete structures." ACI Materials Journal 106-M02 (January/February 2009): 11-18.

Sengul, O., O. E. Gjorv. (2008). "Electrical resistivity measurements for quality control during concrete construction." ACI Materials Journal 105(6): 541-547.

Shariati, M., H. Sulong, M. Arabnejad, P. Shafigh, H. Sinaei. (2011). "Assessing the strength of reinforced concrete structures through ultrasonic pulse velocity and Schmidt Rebound Hammer tests." Scientific Research and Essays 6 (1): 213-220.

Shi, X. (2011). Understanding and mitigating effects of chloride deicer exposure on concrete. Western Transportation Institute. Bozeman, MT, Montana State Univerity.

Shi, X., L. Yajun, M. Mooney, M. Berry, L. Fay, A. B. Leonard. (2010). Effect of chloride-based deicers on reinforced concrete structures. Bozeman, MT, Montana State University: 1-74.

Shi, X., Y. Li., S. Jungwirth, Y. Fang, N. Seeley, E. Jackson. (2013). "Identification and laboratory assessment if best practices to protect DOT equipment from the corrosive effect of chemical deicers." 217 pp.

Sirivivatnanon, V., W. A. Thomas, K. Waye. (2012). Determination of free chlorides in aggregates and concrete. Australian Journal of Structural Engineering. 151-158 .

Song, H., V. Saraswathy. (2007). "Corrosion monitoring of reinforced concrete structures - a review." International Journal of Electrochemical Science 2(2007):1-28.

Standard method of test for surface resistivity indication of concrete’s ability to resist chloride ion penetration. (2011). American Association of State Highway and Transportation Officials, Washington DC.

Sutter, L., K Peterson, G. Julio-Betancourt, D. Hooton, T. V. Dam, k. Smith. The Deleterious Chemical Effects of Concentrated Deicing Solutions on Portland Cement Concrete. (2008). SD2002-01. Federal Highway Administration: 1-198, Houghton, MI.

Swanstrom, J., T. Rogers, G. Bowling, S. Tuttle (2013). ODOT bridge inspection program manual 2013. Oregon Department of Transportation: 1-381, OR.

Wagner, T., D. A. Kulik ,F. F. Hingerl, S. V. Dmytrieva. (2012). "Gem-Selektor geochemical modeling package: TSolmod library and data interface for multicomponent phase models." Canadian Mineralogist 50(5): 1173-1195.

Wang, Q. Z., L. Wang, Y. Yao, K. Li. (2015). "Electrical resistivity of cement pastes undergoing cyclic freeze-thaw action." Journal of Materials in Civil Engineering. 27(1).

Wang, Z., Q. Zeng, L. Wang, Y. Yao, K. Li. (2014). "Effect of moisture content on freeze–thaw behavior of cement paste by electrical resistance measurements." Journal of Materials Science. 49(12): 4305-4314.

Wang, Zhendi, , L. Wang, Y. Yao, K. Li. (2015). "Electrical resistivity of cement pastes undergoing cyclic freeze-thaw action." Journal of Materials in Civil Engineering 27(1) 1-8.

Weydert, R., C. Gehlen. (1999). "Electrolytic resistivity of cover concrete: Relevance, measurement and interpretation." Proceedings of the 8th International Conference on Durability of Building Materials and Components. 409-419. NRC Research Press, Vancouver, Canada.

APPENDICES

APPENDIX A: Type II Cement Composition

WYOMING ANALYTICAL LABORATORIES, INC.
14335 W. 44th Avenue
Golden, CO 80403
www.wal-lab.com
Email: walxray@aol.com
(303) 278-2448
Fax (303) 278-2439

November 5, 2014

Chang Li
Oregon State University
220 Owen Hall
Corvallis, OR 97331-3212

WAL #140913-1
Sample ID: Type I/II Cement
PO#:

CHEMICAL ANALYSIS
Wt%, as Rec'd Basis

Silicon Dioxide	SiO_2	19.93	
Aluminum Oxide	Al_2O_3	4.77	
Iron Oxide	Fe_2O_3	3.50	
Calcium Oxide	CaO	63.47	
Magnesium Oxide	MgO	0.87	
Sodium Oxide	Na_2O	0.29	
Potassium Oxide	K_2O	0.33	
Total Alkalies as Na_2O			0.51
Titanium Dioxide	TiO_2	0.27	
Manganic Oxide	Mn_2O_3	0.12	
Phosphorus Pentoxide	P_2O_5	0.07	
Strontium Oxide	SrO	0.18	
Barium Oxide	BaO	0.11	
Sulfur Trioxide	SO_3	3.11	
Loss on Ignition		3.09	
Total		100.00	

Tricalcium Silicate	C_3S	61.33
Tricalcium Aluminate	C_3A	6.61
Dicalcium Silicate	C_2S	10.86
Tetracalcium Aluminoferrite	C_4AF	10.64

*TiO_2 and P_2O_5 not included in Al_2O_3
*No correction has been made for the possibe use of limestone.
Analysis per ASTM C 114

Charles R. Wilson,
Division Manager

MEMBER
ACIL

APPENDIX B: Silica Fume Compositon

WYOMING ANALYTICAL LABORATORIES, INC.
14335 W. 44th Avenue
Golden, CO 80403
www.wal-lab.com
Email: walxray@aol.com
(303) 278-2446
Fax: (303) 278-2439

September 29, 2014

Chang Li
Oregon State University
220 Owen Hall
Corvallis, OR 97331-3212

Denver Division #: 140912-1
Sample ID: Silica Fume
PO#:

CHEMICAL ANALYSIS
WT%, DRY BASIS

Silicon Dioxide, SiO2	90.17
Aluminum Oxide, Al2O3	0.48
Iron Oxide, Fe2O3	1.49
Total (SiO2 + Al2O3 + Fe2O3)	92.13
Calcium Oxide, CaO	1.01
Magnesium Oxide, MgO	2.55
Sodium Oxide, Na2O	0.20
Potassium Oxide, K2O	0.78
Titanium Dioxide, TiO2	0.00
Manganese Dioxide, MnO2	0.17
Phosphorus Pentoxide, P2O5	0.11
Strontium Oxide, SrO	0.02
Barium Oxide, BaO	0.00
Sulfur Trioxide, SO3	0.13
Loss on Ignition (950°C)	2.90
Total	100.00
Moisture (105°C), as Received	0.56

Analysis per ASTM C 1240

Charles R. Wilson
Division Manager

MEMBER
ACIL

APPENDIX C: Class F Fly Ash Composition

WYOMING ANALYTICAL LABORATORIES, INC.
14335 W. 44th Avenue
Golden, CO 80403
www.wal-lab.com
Email: walxray@aol.com
(303) 278-2446
Fax: (303) 278-2439

September 29, 2014

Chang Li
Oregon State University
220 Owen Hall
Corvallis, OR 97331-3212

Denver Division #: 140917-2
Sample ID: Fly Ash
PO#:
Project#:

CHEMICAL ANALYSIS
WT%, DRY BASIS

Silicon Dioxide, SiO2	49.69
Aluminum Oxide, Al2O3	17.23
Iron Oxide, Fe2O3	5.63
Total (SiO2 + Al2O3 + Fe2O3)	72.54
Calcium Oxide, CaO	13.94
Magnesium Oxide, MgO	4.48
Sodium Oxide, Na2O	3.58
Potassium Oxide, K2O	1.71
Titanium Dioxide, TiO2	0.98
Manganese Dioxide, MnO2	0.09
Phosphorus Pentoxide, P2O5	0.31
Strontium Oxide, SrO	0.35
Barium Oxide, BaO	0.62
Sulfur Trioxide, SO3	0.99
Loss on Ignition (750°C)	0.42
Total	100.00
Moisture (105°C), as Received	0.09

Analysis per ASTM C 311

Charles R. Wilson
Division Manager

MEMBER
ACIL

APPENDIX D: Coarse Aggregate Sieve Analysis

Sieve	*Sieve Wt. (kg)*	*Sample Wt. (kg)*	*Sieve*	*Opening (mm)*	*Percent Retained*	*Sample Weight*	*Percent Passing*	*Cumulative Percent Retained*
1.5"	8.748	8.748	1.5."	38.10	0.00	0.00	100.00	0.00
3/4"	7.468	8.096	3/4"	19.05	5.45	0.63	94.55	5.45
1/2"	7.324	12.556	1/2"	12.70	45.37	5.23	49.18	50.82
1/4"	8.608	13.712	1/4"	6.35	44.26	5.10	4.93	95.07
No. 4	6.954	7.330	No. 4	4.75	3.26	0.38	1.66	98.34
No.8	6.526	6.696	No.8	2.36	1.47	0.17	0.19	99.81
Pan	6.252	6.274	Pan	0.00	0.19	0.02	0.00	100.00
Total	51.880	63.412	11.53		100.0	11.53	250.52	

APPENDIX E: Fine Aggregate Sieve Analysis

Sieve Opening (mm)	*Percent Retained*	*Sample Weight*	*Percent Passing*	*Cumulative Percent Retained*
9.525	0.00	0.0	100.00	0.00
4.75	4.55	59.5	95.45	4.55
2.36	18.71	244.5	76.74	23.26
1.18	13.74	179.5	63.00	37.00
0.6	12.53	163.7	50.47	49.53
0.3	34.51	451.0	15.96	84.04
0.15	14.10	184.2	1.86	98.14
Pan	1.86	24.3		100.00
	100.00	1306.7	403.47	
		Fineness Modulus	2.97	

Sieve Opening (mm)	*Percent Retained*	*Sample Weight*	*Percent Passing*	*Cumulative Percent Retained*
9.525	0.00	0.0	100.00	0.00
4.75	5.29	68.0	94.71	5.29
2.36	20.63	265.2	74.08	25.92
1.18	13.95	179.3	60.13	39.87
0.6	12.42	159.7	47.70	52.30
0.3	33.70	433.2	14.00	86.00
0.15	12.35	158.8	1.65	98.35
Pan	1.65	21.2		100.00
	100.00	1285.4	392.27	
		Fineness Modulus	3.08	

Average Fineness Modulus	*3.02*

APPENDIX F: Deterioration due to Freeze-Thaw Action

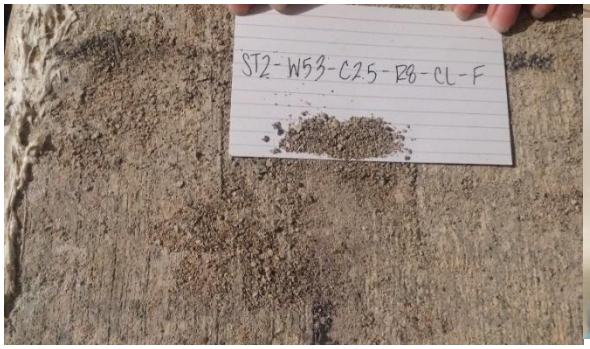

(a)

(b)

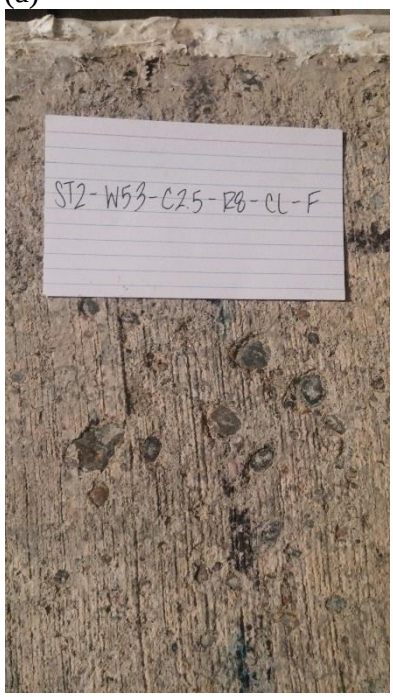

(c)

(d)

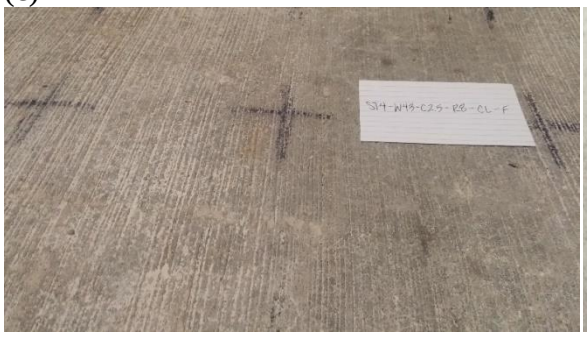

(e)

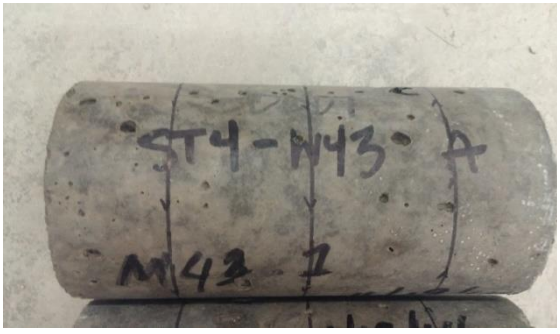

(f)

Appendix D - Deterioration due to F-T action. (a)- (d) represent the non-entrained OPC mixture; (e) and (f) represent the HPC mixture.